



3 0307 00046 3714

Non-Ferrous Mine Waste Characterization Project

Final Report

Minnesota Department of Natural Resources
Division of Minerals
Reclamation Section

June 1993

TD
428
.M56
L37
1993

NON-FERROUS MINE WASTE CHARACTERIZATION PROJECT

FINAL REPORT

JUNE 1993

Kim Lapakko

Minnesota Department of Natural Resources
Division of Minerals
Reclamation Section

TABLE OF CONTENTS

	PAGE
List of Tables	i
List of Figures	iii
List of Appendices	vi
0. Executive Summary	vii
1. Introduction	1
2. Objectives	1
3. Background: Mine Waste Dissolution	3
4. Methods	5
4.1. Materials	5
4.2. Procedures	7
4.2.1. Long Term Dissolution Experiment	7
4.2.2. Variable Mass Experiment	8
4.2.3. Variable Rinse Interval Experiment	10
4.2.4. Elevated Temperature Experiment	11
4.3. Calculations	12
5. Results and Discussion	13
5.1. Geology of Tailing Sample Sites	13
5.2. Long Term Dissolution Experiment	14
5.2.1. Introduction	14
5.2.2. Case 2 Sample (T9): Low NP, High APP	16
5.2.3. Case 3 Samples (T2, T6, T10): High NP, High APP	17
5.2.4. Rates of Sulfide Mineral Oxidation	18
5.2.5. Summary	22
5.3. Variable Mass Experiment	23
5.3.1. Introduction	23
5.3.2. Extent of Acid Neutralization by Carbonate Mineral Dissolution	24
5.3.3. Summary	27

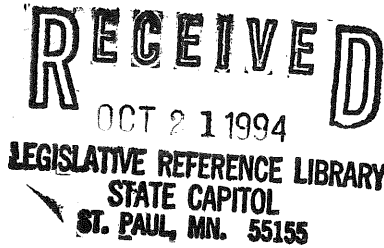


TABLE OF CONTENTS (continued)

	PAGE
5.4. Variable Rinse Interval Experiment	27
5.5. Elevated Temperature Experiment	29
5.5.1. Introduction	29
5.5.2. Temporal Variation of Drainage Quality	29
5.5.3. Rates of Sulfide Mineral Oxidation	31
5.5.4. Summary	32
6. Comparison with Field Drainage Quality	33
7. Treatment of Antimony, Arsenic, and Molybdenum	36
Acknowledgements	37
References	38

LIST OF TABLES

	PAGE
Table 1.	Particle size distribution of tailings. 41
Table 2.	Chemical analysis for regulatory parameters in nonferrous tailings samples. 42
Table 3.	Mineralogical composition of non-ferrous tailings. 43
Table 4.	Mineralogic Acid Production Potential and Neutralization Potential for tailings. 44
Table 5.	Variable Rinse Interval Experiment temperature and relative humidity summary statistics. 45
Table 6.	Percent depletion of APP and NP from Long Term Dissolution Experiment for weeks 0-151. 46
Table 7.	Rates of release for the Long Term Dissolution Experiment for weeks 0-151. 47
Table 8.	Total years of dissolution for depletion of neutralization potential and acid production potential. 48
Table 9.	Rates of release from weeks 20-57 from the Long Term Dissolution Experiment. 49
Table 10.	Specific surface area analysis (m^2/g) and percent recovery. 50
Table 11.	Oxidation rates expressed in terms of pyrite mass and surface area. 51
Table 12A.	Variable Mass Experiment: Acid neutralization by carbonate minerals based on regression data for $([Ca] + [Mg])$ vs. $[SO_4]$, all data. 52
Table 12B.	Variable Mass Experiment: Acid neutralization by carbonate minerals based on regression data for $([Ca] + [Mg])$ vs. $[SO_4]$, for sulfate values less than 1.0 mmole/L. 52
Table 12C.	Variable Mass Experiment: Acid neutralization by carbonate minerals based on regression data for $([Ca] + [Mg])$ vs. $[SO_4]$, for sulfate values less than 0.5 mmole/L. 53
Table 12D.	Variable Mass Experiment: Acid neutralization by carbonate minerals based on regression data for $([Ca] + [Mg])$ vs. $[SO_4]$, for sulfate values less than 0.25 mmole/L. 53

LIST OF TABLES (continued)

	PAGE
Table 13. Trends in pH, sulfate, calcium, magnesium, calcium plus magnesium, and alkalinity vs. oxidation interval.	54
Table 14. Percent APP released during the Elevated Temperature Experiment, weeks 0-48.	55
Table 15. Percent NP released during the Elevated Temperature Experiment, weeks 0-48.	56
Table 16. Comparison of percent APP and NP released in Elevated Temperature and Long Term Dissolution Experiments.	57
Table 17. Comparison of sulfate release rates between Elevated Temperature Experiment and overall rates in the Long Term Dissolution Experiment.	58
Table 18. Comparison of neutralization from the Elevated Temperature Experiment and the Long Term Dissolution Experiment.	59
Table 19. Summary of field vs. laboratory drainage quality data.	60
Table 20. Ratio of trace metal concentrations in the field to those in the laboratory. The upper ends of the observed ranges were used for calculation.	61

LIST OF FIGURES

	PAGE
Figure 1.	Long Term Dissolution Experiment reactor. 62
Figure 2.	Temperature and relative humidity for the Long Term Dissolution Experiment, weeks 0-151. 63
Figure 3.	Variable Mass Experiment reactor (top) and experimental apparatus (bottom). 64
Figure 4.	pH, sulfate, calcium, and magnesium concentrations vs. time for T9, reactor 17 from the Long Term Dissolution Experiment. 65
Figure 5.	Sulfate, calcium plus magnesium, calcium, and magnesium cumulative mass release vs. time for T9, reactor 17 from the Long Term Dissolution Experiment. 66
Figure 6.	Sulfate concentration vs. time for T2, T6, and T10 from the Long Term Dissolution Experiment. 67
Figure 7.	Calcium and magnesium concentrations vs. time for T2, T6, and T10 from the Long Term Dissolution Experiment. 68
Figure 8.	Long Term Dissolution Experiment depletion of APP and NP in 151 weeks. 69
Figure 9.	Rate of sulfate release vs. percent sulfide for the Long Term Dissolution Experiment (Solids T2, T6, T9, and T10), weeks 0-151. 70
Figure 10.	Rate of sulfate release vs. percent sulfide for all twelve solids, weeks 20-57. 71
Figure 11.	Rate of sulfate release vs. iron sulfide surface area for solids T1, T2, T4, T9, and T10. 72
Figure 11A.	T1 (flowsheet A sulfide concentrate). 73
Figure 11B.	T2 (flowsheet A sulfide concentrate). 73
Figure 11C.	T4 (flowsheet A sulfide concentrate). 74
Figure 11D.	T9 (flowsheet A sulfide concentrate). 74
Figure 11E.	T10 (flowsheet A sulfide concentrate). 75
Figure 11F.	T5 (flowsheet B (superpanner only) sulfide concentrate). 75

LIST OF FIGURES (continued)

	PAGE
Figure 12. Extent of acid neutralization as a function of iron sulfide mass (neutralization calculated as $2(\text{SO}_4)/(\text{Ca} + \text{Mg})$).	76
Figure 13. Rate of sulfate release vs. mass of iron sulfide in sample for the Variable Mass Experiment.	77
Figure 14. pH vs. oxidation interval box plots for the Variable Rinse Interval Experiment: T1, T2, and T3.	78
Figure 14 (cont.). pH vs. oxidation interval box plots for the Variable Rinse Interval Experiment: T4, T5, and T6.	79
Figure 14 (cont.). pH vs. oxidation interval box plots for the Variable Rinse Interval Experiment: T7, T8, and T9.	80
Figure 14 (cont.). pH vs. oxidation interval box plots for the Variable Rinse Interval Experiment: T10, T11, and T12.	81
Figure 15. Sulfate concentration vs. oxidation interval box plots for the Variable Rinse Interval Experiment: T1, T2, and T3.	82
Figure 15 (cont.). Sulfate concentration vs. oxidation interval box plots for the Variable Rinse Interval Experiment: T4, T5, and T6.	83
Figure 15 (cont.). Sulfate concentration vs. oxidation interval box plots for the Variable Rinse Interval Experiment: T7, T8, and T9.	84
Figure 15 (cont.). Sulfate concentration vs. oxidation interval box plots for the Variable Rinse Interval Experiment: T10, T11, and T12.	85
Figure 16. Calcium and magnesium concentrations vs. oxidation interval box plots for the Variable Rinse Interval Experiment: T1, T2, and T3.	86
Figure 16 (cont.). Calcium and magnesium concentrations vs. oxidation interval box plots for the Variable Rinse Interval Experiment: T4, T5, and T6.	87
Figure 16 (cont.). Calcium and magnesium concentrations vs. oxidation interval box plots for the Variable Rinse Interval Experiment: T7, T8, and T9.	88
Figure 16 (cont.). Calcium and magnesium concentrations vs. oxidation interval box plots for the Variable Rinse Interval Experiment: T10, T11, and T12.	89

LIST OF FIGURES (continued)

	PAGE
Figure 17. Alkalinity vs. oxidation interval box plots for the Variable Rinse Interval Experiment: T1, T2, and T3.	90
Figure 17 (cont.). Alkalinity vs. oxidation interval box plots for the Variable Rinse Interval Experiment: T4, T5, and T6.	91
Figure 17 (cont.). Alkalinity vs. oxidation interval box plots for the Variable Rinse Interval Experiment: T7, T8, and T9.	92
Figure 17 (cont.). Alkalinity vs. oxidation interval box plots for the Variable Rinse Interval Experiment: T10, T11, and T12.	93
Figure 18. pH, sulfate, calcium, and magnesium concentrations vs. time for T1 (reactors 3 and 4) from the Elevated Temperature Experiment.	94
Figure 19. pH, sulfate, calcium, and magnesium concentrations vs. time for T9 (reactors 9 and 10) from the Elevated Temperature Experiment.	95
Figure 20. Cumulative mass release vs. time for the Elevated Temperature Experiment, weeks 2-48: Solid T9, reactor 10.	96
Figure 21. pH, sulfate, calcium, and magnesium concentrations vs. time for the Elevated Temperature Experiment: Solid T9, reactor 10.	97
Figure 22. Treatment system designs for arsenic removal from tailings water at the Giant and Con mines.	98

LIST OF APPENDICES

Separate Volume

- Appendix A: Tailings Characterization: Particle Size, Chemistry, Mineralogy, and Degree of Liberation
- Appendix B: Long Term Dissolution Experiment
- Appendix C: Variable Mass Experiment
- Appendix D: Variable Rinse Interval Experiment
- Appendix E: Elevated Temperature Experiment
- Appendix F: Short Rinse Interval Experiment
- Appendix G: Elevated Temperature at One Week Interval Experiment
- Appendix H: Iron Sulfide Mineral Characterization: Chemistry, Mineralogy, and Specific Surface Area
- Appendix I: Field Drainage Water Quality Data
- Appendix J: Trace Metal Treatment: Arsenic, Antimony, and Molybdenum

0. EXECUTIVE SUMMARY

The present report is the second phase of a two phase study. In the first phase, ten tailings samples from operating North American gold mines and two titanium tailings generated in pilot plant tests were characterized and subjected to dissolution testing for 52 weeks to examine the relationship between the solid-phase characteristics and drainage quality (Lapakko, 1991). In addressing the objectives of the present study, the following conclusions were made.

1. The tailings collected for this study provide the best presently available approximation of tailings which might be generated if present exploration led to development of a greenstone belt exploration site in Minnesota. The geologic settings from which the gold mine tailings were collected are similar to 73 percent of those presently under exploration in Minnesota. More precise description of tailings composition will be possible only when a mine site in Minnesota is specified and the associated rock samples are available. (For details see report section 5.1.)

The potentially problematic components of these tailings, with respect to water quality impacts, are iron sulfides and trace metal sulfides. The oxidation of iron sulfide minerals leads to acid production, and the oxidation of trace metal sulfides releases trace metals. Calcium carbonate and magnesium carbonate are present in the tailings to neutralize some, or all, of the acid produced as a result of iron sulfide oxidation.

In most of the tailings the amount of these carbonates present is adequate to neutralize the acid produced by the iron sulfides present. One of the tailings samples produced acidic drainage in the laboratory tests at room temperature, and the remaining samples produced drainage of slightly basic pH. Antimony, arsenic, and molybdenum, when occurring in the tailings in elevated concentrations as sulfide minerals, present the greatest potential impact with non-acidic drainages. These metals are released readily from the sulfide minerals, and are soluble in the circumneutral pH range. The two titanium tailings examined present virtually no potential for acid production, due to their minimal sulfide content, and contain only a small amount of metals which will be released under environmental conditions.

2. The quality of drainage generated in short term dissolution experiments may not accurately reflect the drainage quality generated by mine wastes in the many years after abandonment. All of the gold tailings samples produced alkaline drainage during the initial 52 weeks of dissolution, suggesting that the tailings would not produce acidic drainage. Based on solid-phase composition, four of the tailings samples have the potential to produce acidic drainage. Dissolution of these four samples was continued beyond the initial 52-week experiment to obtain a total duration of 151 weeks.

The pH of drainage from one sample (T9) dropped below 6.0 after 122 weeks of dissolution and reached 3.45 after 151 weeks. The three remaining samples continued to produce alkaline drainage throughout the 151 weeks of the Long Term Dissolution Experiment. Based on the composition of these three samples and their rates of dissolution, their drainage could become acidic after six to fourteen years of dissolution. However, this estimation required assumptions which lend considerable uncertainty to the prediction, and more accurate estimation requires additional information on the formation of coatings on the surfaces of sulfide and carbonate minerals present in the mine waste. At present the dissolution behavior of such samples over the long term of interest for abandoned mine waste, can be accurately assessed only by extended dissolution studies. Conducting such studies at a larger scale and under field conditions will further increase their accuracy. (For details see section 5.2.)

3. The surface area of pyrite present in the samples was the critical variable controlling the rate of pyrite oxidation and the attendant acid production. This conclusion is somewhat qualitative since it was not possible to separate all of the pyrite from the tailings samples. Thus the analyses for surface area, as well as those for chemistry, mineralogy, and mineral surface characteristics, were conducted on only twenty to seventy five percent of the iron sulfides present in the tailings samples. Nonetheless, there was no apparent evidence suggesting that something other than the pyrite surface area controlled the rates of pyrite oxidation in the samples examined. Pyrrhotite was present in some of the samples but no extensive analyses were conducted on this mineral and its oxidation rate. (For details see section 5.2.4.)
4. The laboratory drainage quality provided a good indicator of potential for elevated concentrations of antimony, arsenic, copper, lead, molybdenum, nickel, and zinc in the field. Trace metal concentrations in laboratory tests should not be expected to quantify concentrations in the field, but rather provide an indication of whether or not a metal will be released to produce concentrations of concern. However, in fourteen of the twenty-five cases available for comparison, the laboratory concentrations ranged from 20 to 100 percent of the field concentrations. The best quantitative agreement between laboratory and field concentrations was observed for arsenic, molybdenum, and zinc. (For details see section 6.)
5. The addition of ferric chloride is presently used at three Canadian mining operations to remove arsenic, antimony, and/or molybdenum from waters associated with gold tailings. Elevated release of these metals from some of the gold tailings samples was observed in the initial phase of this study. These metals were readily released from the sulfide minerals in which they occurred and were observed at elevated concentrations in slightly basic pH drainages. These metals occur as negatively charged complexes and are not readily removed by methods used for treatment of other trace metals. The ferric chloride treatment may be necessary for tailings

containing sulfides of arsenic, antimony, or molybdenum even at levels of 0.1 percent or less. (For details see section 7.)

6. The mass of mine waste used in laboratory predictive tests affects the extent of acid neutralization by dissolution of calcium and magnesium carbonate minerals present in the waste. This relationship must be considered in the design of predictive tests and the interpretation of their results. Using too small of a mass may underestimate the ability of a mine waste to neutralize acid. Similarly, using too large of a mass may overestimate the ability of a mine waste to neutralize acid. (For details see section 5.3.)
7. The rinse interval used in laboratory tests had only a slight influence on drainage quality and did not suggest extending the rinse interval length beyond the one-week period commonly used for predictive tests. The apparent rate of sulfide mineral oxidation decreased as the rinse interval duration increased beyond one week. Consequently, the use of rinse intervals longer than one week would increase the time required for mine waste drainage quality predictive tests. (For details see section 5.4.)
8. The rate of oxidation of iron sulfide minerals at 97°C was six to nine times that at 25°C. Consequently, the rate of acid production at the higher temperature was also six to nine times that at the lower temperature. The more rapid rate of acid production, in turn, accelerated the rate of calcium and magnesium carbonate dissolution.

The accelerated dissolution of mine wastes at high temperatures indicates that such testing may predict the quality of drainage from mine wastes much more rapidly than predictive tests run at room temperature. For example, eight weeks of testing at 97°C were required to identify sample T9 as an acid producer, while 122 weeks were required at room temperature. Results for four of the remaining six samples subjected to the high temperature dissolution were also consistent with those at room temperature.

However, results from the remaining two samples were difficult to interpret. The unusual oscillation of drainage pH from these samples indicated that caution must be exercised when interpreting the results from this type of testing. The elevated temperatures are not typical of field conditions and the quality of drainage generated in this test may not in general simulate that in the environment. Additional study is required to determine the accuracy of this technique as a predictive tool.

1. INTRODUCTION

Exploration for gold, titanium, and other non-ferrous minerals is presently occurring in Minnesota. If an economic deposit is discovered, the mine wastes must be characterized and the mine waste drainage quality must be projected prior to mine development. This information will be used to identify the types of water quality control required to protect the water resources of the state. Since there is presently no mining of base or precious metals in Minnesota there is little information available on the characteristics of, or drainage quality from, such mining wastes. The lack of such information will inhibit the effectiveness and efficiency of drainage quality prediction, as well as the environmental review and permitting processes.

There is little debate that pre-operational prediction of mine waste drainage quality in order to ensure protection of water resources is conceptually sound. Such prediction is, however, a relatively new field of study. It is recognized that mine waste drainage quality is largely determined by mine waste composition. Whether or not drainage from tailings will be acidic can be predicted with a high degree of certainty if the tailings exhibit a large compositional imbalance of acid-producing minerals relative to acid-neutralizing minerals. However for tailings in general, prediction of the drainage quality of tailings based on their composition is more tenuous. Similarly, laboratory dissolution tests can readily simulate the acidic nature of drainage from tailings which contain an abundance of acid-producing minerals relative to acid-neutralizing minerals. In general, however, there is substantial uncertainty in the design of laboratory dissolution tests, as well as interpretation of their results, to predict the quality of drainage from tailings after a mine has been abandoned.

In the initial phase of this study twelve non-ferrous tailings were collected, characterized (particle size, chemistry, mineralogy, static tests), and subjected to dissolution in a 57-week laboratory experiment (Lapakko, 1991). Although the drainage from all of the tailings was in the neutral to basic range, solid phase analyses and static tests indicated two of the samples had potential to produce acidic (T9, T2) and two others had marginal potential for producing acidic drainage (T6, T10). Elevated concentrations of arsenic, antimony, and molybdenum were observed in drainage from some of the samples. Research needs identified in the initial phase included examination of the geology of the mines from which tailings were collected, additional dissolution testing of tailings identified as potential acid-producers, additional analysis of the tailings, and comparison of drainage quality in the laboratory with that in the field.

2. OBJECTIVES

The objectives of this project were established based on previous investigation of these tailings (Lapakko, 1991) and to examine the effects of dissolution test design on drainage quality generated in the test. The information on the relationship between solid phase characteristics of mine wastes and drainage quality is limited. Increasing the available data on this relationship will improve the ability to predict, prior to operation, the quality of drainage from mine wastes of similar composition.

A more thorough understanding of laboratory dissolution test procedures will also benefit the prediction of mine waste drainage quality. Laboratory dissolution tests are commonly applied tools for mine waste drainage quality prediction (as are static tests which base drainage quality on solid phase characteristics). Little investigation has been conducted on dissolution test experimental design variables, which typically have been established arbitrarily or based on practical convenience. Determination of the influence of design variables on test results will allow better dissolution test design, as well as more meaningful interpretation of test results.

The objectives of this project were as follows.

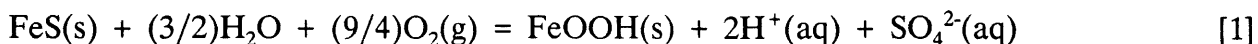
1. Compare the geologic settings from which the tailings were collected to those of non-ferrous exploration sites in Minnesota.
2. Determine the long term drainage quality of tailings which, based on solid phase composition, have the potential to produce acidic drainage. More specifically, describe the temporal variation of drainage quality, as well as rates of sulfide mineral oxidation and carbonate mineral dissolution over an extended period of time.
3. Examine the composition of pyrite present in the samples to determine compositional variables which may influence the rate of pyrite oxidation.
4. Compare the quality of drainage observed in the laboratory with that observed in the field.
5. Survey existing methods for removing arsenic, antimony, and molybdenum from mine waste drainage.
6. Describe the effect of the mass of tailings used in predictive tests on the extent of acid neutralization by dissolution of calcium carbonate and magnesium carbonate. (This objective was not included in the initial project proposal.)
7. Describe the effect of the rinse interval length used for predictive tests on the relative rates of sulfide mineral oxidation and dissolution of calcium carbonate and magnesium carbonate.
8. Describe the effect of elevated temperature on the rate of oxidation of iron sulfide minerals and the dissolution of calcium carbonate and magnesium carbonate minerals.

Previous laboratory dissolution tests identified the needs addressed by objectives one through five. These objectives specifically address the drainage quality of the gold tailings examined and mitigation of drainage quality impacts. Objectives six through eight were established in response to the need for accurate and efficient tests for predicting mine waste drainage quality.

3. BACKGROUND: MINE WASTE DISSOLUTION

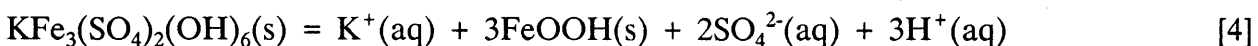
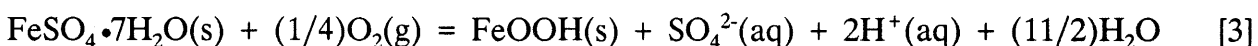
Prior to developing a base or precious metal resource, it is necessary to predict the quality of drainage which will be generated by the mining wastes. The generation of acidic drainage by mine wastes is the primary water quality concern associated with base and precious metal mining. In addition to high acidity, these drainages typically have elevated concentrations of the leachable trace metals present in the mine waste. Either condition can be toxic to aquatic organisms. The release of trace metals in neutral drainage is a secondary concern.

Iron sulfide minerals, trace metal sulfide minerals, as well as calcium carbonate and magnesium carbonate minerals, play a dominant role in the release of acid and trace metals from mine wastes. Acid is produced as a result of the oxidation of iron sulfide minerals present in mine waste, as indicated by reaction 1 (Nelson, 1978) and reaction 2 (Sung and

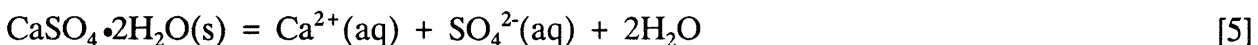


Morgan, 1980). Acid (H^+) and sulfate are released to solution in a molar ratio of 2:1. Oxidation of trace metal sulfide minerals will lead to acid production if, and only if, the trace metal released from the sulfide mineral subsequently precipitates as a metal oxide, hydroxide, or carbonate (or some combination thereof).

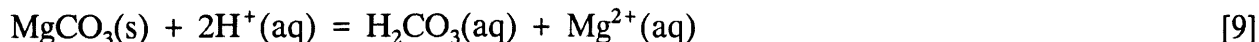
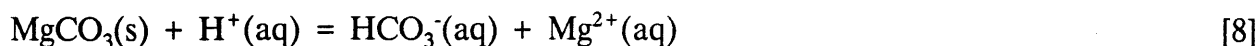
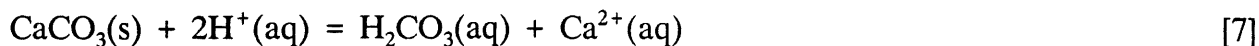
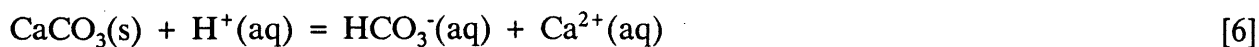
Dissolution of sulfate minerals such as melanterite and jarosite will also produce acid (reactions 3 and 4, respectively). It should be noted that the solubility of jarosite is slight,



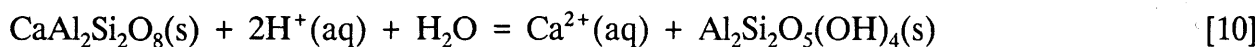
except at low pH. As was the case for the sulfide minerals, the dissolution of melanterite yields two moles of acid per mole of sulfate dissolved. In contrast, the dissolution of jarosite yields 1.5 moles of acid per mole of sulfate dissolved. The dissolution of sulfate minerals such as gypsum (reaction 5, Stumm and Morgan, 1981), anhydrite (CaSO_4), or barite (BaSO_4) will not produce acid.



The most effective minerals for neutralizing (consuming, buffering) acid are those containing calcium carbonate and magnesium carbonate, examples of which are calcite, magnesite, dolomite, and ankerite (CaCO_3), MgCO_3 , $\text{CaMg}(\text{CO}_3)_2$, $\text{CaFe}(\text{CO}_3)_2$, respectively). Dissolution of calcium and magnesium carbonate components neutralizes acid (reactions 6-9). Reactions 6 and 8 are dominant above approximately pH 6.3, while reactions 7 and 9

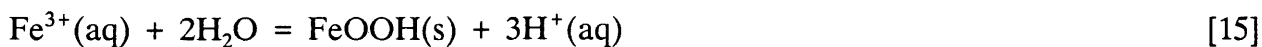
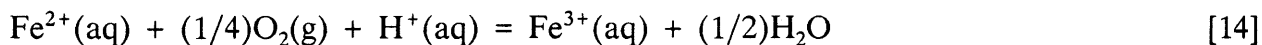
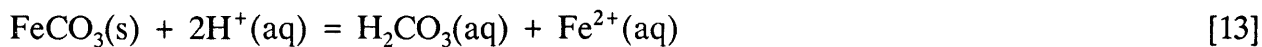
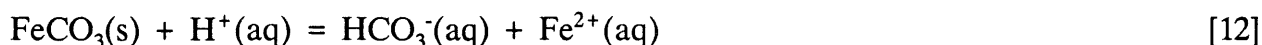


are dominant below this pH. Dissolution of minerals such as anorthite (reaction 10, Busenberg and Clemency, 1976) and forsterite (reaction 11, Hem, 1970) can also neutralize



acid, but their dissolution rate (and associated rate of acid neutralization) is very slow in the neutral pH range. These minerals dissolve more rapidly as pH decreases and, therefore provide more acid neutralization under acidic conditions.

Iron carbonates will provide no net neutralization of acid. The initial dissolution of one mole of iron carbonate will neutralize one or two moles of acid (reactions 12, 13). However, under environmental conditions the one mole of ferrous iron released will oxidize to ferric iron (reaction 14) which will precipitate as ferric oxyhydroxide (reaction 15). The oxidation of ferrous iron is slower than the subsequent ferric oxyhydroxide precipitation, and is reported to be second-order with respect to OH^- concentration (Sung and Morgan, 1980, Eary and Schramke, 1990). The oxidation and precipitation reaction will yield two moles of acid (reaction 16). Thus, iron carbonate will not contribute to acid neutralization.



4. METHODS

4.1. Materials

The methods of sample collection and analysis are presented in Lapakko (1991). The data on particle size distribution, chemistry, mineralogy, and static results are presented in tables 1, 2, 3, and 4 respectively. Additional compositional data collected in the previous phase of this study are presented in appendix A.

Additional analyses were conducted in the present study to more accurately characterize the pyrite present in some of the tailings. In the initial phase of this study it was reported that factors other than sulfur content influenced the rate of sulfate release from the tailings (Lapakko, 1991). In particular the sulfate release rate from sample T10 (3.89 percent sulfide) was higher than expected based on data from the samples examined, while the rates for samples T5 (0.66 percent sulfide) and T9 (3.64 percent sulfide) were lower than expected. The dominant sulfide in these samples was pyrite. The analyses conducted were directed at determining the aspects of pyrite composition which influenced the rates of pyrite oxidation. Additional detail on the analytical methods and results is presented in appendix H.

In order to determine other variables which influenced the oxidation rate of pyrite, analyses were conducted to characterize the specific surface area and composition of the sulfide minerals present in the tailings. Financial resources were not available to analyze all solids. In addition to samples T9 and T10, samples T1, T2, and T4 were selected for analysis since a) pyrite was the dominant sulfide mineral present, b) the relationship between the sulfate release rate and sulfur content was consistent with that for the majority of the samples (that is, these samples behaved in a "normal" manner), c) an adequate amount of sample was available, and d) the samples provided a range of sulfur contents. The mass of sample T5 remaining was limited and this sample was subjected to a less rigorous examination. A few of the sulfide grains were separated using a Haultain Superpanner (Infrasizers Ltd.) and were examined using a scanning electron microscope.

The sulfide minerals were separated using a Haultain Superpanner followed by a heavy liquid separation. To track the sulfide minerals in the separation processes, the tailings, the low-density (non-sulfide) fraction, and the sulfide-rich concentrate were analyzed for sulfur and sulfate, and the water used in the Superpanner was analyzed for sulfate. Four splits of the sulfide concentrate were taken for analyses of specific surface area, chemistry, mineralogy, and surface characteristics. An additional split of the T9 concentrate was leached for 60 minutes at room temperature in 6N HCl (procedure recommended by Ron Nicholson, University of Waterloo). The mixture was stirred manually upon addition and after 30 minutes of contact. The objective of this leach was to remove any iron oxyhydroxide coatings from the sulfide mineral surface. This sample was submitted for surface area determination only and the HCl was analyzed for sulfate and iron.

The surface area was analyzed using the BET nitrogen adsorption technique by Eyasu Mekonnen at the Soil Science Department at the University of Minnesota. The remaining analyses were conducted at Midland Research under the direction of Louis Mattson. Solids were analyzed for sulfur content using a LECO furnace. To determine sulfate present in the tailings were leached with a weak HCl solution and the leachate was analyzed for sulfate by ICP (Analytical Research Laboratory Model 3410). Trace metals were analyzed by digesting solid samples with aqua regia (a mixture of nitric and hydrochloric acid) and analyzing the digestate by ICP. The mineral composition was determined by using a "best fit" between chemical analyses and x-ray diffraction data (XRD instrument by Phillips). The sulfide mineral surfaces were examined using scanning electron microscope (Amray model 1200B). The composition of individual mineral grains examined by SEM was determined using an energy dispersive spectrometer (Noran Instruments model 2010). The photomicrographs produced by the SEM were used to estimate the average grain size. The grains which were mostly unobstructed were measured and those values averaged. For elongate grains, an intermediate value between the long and short dimension was determined (see appendix H).

A second split of samples T9 and T10 was separated using two consecutive heavy liquid separations. This method is more efficient than the Superpanner method for recovering sulfide minerals and is also more expensive. To track the sulfide minerals in the separation processes, the tailings, the low-density (non-sulfide) fraction, and the sulfide concentrate were analyzed for sulfur and sulfate. Five splits of the sulfide concentrates were taken for analyses of specific surface area, chemistry, mineralogy, and surface characteristics. The fifth split was leached for 60 minutes at room temperature in 6N HCl using the procedure described above. The HCl was analyzed for sulfate and iron. The objective of this leach was to remove any iron oxyhydroxide coatings from the sulfide mineral surface. This sample was submitted for surface area determination only. The methods of analysis were the same as those used for the Superpanner-heavy liquid separation.

The sulfide recoveries using the Superpanner-heavy liquid separation were quite low, ranging from 19 to 59 percent of the sulfide in the tailings. With the exception of T9, iron sulfides comprised 85 to 97 percent of the concentrate. Pyrite was by far the predominant iron sulfide present in the concentrates, although the pyrrhotite content of T4 was higher than anticipated based on analysis of the T4 tailings (appendix A). The analysis of the concentrate is assumed to be more accurate than the previous analysis of the tailings sample as a whole. The T9 concentrate contained about 56 percent barite, and siderite (about 12 percent) was present as a contaminant in the T10 concentrate.

The sulfur recovery using two heavy liquid separations on T9 and T10 was considerably higher at 72 percent. The mineralogical composition of the T9 and T10 concentrates was not affected by the method of separation. The increased recovery for the two heavy liquid separations was apparently the due to improved recovery of finer grained tailings.

SEM analysis of the sulfide concentrates indicated that the sulfide grain size decreased in the order T1 (210 μm) \gg T5 (48 μm) > T9 (32 μm) > T10 (27 μm) \approx T2 (25 μm) > T4 (15 μm). Although most of the pyrite grains present were smooth, some of the grain surfaces were irregular. The greatest extent of surface irregularity was observed for the pyrite present in sample T10, in which about one third of the pyrite grains were rough-textured. About 15 to 20 percent of the pyrite present in sample T1 was rough-texture and/or porous, and a few rough-textured grains were observed in sample T2. The remaining pyrite in these and other samples had relatively smooth surfaces. The T4 concentrate was finer than the others and contained more pyrrhotite than indicated by previous analyses. The surfaces of the pyrrhotite grains were reported to be more irregular and rougher than the smooth pyrite grains present in this sample.

The specific surface areas of the sulfide concentrates obtained from the Superpanner-heavy liquid separation ranged from 0.144 to 1.18 m^2/g . The specific surface area of sample T1 was unusually high, which is difficult to explain. Previous particle size distribution analysis indicated this sample was the coarsest of those examined, and examination of the sample under binocular microscope (American Optical, Spencer model, 60X to 120X) and by SEM verified this conclusion. Apparently the rough-textured and/or porous surfaces detected by SEM for 15 to 20 percent of the pyrite grains contributed to the elevated specific surface area.

The specific surface areas of the T9 and T10 concentrates obtained from the two heavy liquid separations were, respectively, 1.75 and 2.75 times the corresponding values for the Superpanner concentrate. Leaching the T9 and T10 samples with HCl decreased the specific surface area by 20 to 75 percent, with the largest decrease observed for sample T10. The decreases were apparently due to the dissolution of some of the finer grained particles present.

4.2. Procedures

4.2.1. Long Term Dissolution Experiment

Duplicate samples of all twelve tailings (T1 through T12) were subjected to the Long Term Dissolution Experiment, which began on 6 June 1990 (week 0). All samples were terminated after 57 weeks except for T2, T6, T9, and T10, for which single reactors were continued through week 151 (28 April 1993). In this experiment, a 75 g sample of unmodified tailings (i.e. as received) was placed into the upper segment, or reactor, of a two-stage filter unit (figure 1). On week 0, all samples were rinsed with 200 mL of distilled-deionized water, to remove products which accumulated from oxidation during sample storage. The distilled water was added slowly with a burette, to minimize disturbance of the solids, and allowed to drain overnight through the mine waste sample. This rinsing was repeated weekly throughout the course of the experiment.

Between rinses the solids were retained in the reactors and stored for further oxidation within individual compartments in a box. A thermostatically controlled heating pad was placed beneath the box to control temperature. The box was stored in a small room equipped with an automatic humidifier and dehumidifier, to maintain a stable range of humidity. During the 151-week experiment temperature and relative humidity were monitored a total of 538 times, typically three to four times a week, using a Taylor wet-bulb/dry-bulb hygrometer. The average weekly temperatures ranged from 21.7 to 29.0 °C, with an average of 25.8°C and a standard deviation of 1.5°C (n=148). The average weekly relative humidities ranged from 42 to 80%, with an average of 54% and a standard deviation of 6.7% (n=148, see also figure 2 and appendix B).

The volume of rinse water, or drainage, was determined by weighing the lower stage (receiving flask) of the reactor. pH and specific conductance were analyzed directly in the lower stage of the reactor, after which a 20 mL sample was taken for analysis of alkalinity (if pH exceeded 6.30) or acidity. The remaining sample was then filtered for subsequent analysis of metals and sulfate. Samples taken for metal analyses were acidified with 0.2 mL AR Select nitric acid (Mallinckrodt) per 50 mL sample.

An Orion SA 720 pH meter equipped with a Ross combination pH electrode (8165) was used for pH analysis, and a Myron L EP conductivity meter was used to determine specific conductance. Alkalinity and acidity were analyzed using standard titration techniques (APHA et al., 1992). Sulfate was analyzed using an HF Scientific DRT-100 nephelometer for the barium sulfate turbidimetric method (APHA et al., 1992). Metals samples collected through week 51 were analyzed by Bondar Clegg (Ottawa, Ontario) using ICP. Subsequent metal samples were analyzed for calcium and magnesium only using a Perkin Elmer 603 atomic absorption spectrophotometer in the flame mode.

4.2.2. Variable Mass Experiment

Samples T2, T4, and T10 were subjected to the Variable Mass Test, which was conducted from 5 March 1992 to 19 November 1992 (week 0 to week 37). Masses of 225, 375, 750, 1125, and 1500 g of each sample were used. The solids were placed onto a Whatman GF/A microfibre filter, which rested on the perforated support in the upper section of a two-piece polypropylene Buchner funnel. The upper section of the funnel is referred to as the reactor in this experiment (figure 2). A 110-mm diameter funnel was used for the 225g and 375g masses, and a 150-mm diameter funnel was used for the 750g, 1125g, and 1500g masses.

Prior to the experiment each solid was rinsed with varying amounts of distilled-deionized water to remove soluble calcium, magnesium, and sulfate from the solids. For rinsing the reactors and the lower section of the two-piece funnel were assembled and placed into a rack. A sample bottle was placed beneath the rack for drainage collection (figure 2). The number of rinses for T2, T4, and T10 were 17, 9, and 12, respectively. The volume used for each rinse ranged from 275 mL for the 225 g samples to 925 mL for the 1500 g samples. The volume of drainage was determined and the drainage samples were analyzed for pH,

alkalinity, specific conductance, sulfate, calcium, magnesium, sodium, and potassium (appendix C).

Following the initial rinses, the samples were rinsed weekly for 37 weeks. At times, surface cracks were observed and were smoothed over to reduce the potential for preferential flow. Distilled water was added slowly from a graduated cylinder to each reactor and allowed to drain overnight through the tailings sample. The volume of water added to the samples was selected to produce a target drainage volume. The target drainage volumes for T2, T4, and T10 were 155, 163, and 167 mL, respectively. These were the average drainage volumes from the respective 75-g samples during the first 52 weeks of the Long Term Dissolution Experiment. This volume was chosen to facilitate comparison of the quality of drainage from the larger masses with that from the 75 gram sample.

Between rinses the solids were retained in the reactors and stored on a thermostatically controlled heating pad to further oxidize (figure 2). The reactors were stored on three shelves in a small room equipped with an automatic humidifier and dehumidifier, to maintain a stable range of humidity. Temperature and relative humidity for each shelf were determined with a Taylor wet-bulb/dry-bulb hygrometer two to three times a week. The temperature and relative humidity did not vary greatly among the shelves. The average temperatures for the bottom, middle, and top shelves were 23.5°C, 23.8°C, and 23.5°C, respectively. The corresponding relative humidities were 53.6%, 53.6%, and 55.1%, respectively. Additional data on the temperature and relative humidity during the experiment are presented in appendix C.

The volume of rinse water, or drainage, was determined by weighing the sample bottle into which the tailings drained. pH and specific conductance were analyzed directly in the bottle, after which a 20 mL sample was taken for analysis of alkalinity (if pH exceeded 6.30) or acidity. The remaining sample was then filtered for subsequent analysis of metals and sulfate. Samples taken for metal analyses were acidified with 0.2 mL AR Select nitric acid (Mallinckrodt) per 50 mL sample.

Following the experiment all samples were rinsed five times (1, 2, 3, 4, and 7 December 1992). The volume of drainage from each reactor was determined and the drainage samples were analyzed for pH, alkalinity, specific conductance, and sulfate. The objective of these analyses was to assess the extent of oxidation products retained on the tailings. The data for these rinses are presented in appendix C.

An Orion SA 720 pH meter equipped with a Ross combination pH electrode (8165) was used for pH analysis, and a Myron L EP conductivity meter was used to determine specific conductance. Alkalinity and acidity were analyzed using standard titration techniques (APHA et al., 1992). Sulfate was analyzed using an HF Scientific DRT-100 nephelometer for the barium sulfate turbidimetric method (APHA et al., 1992). Metal samples were analyzed for calcium and magnesium using a Perkin Elmer 603 atomic absorption spectrophotometer in the flame mode.

4.2.3. Variable Rinse Interval Experiment

The reactors terminated at week 57 of the Long Term Dissolution Experiment were used in the Variable Rinse Experiment. As a result, week 0 for this experiment was 10 July 1991. Two reactors were available for samples T1, T3, T4, T5, T7, T8, T11, and T12, since both of the duplicate reactors containing these samples were terminated after 57 weeks of the Long Term Dissolution Experiment. Only one reactor was available for each of samples T2, T6, T9, and T10, since one of the reactors remained in use for the Long Term Dissolution Experiment. The sample mass, experimental apparatus, as well as methods of rinse water addition and sample collection were the same as those described for the Long Term Dissolution Experiment.

For each of the twelve tailings samples, one reactor was subjected to seven rinses at an interval of five weeks followed by seven rinses at an interval of seven weeks. The last rinse for these samples was on 17 February 1993. The second reactors for samples T1, T3, T4, T5, T7, T8, T11, and T12 were rinsed seven times at an interval of three weeks followed by seven rinses at an interval of ten weeks. The last rinse for these reactors occurred on 7 April 1993. All reactors were rinsed with 200-mL of distilled-deionized water at the designated interval. No duplicate reactors were run. To describe the one-week rinse interval data were used from weeks 58 to 151 of the Long Term Dissolution Experiment (samples T2, T6, T9, T10) and weeks 30 to 57 from the previous phase of this project (samples T1, T3, T4, T5, T7, T8, T11, T12).

Between rinses the solids were retained in the reactors and stored for further oxidation within individual compartments in a box. A thermostatically controlled heating pad was placed beneath the box to control temperature. The box was stored in a small room equipped with an automatic humidifier and dehumidifier to maintain a stable range of humidity. Temperature and relative humidity were typically monitored three to four times a week using a Taylor wet-bulb/dry-bulb hygrometer. For the various rinse intervals, the average temperature ranged from 25 to 26°C and the average relative humidity ranged from 51 to 57 percent (table 5, with additional detail in appendix D).

Other than the use of a Perkin Elmer atomic absorption spectrophotometer in the flame mode for all metals analyses, analytical methods were the same as those for the Long Term Dissolution Test.

A brief experiment was conducted near the end of the project to examine the rate of sulfate release at rinse intervals shorter than one week. A 75 g sample of T2 was subjected to rinse intervals of 6, 24, and 86 hours. A 75 g sample of Duluth Complex rock (1.64 percent sulfur) was also subjected to these rinse intervals. Both solids were subjected to extensive rinsing with distilled water prior to the experiment, to remove oxidation products from the surfaces of the solids.

The solids were retained in the same type of reactor described above, and a timer-activated peristaltic pump was used to provide the rinse water. The volume of rinse water added was approximated to produce a drainage volume equal to that produced when the rinse interval was one week. Since this experiment was conducted near the end of the project, analysis of the data generated was limited.

4.2.4. Elevated Temperature Experiment

The Elevated Temperature Test was a modification of a procedure called the Soxhlet Extraction Test (Renton 1983; Renton et al. 1985, 1988). Duplicate reactors were used for all tailings except for T2 and T10, for which triplicate reactors were used. 75 g samples of each tailing were placed onto a Whatman GF/A glass microfibre filter which rested on the perforated plate in the upper segment of a two-piece polypropylene Buchner funnel. Prior to the inception of the experiment all samples were rinsed with three 200-mL volumes of distilled-deionized water, to remove products accumulated from oxidation during sample storage. The distilled water was added slowly from a graduated cylinder, to minimize disturbance of the solids. For each reactor, all preliminary rinse samples were analyzed for pH, alkalinity/acidity, and specific conductance. Two of the three preliminary rinse samples from each reactor were analyzed for sulfate, calcium, and magnesium (appendix E).

The solids were retained in the reactors and, beginning 19 February 1992, stored between rinses in a Thelco Precision Scientific oven. Temperature in the oven ranged from 93.4 to 101°C, with an average of 96.7°C and a standard deviation of 1.8°C (n=25, additional detail in appendix E). Prior to the first rinse, it was recognized that some of the solids had consolidated. This consolidation resulted in the formation of cracks in the solids bed, which was only about 1.5-cm deep. It was clear that these cracks would have resulted in preferential flow through the solids. To improve flow through the bed and the resultant removal of reaction products, the solids were gently mixed with a stainless steel spatula then leveled prior to rinsing. To maintain uniformity in the methods, this procedure was applied to all solids, regardless of observed cracks.

The solids were rinsed every two weeks for 48 weeks. To each reactor 200 mL of distilled-deionized water, heated to 85°C, was added from a graduated cylinder and allowed to drain overnight through the tailings sample into a 500-mL sample bottle. This procedure was repeated on the following day. The third reactor used for samples T2 and T10 and rinsed with water at room temperature (reactors 16 and 13, respectively). The experiment was terminated after 48 weeks (6 January 1993).

For both of the bi-weekly drainage samples, the volume of drainage was determined by weighing the sample bottle, and pH and specific conductance were determined directly in the sample bottle. The two samples were composited and a 20 mL sample was taken for analysis of alkalinity (if pH exceeded 6.30) or acidity. The remaining sample was then filtered for subsequent determinations of sulfate, calcium, and magnesium. Samples for analysis of calcium and magnesium were acidified with 0.2 mL AR Select nitric acid

(Mallinckrodt) per 50 mL sample. The analytical methods were the same as those used for the Variable Rinse Interval Experiment.

For 16 weeks after the Elevated Temperature Experiment (through 28 April) the solids were rinsed weekly to determine the influence of this procedural modification. The third reactors containing T2 and T10 were rinsed with a single 200-mL volume of heated water in this phase of the experiment. This experiment was conducted near the end of the project and limited data analyses were conducted.

4.3. Calculations

The mass of sulfate release was calculated as the product of the observed concentration and the drainage volume. Some samples were not analyzed for sulfate. The sulfate concentration for these samples was estimated as the average of the previous and subsequent analyses.

Cumulative sulfate release was plotted as a function of time for each reactor. Periods of linear release were selected based on visual examination of the graphs produced, and the release rate for each period was determined by linear regression. For some of the reactors the sulfate release in the initial weeks was inconsistent with that observed over the experiments as a whole. Consequently, the initial period was often omitted from calculations of sulfate release. The "average" rate of release was calculated by conducting linear regression on all data after this initial period.

The masses of calcium and magnesium release were calculated in the same manner as the sulfate mass release. The rates of release for these parameters were calculated for the same time periods as the sulfate release rates. The method used for rate calculation was the same as that used for sulfate release rates. The molar mass releases, as well as mass release rates, of calcium and magnesium were at times summed to represent the dissolution of calcium and magnesium carbonate minerals.

5. RESULTS AND DISCUSSION

5.1. Geology of Tailings Sample Sites

There has been virtually no mining of base or precious metals in Minnesota. Although two tailings samples generated from bench scale tests on titanium ore from Minnesota were available, there were no known gold mine tailings generated from Minnesota rock. Consequently it was necessary to locate tailings generated from development of gold deposits in areas geologically similar to land under exploration in Minnesota.

There are approximately 159 current metallic mining leases in the state (Division of Minerals, 1993a). The bedrock associated with the individual leases was identified using a map of the leases (Division of Minerals, 1993b) overlain on a bedrock map of Minnesota (Division of Minerals, 1993b). About 33 percent of the leases are in metavolcanic rocks of greenschist (which constitutes the major portion) to amphibolite grades. These rocks include the Ely Greenstone and the Newton Lake Formation. Another 40 percent of the leases are in metasedimentary rocks, including the Knife Lake Group and the Lake Vermillion Formation. Again, these are mainly greenschist with some amphibolite metamorphic grades.

The third group of 13 percent are in metamorphosed felsic volcanic rocks. A fourth group of approximately 4 percent lie in metamorphosed mafic-intermediate volcanics (including the Mille Lacs Group). The North Shore Volcanics contain about five percent. The remaining five percent are scattered among quartzite, granitoid, felsic-intermediate volcanics, iron formation, and migmatitic gneiss. Each of these five rock units contains about one percent of the leases.

Thus, approximately 73 percent of the leases (the first two groups) lie in Archean age greenstone belts of the Superior province, comprised of metavolcanic and metasedimentary rocks. The Superior province lies in the Canadian Shield, which covers much of eastern and northern Canada and most of Minnesota (Ojakangas and Matsch, 1982). Greenstone belts, which lie in the center of every continent, are comprised of volcanic and volcano-sedimentary rocks that were formed 2.6 to 2.7 billion years ago in the middle of the Precambrian Era (Windley, 1977). The rocks were later deformed, specifically folded, faulted, sheared, and intruded (Eckstrand, 1984). Metamorphism occurred to the grade of greenschist/amphibolite, which are high temperature, low pressure deformations (Jiran, 1990).

The characteristics of gold deposits in greenstone belts are universally similar (Windley, 1977). Almost every gold deposit in the Superior Province is found within or adjacent to the greenstone belts (Colvine, 1989). Folds, faults, and intrusions are important controlling factors in deposit location (Eckstrand, 1984). Folds and faults create conduits for the introduction of hydrothermal solutions, which recrystallize local minerals and add new minerals by precipitation. The resulting hydrothermal veins are primarily composed of

quartz and carbonates, with accessory minerals including veins of gold (Jiran, 1990). Gold deposits can also be found at felsic-mafic volcanic contacts, in carbonate facies iron formations, mafic igneous rocks, felsic intrusives, and marginal zones of greenstone belts near an intrusion (Windley, 1977). Large quantities of disseminated gold can be found in these highly sheared contact zones (Eckstrand, 1984).

Since the characteristics of gold deposits in greenstone belts are similar, tailings samples were collected from gold mines developed in the greenstone belts of the Superior province. As described above, these are typically hydrothermal vein deposits, composed primarily of quartz and carbonates. Lacking samples generated in Minnesota, this was the best available method of approximating the composition of tailings generated by a gold mine in the state. Since the composition of tailings varies among and even within operations, the results will provide a general reflection of the compositional characteristics and dissolution behavior of tailings generated by gold mining in Minnesota. More precise description can be made only when a mine site is specified and rock samples are available.

5.2. Long Term Dissolution Experiment

5.2.1. Introduction

The generation of acidic drainage is the primary drainage quality concern associated with abandoned mine wastes, which include tailings, waste rock, and the mine itself. The time frame over which these wastes will generate drainage is difficult to simulate in the relatively short period over which predictive dissolution testing can be conducted. That is, it is difficult to simulate the dissolution of mine wastes over a period of decades and centuries in the course of weeks or even years of laboratory testing.

Mine wastes often contain iron sulfide minerals, which will oxidize in the presence of atmospheric oxygen and water. This oxidation leads to the production of acid. The dissolution of other minerals present in the mine waste will neutralize acid. Minerals containing calcium carbonate and magnesium carbonate are the most effective acid-neutralizing components of mine waste. If the rate of acid production exceeds the rate of acid neutralization, the drainage from the mine waste will become acidic.

The following three variations in the neutralizing mineral content of sulfide bearing mine wastes are presented to describe potential variations in mine waste drainage pH over time.

Case 1: A sulfide-bearing mine waste which contains no neutralizing minerals will generate acidic drainage almost immediately. Iron sulfide oxidation, and the consequent acid production, will begin as soon as the iron sulfide minerals are removed from depth and exposed to atmospheric oxygen and water at the earth's surface.

Case 2: A sulfide-bearing mine waste which contains a small amount of neutralizing minerals will initially produce a neutral drainage. The acid produced by sulfide oxidation will be neutralized by the dissolution of the acid-neutralizing minerals. The drainage will remain neutral until these minerals are depleted, at which time it will become acidic.

Case 3: A sulfide-bearing mine waste which contains a substantial amount of neutralizing minerals will produce neutral drainage for an extended time. During this long time frame precipitates may gradually accumulate on the surfaces of both iron sulfide minerals and acid neutralizing minerals. Such coatings will inhibit the reactivity of the minerals on which they form. If coatings form on the acid-neutralizing minerals and iron sulfide oxidation continues, drainage from the waste will become acidic. If coatings form on the iron sulfide minerals and the rate of iron sulfide oxidation is adequately inhibited, the drainage will not acidify. At present it is not possible to quantitatively model the formation of coatings with the accuracy required to predict the effects on drainage quality.

The first case can be readily detected by dissolution testing, since the drainage will acidify within a few weeks. In the second case, the duration of the dissolution test must be fairly long. For example, laboratory dissolution tests were conducted on a mixture of 75 g rock (2.1 percent sulfur, mostly as pyrrhotite) and 0.79 g rotary kiln fines (a waste generated in the production of lime from limestone; the waste is largely comprised of limestone and CaO). The drainage pH from this mixture, which had a neutralization potential of 8.4 kg CaCO₃/t, was above 7.0 for 75 weeks then decreased below pH 6.0 (Lapakko, 1990). A mixture of 75 g of the same rock and 0.79 g -10 mesh limestone yielded a neutralization potential of 11 kg CaCO₃/t. This mixture produced neutral drainage for 109 weeks, at which time the drainage pH decreased below 6.0 (Lapakko and Antonson, 1991).

As is clear from the previous examples, a very long dissolution test would be required to identify the acid producing character of a sample containing a substantial fraction of calcium/magnesium carbonate minerals. Such a test would be conducted until the drainage acidified or until the iron sulfide minerals present became unreactive. The decrease in this reactivity would be indicated by a decrease in sulfate release.

In the initial phase of this project all twelve tailings samples generated drainage in the neutral pH range during the 52-week dissolution experiment (Lapakko, 1991). Since none of the samples produced acidic drainage, it is clear that none of the samples examined conformed to the profile described in Case 1. Samples T2, T6, T9, and T10 were continued for an additional 99 weeks of dissolution in the Long Term Dissolution Test. Based on chemical and mineralogic analyses, the acid production potentials of samples T2, T6, and T9 exceeded their respective potentials to neutralize acid (table 4). This suggests that the neutralization potential of these samples would be depleted while acid was yet being generated, at which time drainage would become acidic. The acid neutralization potential of sample T10 exceeded its acid production potential but this difference was small.

5.2.2. Case 2 Sample (T9): Low NP, High APP

Sample T9, with an NP of 14 kg CaCO₃/t and an APP of 156 kg CaCO₃/t, was generally consistent with the Case 2 description. The pH of drainage from the T9 tailings was in the approximate range of 7.7 to 8.1 during the initial 100 weeks of the experiment. At this time drainage pH began to decline, dropping below pH 6.0 after 122 weeks and ultimately reaching pH 3.45 after 151 weeks (figure 5). The alkalinity concentrations followed a similar trend (appendix B).

Sulfate concentrations generally increased throughout the experiment, indicating an increase in the rate of acid production (figure 5). Anomalously high sulfate concentrations were observed between weeks 50 and 65. The relative humidity was also high during this period (figure 2) and apparently accelerated the rate of sulfide oxidation.

The elevated sulfate concentrations after week 130 were roughly eight times those typical of the earlier phase of the experiment, when drainage pH was near neutral. The elevated values were likely related to the pH, which decreased below 4.0 near week 130. Research on pyrite oxidation indicates that as "pH decreases to 4.5, ferric iron becomes more soluble and begins to act as an oxidizing agent" (Nordstrom, 1982). As pH further decreases, bacterial oxidation of ferrous iron becomes the rate limiting step in the oxidation of pyrite by ferric iron (Singer and Stumm, 1970), which is the only significant oxidizing agent in this pH range (Nordstrom, 1982; Singer and Stumm, 1970; Kleinmann et al., 1981). This indicates that the elevated sulfate concentrations near the end of the experiment were probably due to increased biologically mediated ferric iron oxidation of the sulfide minerals as pH decreased below 4.0. The rate of chemical oxidation may have increased also, although the extent of this increase was most likely slight relative to the increase in biological oxidation (Nordstrom, 1982).

In contrast, calcium concentrations in the drainage generally decreased throughout the experiment, and the decrease was particularly marked as the drainage pH declined (figure 5). This suggested that the calcium carbonate initially present in the sample (table 3) was being depleted or rendered unreactive. Consequently, the acid produced by the iron sulfide oxidation, as indicated by sulfate concentrations, was not neutralized and the drainage acidified.

The cumulative release calculations support the contention that the carbonate minerals initially present in the sample had been depleted. The cumulative release of calcium plus magnesium from T9 was calculated as 12 millimoles at week 122 (figure 5). Using this value to represent the depletion of carbonate minerals from the solid indicates that 114% of the 10.5 millimoles initially present had been depleted. In contrast, less than eight percent of the total sulfur initially present in the sample had been depleted (table 6). The remaining iron sulfides (mostly pyrite) continued to produce acid, of which only a fraction was neutralized, and the drainage pH decreased. The acid neutralized during this phase was apparently due to dissolution the minerals listed below which were present in the tailings

(appendix A, mineral compositions from Klein and Hurlbut, Jr., 1985). This dissolution was reflected by continued low-level release of calcium and magnesium.

feldspar group	
orthoclase-albite	$\text{KAlSi}_3\text{O}_8\text{-NaAlSi}_3\text{O}_8$
albite-anorthite	$\text{NaAlSi}_3\text{O}_8\text{-CaAl}_2\text{Si}_2\text{O}_8$
mica group	
muscovite	$\text{KAl}_2(\text{AlSi}_3\text{O}_{10})(\text{OH})_2$
phlogopite	$\text{KMg}_3(\text{AlSi}_3\text{O}_{10})(\text{OH})_2$
biotite	$\text{K}(\text{Mg, Fe})_3(\text{AlSi}_3\text{O}_{10})(\text{OH})_2$
lepidolite	$\text{K}(\text{Li, Al})_{2-3}(\text{AlSi}_3\text{O}_{10})(\text{O, OH, F})_2$
margarite	$\text{CaAl}_2(\text{Al}_2\text{Si}_2\text{O}_{10})\text{OH}_2$
chlorite group	
chlorite	$(\text{Mg, Fe})_3(\text{Si, Al})_4\text{O}_{10}(\text{OH})_2 \cdot (\text{Mg, Fe})_3(\text{OH})_6$
apophyllite	$\text{KCa}_4(\text{Si}_4\text{O}_{10})_2\text{F} \cdot 8\text{H}_2\text{O}$
prehnite	$\text{Ca}_2\text{Al}(\text{AlSi}_3\text{O}_{10})(\text{OH})_2$
amphibole group	$\text{W}_{0-1}\text{X}_2\text{Y}_5\text{Z}_8\text{O}_{22}(\text{OH, F})_2$, where W represents Na^+ and K^+ , X represents Ca^{2+} , Na^+ , Mn^{2+} , Fe^{2+} , Mg^{2+} , and Li^+ , Y represents Mn^{2+} , Fe^{2+} , Mg^{2+} , Fe^{3+} , Al^{3+} , and Ti^{4+} , and Z represents Si^{4+} and Al^{3+}

5.2.3. Case 3 Samples (T2, T6, T10): High NP, High APP

The relatively high neutralization potentials (45 to 200 kg CaCO_3/t) and acid production potentials of samples T2, T6, and T10 (66 to 247 kg CaCO_3/t , table 4) were consistent with the Case 3 characteristics. These samples generated basic drainage throughout the 151 weeks of the Long Term Dissolution Experiment. For the vast majority of drainage from these three samples, pH ranged from 7.8 to 8.4 and alkalinity from 40 to 120 mg/L. The pH and alkalinity values from sample T6 were at the lower end of these ranges, and the values from T10 were at the upper end of the ranges.

The concentrations of sulfate, calcium, and magnesium in the drainages from T2, T6, and T10 were highest at the beginning of the experiment. These elevated values reflected the removal of reaction products which accumulated between the time the samples were collected and the beginning of the experiment. Elevated sulfate concentrations were also observed between weeks 50 and 65. This was possibly due to the acceleration of iron sulfide oxidation due to the elevated relative humidity during this period (figure 2).

Subsequently, the sulfate, calcium, and magnesium concentrations from T2 and T6 were fairly stable. In contrast, sulfate and calcium concentrations in the drainage from T10 increased fairly steadily from week 75 to the end of the experiment, while magnesium concentrations decreased (figures 6, 7). The reason for the steady increase in the rate of sulfide mineral oxidation is not apparent. In some cases, such as T9, increasing sulfate concentrations have been a precursor of drainage acidification (figure 4).

The cumulative mass release from these samples was calculated for sulfate, calcium, and magnesium (appendix B). These values were then compared to the iron sulfide and calcium/magnesium carbonate content of the samples. The values determined indicated that for samples T2, T6, and T10, from 14 to 27 percent of iron sulfides initially present oxidized, and 30 to 52 percent of the total calcium carbonate and magnesium carbonate initially present dissolved during the 151 week experiment (figure 8, table 6).

The average rates of release during the experiment were also calculated (table 7). These rates, in conjunction with the initial APP and NP, were used to estimate the dissolution time required to deplete the APP (iron sulfide minerals) and NP (calcium and magnesium carbonate minerals) present in the samples. The time required for APP depletion was calculated by dividing the initial APP (millimoles CaCO_3/g) by the rate of sulfate release (millimoles per week). This quotient was divided by 52 to convert from the time from weeks to years. The time required for NP depletion was calculated similarly. This method of estimation does not account for the possible accumulation of coatings on sulfide and carbonate mineral surfaces. As previously discussed, these coatings will inhibit the dissolution of the minerals on which they formed. This phenomenon has been observed in other laboratory studies (Lapakko and Antonson, 1991, MN DNR unpublished data).

Based on this calculation, the NP of all samples would be depleted before the APP (table 8). This implies that all three samples would eventually produce acidic drainage. For example, sample T2 would produce neutral drainage for 14 years, at which time the NP would be depleted. Subsequently, the drainage would become acidic until the APP was depleted after an additional 31 years. This estimation provides only a "first-cut" guess on the variation of drainage pH over the long term. Given the potential for coating formation on the mineral surfaces, a high degree of uncertainty is associated with this estimation.

The dissolution behavior of the samples over time can be accurately assessed only by extended dissolution studies. Although conducting such studies under field conditions would most closely approximate the conditions of actual mine waste disposal, and therefore the quality of drainage generated, laboratory tests may provide a more practical approach. Such studies would be difficult, at best, within the typical regulatory time frame. Consequently, projects must be conducted specifically to address the long term dissolution behavior of mine wastes in general, in anticipation of mineral resource development. In such studies the relationship between solid-phase composition and drainage quality must be established with as much accuracy as possible, so results can be more readily extrapolated to specific mine wastes when mineral development is proposed.

5.2.4. Rates of Sulfide Mineral Oxidation

For the Long Term Oxidation Experiment the rates of sulfate release for numerous periods were calculated, and an overall rate was determined for the duration of the experiment (table 7). For pyrrhotite oxidation, the rate of mineral oxidation equals the rate of sulfate release, while for pyrite the rate of mineral oxidation is half the rate of sulfate release.

Rates of calcium and magnesium release were determined for the same periods. Rates were also determined for weeks 20 to 57 in the previous phase of this project (table 9).

The overall rates of sulfate release for the 151-week and 57-week periods of record were plotted as a function of the sulfide content of the samples (figures 9 and 10, respectively). The data from the Long Term Dissolution Test indicate that the rate of sulfate release from T10 was anomalously high with respect to the rates observed for the other three samples.

Regression analysis conducted on the data presented in figure 10 yielded the following equation. The r^2 value indicates that the variation in percent sulfur accounts for 69

$$d(\text{SO}_4)/dt = 0.013 (\%S^2) - 0.000, n = 24, r^2 = 0.693$$

percent of the variation in the sulfate release rate. It is clear that other variables also influence these rates. The data from weeks 20 to 57 indicate, as did those from the Long Term Dissolution Experiment, that the oxidation rate for T10 is elevated with respect to the rates observed for the samples in general. Furthermore, the rates observed for samples T5, T8, and T9 were low when compared to the general trend for the samples (figure 10). It is worth noting that the rate for T9 in this analysis is limited to a period when the pH of drainage from the sample was near neutral. Data from the Long Term Dissolution Experiment include those from the period during which the drainage was acidic and the sulfate release rate was accelerated.

The oxidation rates vary among iron sulfide minerals. Whereas pyrite is the predominant sulfide mineral in most of the samples, pyrrhotite predominates in samples T6 and T7. It also constitutes about 30 percent of the iron sulfide content of sample T8 (table 3). Although the oxidation rate for T8 is lower than expected based on the variation of rate with sulfide content, the rates for T6 and T7 are reasonably consistent with the samples in general. Thus the presence of pyrrhotite does not appear to substantially affect the iron sulfide oxidation rate for these samples. (As noted previously, for pyrrhotite the rate of mineral oxidation equals the rate of sulfate release, while the rate of pyrite oxidation equals half the rate of sulfate release.)

The influence of specific surface area may explain some of the deviation observed in the relationship between oxidation rate and solid-phase sulfide content. The oxidation rate for specific sulfide minerals is reported to be directly proportional to the mineral surface area available for reaction. The sulfide mineral surface area available is the product of the mass of sulfide minerals present and their specific surface area, since the sulfide minerals present in these samples are virtually totally liberated (appendix A). Whereas the solid-phase sulfide content provides a good indication of the iron sulfide mass, it does not account for variation in the specific surface area of the minerals present. Such variation among the samples is highly likely, as indicated by the differences in particle size distribution.

In an attempt to quantify the relationship between pyrite surface area and the rate of pyrite oxidation, the sulfide minerals were separated from samples T1, T2, T4, T9, and T10. Pyrite was the dominant iron sulfide present in all of these solids (table 3). The surface area of the sulfides separated was then determined using the BET method. Some of the sulfides present in sample T5, of which a limited mass was available, were separated for SEM analysis. The oxidation rates relative to sulfide content for samples T1, T2, and T4 were generally consistent with those of the samples on the whole. In contrast the oxidation rates for samples T5 and T9 were lower, while that for T10 was higher, than the general trend (figure 10).

Based on iron sulfide content the sulfate release from T10 was considerably higher than that from T9 (figure 10). This may be explained to a large degree by the differences in surface area between the two samples, as indicated by analyses of the concentrates obtained by both methods of separation. For the Superpanner concentrates the specific surface area of T10 was three times that of T9, most likely due to the smaller size and rougher surface texture of the T10 sulfide grains, as detected by SEM (figures 11D, 11E). The same reasoning would explain the low sulfate release from sample T5 (figures 11A-11F), which contained relatively large, smooth sulfide grains. The rougher surface texture of T10 may also have been an indication of a higher density of surface dislocations. The specific surface areas of sulfide mineral concentrates separated using the two heavy liquid separations were higher, apparently due to more efficient recovery of finer particles. For these concentrates the T10 surface area was 4.6 times that of T9 (table 10). (See appendix H for details of sulfide mineral analysis.)

These values suggest that the differences in the sulfate release rates for these samples can be explained based on differences in the specific surface areas of the sulfide minerals. However, since the sulfide recovery was low, it is difficult to draw quantitative conclusions from analyses of the concentrates, which probably represent the larger sulfide minerals present.

Furthermore, barite and siderite were present in the concentrates of T9 and T10, respectively, and it is difficult to quantify the relative contributions of these contaminants to the specific surface area values. Examination of the SEM photographs indicates that the barite present in the T9 concentrate was similar in size and surface texture to the pyrite particles. This suggests that the specific surface area determination was reasonable representative of the pyrite grains present in the concentrate. The siderite grains present in the T10 concentrate appear to be larger than the average pyrite grains. The siderite grain surfaces were also smooth in comparison to the pyrite grains. This suggests that the specific surface area of the pyrite present is somewhat higher than the value determined.

Other qualitative evidence suggests that the specific surface area of pyrite present in T10 was greater than that for the samples in general. The Superpanner-heavy liquid separation recovered less pyrite from T10 than from the other samples (table 10). This implies that there was a greater fraction of very fine sulfides present in this sample than in other

samples. The abundance of fine pyrite grains would increase the pyrite surface area. This supports the hypothesis that the sulfate release rate from sample T10 was the result of the higher pyrite surface area of this sample.

The sulfides separated in the Superpanner concentrates represented only the larger sulfide grains present in the tailings. Consequently, the specific surface areas represent a lower bound of the actual surface area since the smaller grains, of high specific surface area, were not accounted for. The specific surface areas determined for the concentrates were multiplied by the iron sulfide content of the samples to estimate the iron sulfide area present.

In order to estimate the relationship between iron sulfide mineral surface area and the rate of sulfate release, it was necessary to assume that either a) the estimated iron sulfide surface areas were proportional to the actual values or b) the difference among the unmeasured specific surface areas was negligible. It is recognized that either assumption is tenuous. The rates of sulfate release were then plotted as a function of the estimated iron sulfide surface area (figure 11). Linear regression was used to determine the equation of the line which best fit the data. The r^2 value for the regression was 0.929, which indicates that the variation in the estimated pyrite surface area explained 93 percent of the variation in the sulfate release rate. Despite the uncertainty in the specific surface area measurements, this suggests that variations in sulfate release rate which were not explained by sulfur content may have been the result of differences in sulfide mineral surface area. The slope of the line, which represents the sulfate release rate in terms of sulfide mineral surface area, was 5.6×10^{-11} moles/m²(FeS₂) • s.

The iron sulfide surface areas were used to express the rates of sulfide oxidation in terms of the sulfide mineral surface area (table 11). The rates calculated in terms of iron sulfide surface area were considerably closer than those expressed in terms of the mass of iron sulfide present. The ratio of the maximum to minimum rates for the former was seven as compared to 25 for the latter. With the exception of sample T1, the maximum rate expressed in terms of iron sulfide surface area was within a factor of two of the minimum rate. As mentioned previously, the specific surface area determined for T1 was higher than that expected based on the particle size, which resulted in a low sulfate release rate per unit iron sulfide surface area. Apparently the surface irregularities observed on the pyrite grains present in this sample contributed some surface area which was of lesser reactivity. Perhaps the surface area present in the pores of these grains released less sulfate due to transport limitations within the pores.

In conclusion, the rate of sulfate release (i.e. the apparent rate of iron sulfide oxidation) was apparently controlled by the iron sulfide mineral surface area present. Other factors such as iron sulfide chemistry, crystal structure (including lattice dislocations), and surface coating may also affect release rates. However, for the samples examined by the methods in this study, these effects were not discernible.

5.2.5. Summary

1. Only one of the ten gold tailings samples examined in this study produced acidic drainage during the Long Term Dissolution Experiment. Sample T9 produced circumneutral drainage for 120 weeks and at week 121 the drainage pH dropped below 6.0, eventually reaching pH 3.45 at week 151. This demonstrates that the quality of drainage generated in short term dissolution experiments may not accurately reflect the drainage quality generated by mine wastes over a longer time frame. In order to extrapolate dissolution test results to the longer time frame relevant to abandoned mine waste, first, the capacity for acid production and acid neutralization should be determined for samples subjected to dissolution testing. Second, the drainage generated in dissolution test should be analyzed for sulfate, calcium, and magnesium in addition to pH. The rates of release for sulfate, calcium, and magnesium can be calculated from these values.

Using these rates in conjunction with the capacities for acid production and acid neutralization, the time to deplete these capacities can be calculated. This will yield a first-cut estimate of whether drainage will remain basic (i.e. acid producing capacity will be depleted before acid neutralizing capacity) or become acidic (i.e. acid neutralizing capacity is depleted before acid producing capacity). This estimation ignores the formation of precipitate coatings on the surfaces of acid producing and acid neutralizing minerals. Although these coatings are known to form, knowledge of their formation in mine wastes is inadequate to quantify their influence on drainage quality.

2. Samples T2, T6, and T10 continued to produce drainage of slightly basic pH for a total of 151 weeks. Even after 151 weeks of dissolution, these samples contain a substantial amount of calcium and magnesium carbonate minerals. The technique described above indicated that the drainages from these three samples would become acidic in six to fourteen years. However, over this duration the pH within the tailings will be neutral to basic, and coatings may form on the iron sulfide minerals present. Such coatings may effectively inhibit their oxidation, thereby precluding the generation of acidic drainage.
3. Long term dissolution tests can reduce the uncertainty associated with predicting precipitate coating formation on sulfide and carbonate mineral surfaces and the influence of these coatings on mine waste drainage quality. Conducting such tests with operational size waste under actual field conditions provides the best simulation of the environmental behavior of the mine waste. Long term laboratory testing provides the next best approximation.
4. The pyrite surface area was the predominant control on the rate of pyrite oxidation observed in this experiment.

5. The release of arsenic, antimony, or molybdenum in slightly basic drainage was observed from three of the samples. The potential for such trace metal release must be considered with tailings generated from hydrothermal gold deposits such as these.

5.3. Variable Mass Experiment

5.3.1. Introduction

The Variable Mass Experiment was conducted to examine the effect of the mass of sample used in a dissolution experiment on the amount of acid neutralized for each mole of carbonate mineral dissolved. (Drainage quality and mass release data, as well as additional figures, are presented in appendix C). This amount can vary from zero to two moles of acid per mole of carbonate mineral dissolved. Carbonate minerals will dissolve to a given extent in the absence of acid (reaction 17). The presence of acid will lead to dissolution by



reaction 6 or 7. When calcium carbonate or magnesium carbonate is present in a mine waste, this dissolution can neutralize acid produced as a result of iron sulfide oxidation.

Carbonate minerals will always dissolve to some degree due to their solubility, that is, by reaction 17. If the acid produced by iron sulfide oxidation is relatively small, reaction 17 will be the dominant path of carbonate dissolution. The low acid production is more likely to occur when the mass of iron sulfide minerals present is small, that is, when the sample mass is small or the concentration of iron sulfides in the sample is low. As the iron sulfide mass and attendant acid production increases, the extent of acid neutralization by carbonate mineral dissolution will increase. That is, one to two moles of acid will be neutralized per mole carbonate mineral dissolved.

In the field, the mass of mine waste will be very large in comparison to that used in laboratory experiments. Consequently, the acid production will be greater and carbonate minerals will be more apt to dissolve according to reactions 6 and 7. Thus, under field conditions one to two moles of acid will be neutralized by the dissolution of one mole of calcium or magnesium carbonate.

If the carbon dioxide generated by the carbonate mineral dissolution can escape to the atmosphere, two moles of acid would be neutralized per mole of calcium carbonate or magnesium carbonate dissolved (reaction 7). However, as carbonate minerals present in fine particles dissolve, the carbon dioxide gas evolved may become trapped within the pores between the particles. This will cause an increase in the carbon dioxide partial pressure, which will then control the extent of acid neutralization by carbonate mineral dissolution. Based on field results from coal mines (Brady et al., 1990) and considerations of carbonate equilibria (Cravotta III et al., 1990), an acid neutralization of one mole per mole of calcium/magnesium carbonate dissolved would be expected (reaction 6). Thus the extent

of acid neutralization under field conditions may vary from one to two moles per mole of calcium or magnesium carbonate. The extent of neutralization at the specific site must be considered when selecting the sample mass for predictive tests and interpreting test results.

The extent of acid neutralization by carbonate mineral dissolution was calculated using observed molar concentrations in the drainages. The sum of calcium and magnesium concentrations vs. the corresponding sulfate concentrations in drainage samples were plotted for each sample. Linear regression analyses were conducted to determine the constants for the equation:

$$[\text{Ca}^{2+}] + [\text{Mg}^{2+}] = m[\text{SO}_4^{2-}] + b \quad [18]$$

Twice the inverse of the slope, m , yields the number of moles of acid neutralized by the dissolution of carbonate minerals. The value b is the y-intercept, which is the molar sum of calcium and magnesium concentrations when no sulfate is present. This represents the amount of calcium and magnesium carbonate which dissolves in the absence of the acid produced by iron sulfide oxidation (i.e. by reaction 17).

Error is introduced in this approach since a single slope will be applied to the entire data set. In actuality, each of reactions 6, 7, and 17 will generate its own distinct slope for equation 18. If iron sulfide oxidation is very small, the generation of sulfate and acid will be small. In this case reaction 17 will dominate and the slope will be near zero. That is, the release of calcium and magnesium by carbonate dissolution will be independent of sulfate concentration.

As iron sulfide oxidation and the consequent acid production increases, reaction 6 will represent the dominant path of carbonate dissolution, and the slope of the line ($\{[\text{Ca}] + [\text{Mg}]\}/[\text{SO}_4]$) would be 2.0. As the concentration of acid produced by iron sulfide oxidation increases, bicarbonate concentrations produced by reaction 6 will increase and carbonic acid will form (reaction 19). The net reaction is represented by reaction 7, which would generate a slope of 1.



The slope determined in the regression analysis will reasonably reflect the dominant carbonate mineral dissolution reaction and the attendant extent of acid neutralization. However, the intercept will provide only a first-cut approximation of the extent of dissolution occurring by reaction 17.

5.3.2. Extent of Acid Neutralization by Carbonate Dissolution

Regression analysis was conducted on the drainage data for the individual samples (T2, T4, T10), as well as the combined data for all samples. The correlations were very high, as indicated by r^2 values of 0.864 to 0.986 for data sets of 100 to 310 points. The extent of acid

neutralization was close to two moles acid per mole of carbonate mineral dissolved in all cases (table 12A). The carbonate mineral dissolution by reaction 17 was estimated to be in the range of 0.66 to 0.80 mmol/L, based on the y-intercepts obtained.

The extent of acid neutralization by carbonate mineral dissolution decreased as sulfate concentrations decreased. For sulfate concentrations less than 1.0 mmol/L the acid neutralization was about 1.6 mole acid per mole carbonate mineral dissolved. When the data were limited to sulfate concentrations less than 0.5 mmol/L and 0.25 mmol/L, the extent of acid neutralization decreased further, although the r^2 also decreased substantially (table 12B, 12C, 12D). The y-intercepts for the regressions based on the lower sulfate concentrations indicated the carbonate mineral dissolution by reaction 17 was in the approximate range of 0.5 to 0.6 mmol/L. It is assumed that this range is more accurate than that obtained using the higher sulfate concentrations, since the values used were in closer proximity to the intercept.

The mass release data reflect the water quality trends. That is, the acid neutralized per mole of calcium/magnesium carbonate mineral dissolved tends to increase as the mass of iron sulfide present increases. The iron sulfide mass is a function of the iron sulfide content of the tailings and the mass of tailings present. The acid neutralized per mole of carbonate mineral dissolved increased from less than one at low masses to a maximum of two at a higher mass, at which point it plateaus (table 13).

For the individual reactors in this study, the extent of acid neutralization was calculated as twice the molar release of sulfate divided by the sum of the molar releases of calcium and magnesium (appendix C, table C9.1). The extent of acid neutralization increased from about 0.3 to 1.8 moles H^+ neutralized per mole calcium/magnesium carbonate dissolved as the mass of iron sulfide present increased from 0 to 40 g. A value of one mole H^+ neutralized per mole calcium/magnesium carbonate dissolved occurred at about 15 g iron sulfide (figure 12). The extent of acid neutralization by calcium/magnesium carbonate mineral dissolution increased to two moles H^+ neutralized per mole calcium/magnesium carbonate dissolved when the mass of iron sulfide exceeded 100 g (figure 12). Thus 15 to 100 g of iron sulfide provided the range of one to two moles H^+ neutralized per mole calcium/magnesium carbonate dissolved, the range expected under field conditions.

It should be noted that the use of 100 g of iron sulfide per reactor may be limited by the amount of sample available. For example, 5000 g of a sample containing two percent pyrite would be required to obtain a pyrite mass of 100 g. It should also be noted that use of an excessively large mass of samples may yield drainage concentrations of sulfate and calcium which exceed the solubility of gypsum ($\log K_{s0} = -4.60$, Stumm and Morgan, 1981). The precipitation of gypsum will prohibit accurate calculation of the rates of sulfide oxidation and calcium carbonate dissolution using the observed concentrations of sulfate and calcium in the drainage from the sample.

The 15 to 100 g pyrite mass suggested above provides a "first-cut" approximation of the mass of iron sulfide minerals required to simulate the extent of neutralization by calcium/magnesium carbonate minerals under field conditions. The extent of acid neutralization is dependent on the rate of acid production which, in turn, is dependent upon the rate of iron sulfide oxidation. Consequently, other factors must be considered when determining the mass of mine waste to be used for dissolution testing. As discussed in section 5.2.4, the iron sulfide minerals present and the mineral surface area available for reaction must be determined.

For the samples examined in this study, the iron sulfide was present predominantly as fine grained (61 to 91 percent minus 500 mesh) pyrite, roughly 90 percent of which was liberated (i.e. roughly 90 percent of the pyrite surface area was available for oxidation). For larger pyritic mine wastes or mine wastes in which the degree of liberation is lower, a larger sample mass would be required to simulate the extent of acid neutralization by carbonate mineral dissolution.

To provide a point of reference for the "reactivity" of the samples in this study the sulfide oxidation rates, normalized for iron sulfide mass, were calculated for samples T2, T4, and T10. For each sample, regression analysis was conducted on the variation of the observed sulfate release rate with the variation of iron sulfide mass (figure 13). The rates determined varied from about 2.3×10^{-11} to 2.6×10^{-11} moles/g(FeS_2) \cdot s. The average specific surface area for the three samples ($0.42 \text{ m}^2/\text{g}$ iron sulfide) was used to approximate the rate in terms of pyrite surface area. Since the fine sulfide particles were not recovered for this analysis, the specific surface area represents a lower bound of the actual value. Consequently the range of rates determined, 5.5×10^{-11} to 6.3×10^{-11} moles/ $\text{m}^2(\text{FeS}_2)\cdot$ s, represents an upper bound for the reaction rate. These rates are roughly an order of magnitude lower than other rates reported for pyrite oxidation.

It is worth noting that the rates of sulfate release, normalized for the sample mass, were higher at the higher sample masses. This may have been the result of more humid conditions at the sulfide mineral surfaces. Such conditions would have resulted from the greater degree of water retention by the larger masses. This may also have been an artifact of the experimental design. When the samples were rinsed prior to the experiment, the volume of rinse water per unit mass solid was lower at the higher masses. The rinse volume per unit mass decreased as the mass increased. For all three solids the rinse volume per unit mass for the 225 g mass was about twice that for the 1500 g mass (appendix C, table C1.16) Consequently, some soluble oxidation products (due to sulfide oxidation occurring between sample collection and the start of the experiment) may have remained in the higher mass samples. The removal of these products during the weekly rinses would have artificially elevated the sulfate release rate.

5.3.3. Summary

The variation in the extent of acid neutralization as a function of sample mass must be considered when designing predictive dissolution tests. Under field conditions, when the mass of mine waste is large, the acid neutralization will likely be between one and two moles of acid per mole of carbonate mineral dissolved. By using too small of a mass in predictive tests, the acid neutralization capacity of a mine waste may be underestimated. Similarly, by using too large of a mass, the acid neutralization capacity of the waste may be overestimated. The use of too large of a mass may also result in the precipitation of gypsum from the drainage, which would impair drainage data interpretation. Thus, the variation in the extent of acid production as a function of sample mass must be accounted for in predictive test design and considered in the interpretation of experimental data. For the samples examined in this study the sample mass used should contain 15 to 100 g of iron sulfide minerals. The mass required for other samples will depend on the sulfide minerals present and the sulfide mineral surface area available for reaction.

5.4. Variable Rinse Interval Experiment

Predictive dissolution tests are typically conducted using a rinse interval of one week. The rinse interval length was varied for all twelve tailings samples to examine its effect on drainage quality and mass release. The rinsing intervals used were 1, 3, 5, 7, and 10 weeks except for samples T2, T6, T9, and T10, which were subjected to rinsing intervals of 1, 5, and 7 weeks. Detailed data on drainage pH and sulfate concentrations are presented in appendix D.

For all samples except T6, T11, and T12 the median pH values varied less than 0.1 units as the rinse interval ranged from one to ten weeks (figure 14). For these nine samples the drainage pH values were generally in the range of 8.0 to 8.2, with values from T5 at the lower end of this range. The drainage from sample T9, which became acidic after 122 weeks of the one-week rinse interval in the Long Term Dissolution Experiment, exhibited pH values slightly below 8.0 for rinse intervals of five and seven weeks.

The sulfate concentrations from samples other than T6, T11, and T12 were generally lowest at the one-week oxidation interval but did not increase greatly at longer oxidation intervals (figure 15). This indicates that the majority of the sulfide oxidation occurred within one week after rinsing. Concentrations of calcium, magnesium, and alkalinity increased as the length of the rinse interval increased, indicating an increase in the dissolution of calcium carbonate and magnesium carbonate minerals. pH values in the range of those observed, approximately 8.0 to 8.2, indicate that the drainage pH was controlled by dissolution of calcium carbonate and/or magnesium carbonate minerals present in the tailings.

The median pH of drainage from sample T6 decreased from about 8.0 at the one-week rinse interval to 7.85 at the seven-week interval (figure 14). This was apparently the result of an increase in the extent of sulfide oxidation with increasing rinse interval duration. The

variation in sulfate concentrations indicate that the extent of sulfide oxidation increased by less than a factor of two as the rinse interval duration increased from one to seven weeks (figure 15). Concentrations of calcium, magnesium, and alkalinity in the drainage from T6 were comparatively stable over the range of rinse intervals examined (figures 16, 17).

The pH of drainage from T11 and T12 was lowest at the one-week interval. These samples contained virtually no sulfide minerals and 0.4 percent calcite. The pH elevation observed for the longer rinse intervals was apparently due to increased dissolution of the small amount of calcite present. This contention is supported by increasing concentrations of cations and alkalinity with increasing rinse interval duration (figures 16, 17).

In summary, for the gold mine tailings (T1 to T10) the variation in drainage pH with the length of rinse interval was usually less than 0.1 unit. The majority of sulfide oxidation occurred within the one-week period following rinsing. Furthermore, the acid produced as a result of this oxidation was readily neutralized by the dissolution of the calcium carbonate and magnesium carbonate present in the samples. This dissolution maintained drainage pH values in a typical range of 8.0 to 8.2, and increased as the length of the oxidation interval increased. Furthermore, the extent of acid neutralization did not vary substantially over the range of rinse intervals examined (appendix D, figures D4.25 to D4.28). An increase in sulfide oxidation with rinse interval duration was observed for sample T6, and lesser increases may have occurred with samples T7 and T8. These were the only samples which contained substantial amounts of pyrrhotite, but more extensive experimentation would be required to determine if this mineralogical influence was significant.

The subtle trends observed would not suggest alteration of the rinse interval length for predictive tests beyond the typical duration of one week. The influence of the rinse interval length on drainage quality was slight (table 13), and increasing the rinse interval would increase the time required for mine waste drainage quality predictive tests. The variation in rinse interval length may affect the accumulation of reaction products on mineral surfaces, but examination of this relationship was beyond the scope of the present project.

An additional brief test (15 weeks) was conducted to examine the effect of shorter rinse intervals on the rate of sulfate release. Sample T2 and a Duluth Complex rock sample containing 1.64 percent sulfur were subjected to rinse intervals of 6, 24, and 84 hours. The predominant iron sulfide in sample T2 is pyrite, while pyrrhotite was the major iron sulfide in the Duluth Complex sample. The detailed experimental methods and results are presented in appendix F.

The weekly sulfate release from sample T2 did not vary substantially among the three shorter rinse intervals examined. The release at these intervals appeared to be less than or equal to that at the one-week rinse interval. However, the sulfate release at the 6 and 24 hour rinses of the Duluth Complex rock was about 25 percent higher than that at the 84 hour rinse interval. cursory examination indicated that the weekly release at the 6 and 24 hour intervals was not substantially different from that at a rinse interval of one week.

Additional experimental work and data analyses are required to accurately compare these results with those at a rinse interval of one week.

5.5. Elevated Temperature Experiment

5.5.1. Introduction

Samples T1, T2, T4, T8, T9, T10, and T12 were submitted to the Elevated Temperature Test. The samples were rinsed every two weeks and stored between rinses in an oven with an average temperature of 96.7°C. The results from this 48-week test were compared to those from the Wet-Dry Cycle Test conducted at 25°C. Detailed results from the Elevated Temperature Experiment are presented in appendix E.

5.5.2. Temporal Variation of Drainage Quality

The temporal variation of drainage quality followed three general trends. First, samples T1, T4, T8, and T12 continuously produced drainage pH values above 6.0. These drainage pH values are consistent with those observed at room temperature. Samples T1, T4, and T8 produced drainage with typical pH and alkalinity ranges of 7.4 to 8.2 and 50 to 100 mg/L, respectively (figure 18). Sulfate concentrations in the drainages tended to decrease over time, although the decrease was less pronounced for sample T1. This decrease was probably influenced by the decrease in available iron sulfides (table 14) and possibly the formation of ferric oxyhydroxide coatings on the iron sulfide mineral surfaces.

The temporal variation of calcium concentrations was similar to that for sulfate, while magnesium concentrations were relatively constant or increased slightly over time. The similarity between calcium and sulfate is not coincidental, since the calcium release from carbonate minerals was driven by the acid produced by sulfide mineral oxidation. The fraction of neutralizing minerals depleted ranged from eight to twenty percent (table 15), considerably less than the sulfide mineral depletion. These results suggest that samples T1, T4, and T8 would not generate acidic drainage if the tests continued.

The pH of drainage from sample T12 was typically between 6.5 and 7.0 for the first 40 weeks of the experiment, and then decreased to around 5.0 at week 48. The only pH values below 6.0 occurred at weeks 47 and 48. (More recent data indicate that drainage pH increased above 6.0 after week 48.) The low pH values are difficult to explain. The iron sulfide content of this sample was low. Sulfate concentrations after week 12 were uniformly low throughout the experiment, from less than two to eight mg/L, indicating that the rate of iron sulfide oxidation and consequent acid production was consistently low. Consequently, it is difficult to identify the source of the acid release and resultant pH decrease at the end of the experiment. It is concluded that the anomalously low pH values are not an indicator of any great potential to produce acid.

Second, the pH of drainage from sample T9 ranged from 7 to 8 during the first six weeks of the experiment. The drainage pH at week 8 dropped to about 2.7 then slowly increased to around 3.5 at the end of the experiment (figure 19). The temporal variation of net alkalinity (alkalinity - acidity) was consistent with that of pH. Values were typically around 50 mg/L as CaCO₃ during the first six weeks of the experiment, and subsequently dropped to around -1300 mg/L as CaCO₃. The net alkalinity subsequently increased slowly to around -150 mg/L as CaCO₃.

The sulfate concentrations in drainage from T9 peaked around week 10, and subsequently decreased to a fairly stable lower level (figure 19). Although the sulfate concentrations after week 20 were low relative to those near week 10, they were still in the typical range of 30 to 300 mg/L. This indicates that iron sulfide mineral oxidation continued, with its consequent acid production. The decrease in the oxidation rate may have been the result of the decrease in sulfide minerals (table 14) or precipitate coating of the pyrite present.

Calcium and magnesium concentrations peaked near week eight then decreased. After week 20 the calcium concentrations were typically in the range of three to eight mg/L, and magnesium concentrations were typically less than one mg/L (figure 19). The decrease in calcium and magnesium concentrations, in conjunction with the decrease in drainage pH, imply the depletion of calcium and magnesium carbonates from T9.

Sample T9 contained 1.4 percent calcite, which was the lowest acid neutralizing carbonate mineral content of the gold mine tailings examined (T1-T10, table 4). By week eight, 60 to 70 percent of the calcite was depleted and more than 80 percent was depleted by week ten (figure 20). Despite the presence of some calcium carbonate, the drainage from the sample became acidic at week eight. This indicates that the rate of iron sulfide oxidation (and consequent acid production) exceeded the rate of calcium carbonate dissolution (and consequent acid neutralization).

This may have been due, in part, to the lack of adequate contact between the acid generated by the iron sulfide oxidation and the calcium carbonate minerals. Water present in the solids after the rinses would evaporate rapidly at the high temperatures in the oven. As a result, this would inhibit the aqueous phase transport of acid from the iron sulfide mineral surfaces to the calcium carbonate minerals. It has also been suggested that "air locks" may form in the pores among small tailings particles to inhibit flow (Bradham and Caruccio, 1991). The potential for such localized areas of elevated gas pressure would be greater in the neighborhood of carbonate minerals, since their dissolution under acidic conditions releases carbon dioxide gas. This gas could become entrapped in the pores near the calcium carbonate grains and limit the transport of acid to the carbonate mineral surface.

The available neutralizing minerals were virtually totally depleted by week 20 (figure 20, table 15). This fairly rapid depletion of calcium carbonate was due to the accelerated iron sulfide oxidation, and consequent acid production, in the Elevated Temperature Experiment. The subsequent low-level release of calcium and magnesium was apparently due to

dissolution of feldspar, mica, chlorite, and amphibole present. The observed drainage quality data from the Elevated Temperature Experiment indicate that sample T9 would produce acidic drainage in the field.

Third, the drainage quality from samples T2 and T10 oscillated over time. These samples had the highest iron sulfide mineral content (13.6 and 6.7 percent, respectively) of the samples examined and a high combined content of calcium carbonate and magnesium carbonate (19 and 20 percent as CaCO_3 , respectively). During the initial 20 to 30 weeks of the experiment, pH oscillated between 3 and 7.8, and the associated net alkalinity oscillated from about -1500 to 100 mg/L as CaCO_3 . Sulfate concentrations in drainage from both solids decreased from roughly 3000 to 100 mg/L over the course of the experiment (figure 21), suggesting that the iron sulfide minerals available for reaction had been substantially depleted. The sulfate released from samples T2 and T10 accounted for approximately 70 and 100 percent, respectively, of the sulfur initially present in the samples (table 14).

The erratic oscillation of drainage pH and alkalinity make the prediction of field drainage quality for samples T2 and T10 difficult. The oscillation may have been due, in part, to the elevated contents of iron sulfides and carbonates of calcium and magnesium. Variations in the degree to which acid was transported to the carbonate mineral surfaces would be accentuated by the elevated amounts of iron sulfides and carbonates present. The high rates of acid production and neutralization would generate a relatively large amount of carbon dioxide. If acid transport were limited by elevated carbon dioxide pressure in pores near the carbonate minerals, the high carbon dioxide generation by this samples would tend to inhibit neutralization until the carbon dioxide escaped to the atmosphere.

The mineral form of the carbonate may influence the effectiveness of acid neutralization in the Elevated Temperature Experiment, and under other conditions also. The dominant buffering carbonate mineral in sample T9 was calcite. In contrast, the dominant buffering minerals present in T2 and T10 were dolomite and ankerite, respectively. Solid phase analyses of leached solids may provide additional insight into the carbonate dissolution process in this test.

5.5.3. Rates of Sulfide Mineral Oxidation

The oxidation of sulfide minerals was obviously accelerated by the high temperature in this test. The sulfate mass release during 48 weeks of biweekly rinses in the Elevated Temperature Experiment was six to nine times that in 55 weekly rinses at 25°C (table 16). The sulfate release rates in the Elevated Temperature Experiment decreased over time, due to the diminishing sulfide mineral mass and, possibly, the formation of coatings on the sulfide mineral surfaces. The rates at the beginning of the experiment exceeded overall rates at room temperature by a factor of 40 (table 17). The mass of sulfate release from samples T2 and T10 using the cold water rinse were no different than those with the hot water rinse (table 14). The NP release was slightly lower with the cold water but this difference was not deemed of consequence.

The rate of calcium and magnesium carbonate mineral dissolution was also accelerated in the Elevated Temperature Experiment, although to a lesser degree than the sulfide mineral oxidation. As a result of the preferential acceleration of the sulfide mineral oxidation, more acid was produced per mole of carbonate mineral dissolved (table 18). The dissolution of calcium or magnesium carbonate minerals will neutralize between zero and two moles of acid, as discussed in section 5.3.1. Tailings samples T1, T4, and T8 generated neutral drainage throughout the Elevated Temperature Experiment, as was the case in the Long Term Dissolution Experiment. However, the acid produced per mole carbonate mineral dissolved at the high temperature was two to three times that at the lower temperature. The high acid neutralization at the high temperature was most likely the result of the higher rate of acid production. A similar occurrence was observed for elevated sulfide oxidation, and attendant acid production, resulting from a high mass of iron sulfide present, as discussed in section 5.3.2.

After the 48-week Elevated Temperature Experiment, the samples were retained in the reactors and rinsed weekly, rather than biweekly, for 16 weeks (appendix G). The objective of this experiment was to determine if the rate of sulfate release would be higher at the shorter rinse interval. A cursory examination of the drainage quality data indicated that the sulfate release rate was lower at the shorter rinse interval. The sulfate release decreased with time in the original experiment and this trend most likely continued (appendix G, figures G4.1-4.4). Thus, to some degree the lower sulfate release was the result of previous dissolution. Nonetheless, there appears to be little indication that a one week rinse interval provides an advantage to offset the increased sampling and analysis required. However, an experiment with fresh solids would be required to verify this preliminary observation.

5.5.4. Summary

The data from sample T9 suggest that the Elevated Temperature Experiment may predict the quality of drainage from mine wastes, of composition similar to these (typically quartz-carbonate tailings), much more rapidly than the Long Term Dissolution Experiment at lower temperature. This sample produced acidic drainage in eight weeks in the Elevated Temperature Experiment as opposed to 122 weeks in the Long Term Dissolution Test. The shorter test duration is due to the accelerated sulfide oxidation at the higher temperature. Samples T1, T4, T8, and T12 produced drainage in the neutral pH range, which was also consistent with results at room temperature.

However, the elevated temperatures are not typical of the reaction environment in the field and, consequently, the drainage quality in this test may not simulate that in the field. The high temperatures accelerate evaporation rates. This may limit the aqueous phase transport of acid from sulfide mineral surfaces to carbonate mineral surfaces and inhibit acid neutralization. The accelerated accumulation of carbon dioxide (contributing to the formation of "air locks") in the neighborhood of carbonate minerals may further inhibit acid transport to their surfaces for neutralization. Cementation of particles may also be enhanced at elevated temperature, thus producing a physical deviation from environmental

conditions, which may be accompanied by a deviation in the resultant drainage quality. The formation of coatings on mineral surfaces at the high temperatures may not reflect their formation at environmental temperatures.

Two obvious cases of unusual variations in drainage quality were observed. The pH of drainage from samples T2 and T10 varied erratically throughout the test. Such variation was not observed for any of the samples run at room temperature. Furthermore, it is difficult to conceive of the conditions in the field which would produce such results.

Test results indicated that the release of sulfate, calcium, and magnesium from these solids was not affected by the temperature of the rinse water. Future experiments should consider the use of a room temperature rinse water, since it simplifies the procedure. Furthermore, the mass release at a rinse interval of one week was not substantially greater than that at two weeks. The use of the two week rinse interval in the original design was more efficient procedure, since it generated results at the same rate and it was less labor intensive. Additional experimentation is required to determine the rate of sulfate release from unleached solids at rinse intervals of one and two weeks.

6. COMPARISON WITH FIELD DRAINAGE QUALITY

The nine firms which submitted gold tailings samples for testing were contacted for additional information on the tailings. Of the nine firms, six sent recent field water quality data from their tailings basins: samples T3/T4 (these were two samples from the same site), T5, T6, T7, T9, and T10. No field data were available for samples T1 and T2. No field data were available for the titanium tailings which were obtained from bench scale process tests. The data received are presented in appendix I.

Trace metal concentrations reported for the field were compared to those observed in the laboratory drainage from the corresponding sample. The laboratory dissolution tests are better suited to indicate if release of a given metal will be elevated, as opposed to predicting specific metal concentrations in the field. Three factors lend to quantitative differences between metal concentrations in the laboratory and those in the field. First, metal concentrations in the laboratory drainage are the result of rinsing a 75-gram sample weekly with 200 mL of distilled water. The ratio of tailings to water in the field may be significantly different. Consequently, the trace metal release from the tailings will result in different concentrations due to the different ratios. Second, trace metal concentrations in the field may also be influenced by processing variables. The tailings basin water may contact ore materials which contribute metals to solution. Furthermore, processing reagents may influence trace metal solubility. In particular, the cyanide used in gold processing tends to complex cationic trace metals and thereby increase their solubility. Third, environmental variables in the field may influence trace metal concentrations.

Although trace metal concentrations in the laboratory tests were not expected to approximate field concentrations, this was often the case. For samples T3 and T4, the field concentrations of arsenic and zinc were three and five times those observed in the laboratory, which is reasonably close agreement given the factors cited above. In contrast the field concentrations of copper, lead, and nickel were at least 30 to 1000 times the corresponding laboratory concentrations (table 19). The range of aqueous zinc concentrations in the T5 tailings basin was consistent with that observed in the laboratory, particularly in the early stage of the dissolution experiment (table 19).

Field data for T6 were received as the report was being prepared for printing. Although data for the years 1978 to 1992 were received, only data from 1989 to May 1992 are presented. Field concentrations of silver, arsenic, cadmium, chromium, copper, mercury, lead, zinc, as well as total and WAD cyanide were reported. The water quality samples were apparently collected from a "pump-back" sump downstream of the tailings basin. Zinc was the only metal for which measurable concentrations were regularly observed in the laboratory drainage from this sample. The field concentrations were roughly two to twenty times those in the laboratory, which is consistent with the other laboratory-field relationships (table 19).

Silver, arsenic, cadmium, chromium, copper, mercury, and lead were rarely detectable in the laboratory drainages and generally occurred at low concentrations in the field. With the exception of mercury and lead, the field concentrations of these metals typically ranged from about five to thirty parts per billion (ppb). Mercury concentrations were lower, ranging from 0.00 to 0.03 ppb. For these six metals the laboratory data are viewed as being in reasonably good agreement with the field data. That is, the laboratory data indicated little potential for release and the observed concentrations in the field were reasonably low. Lead concentrations were highest of the trace metals, with a typical range of 60 to 80 ppb. Since no lead release was detected in the laboratory, a lack of agreement between the laboratory and field data is assumed.

The arsenic concentrations in the T7 tailings basin were consistent with the range of values observed in the laboratory, but field concentrations of copper, nickel, and zinc were often about three orders of magnitude higher than the associated laboratory concentrations. The copper concentrations in laboratory drainage from this sample were usually above the 0.01 mg/L detection limit and less than 0.02 mg/L, suggesting that copper some copper release was occurring in the laboratory. In contrast, neither the drainage quality nor the solid phase chemistry suggested that release of nickel or zinc would be elevated. The elevated copper, nickel, and zinc concentrations observed in the field may be the result of a compositional difference between the laboratory and field tailings or processing chemical inputs. For example, copper may be added as a catalyst for the oxidation of cyanide by hydrogen peroxide (Meyer, 1992).

The maximum arsenic and antimony concentrations in the T9 tailings basin were roughly two orders of magnitude lower than the corresponding concentrations in laboratory drainage.

It is surprising that laboratory concentrations were so much higher than those in the field. Additional information on the field sample site and processing methods, as well as a comparison of laboratory and field tailings composition, is necessary to address this point. The ranges of molybdenum and zinc concentrations in the field were similar to the corresponding ranges in the laboratory. The molybdenum concentrations in the laboratory drainage, however, were usually at the low end of the reported range, typically between 0.02 and 0.05 mg/L. Nonetheless, the laboratory data suggested concentrations of molybdenum, as well as arsenic, antimony, and zinc, would be elevated in the field.

The copper, zinc, and nickel concentrations in the T10 tailings basin were generally low, as was the case with the concentrations observed in the laboratory. The range of copper and zinc concentrations in the field were in good agreement with those from the laboratory. The upper end of nickel concentrations in the field was roughly five times that in the laboratory (table 19), although over 80 percent of the nickel concentrations in the laboratory drainage were reported as less than 0.01 mg/L. Thus maximum nickel concentrations in the field were more closely approximated by the maximum laboratory concentrations than the "typical" concentrations.

One method of summarizing the comparison of field and laboratory data is by calculating the ratio of concentrations in the field to those observed in the laboratory. That is, by

$$F_i = C_{i,f}/C_{i,l}, \text{ where}$$

F_i is the field to laboratory ratio for parameter i (dimensionless),

$C_{i,f}$ is the concentration of parameter i in the field, and

$C_{i,l}$ is the concentration of parameter i in the laboratory in the same units.

The F values for all metals were calculated using the upper end of the concentration range observed in both the field and laboratory (table 20).

In summary, the laboratory data provided a surprisingly good indication of potential for trace metal release in the field. Twenty-five cases of trace metal concentrations in the field were available for comparison with laboratory values. In fourteen of the cases the field concentrations ranged from 1 to 5 times those in the laboratory, indicating reasonably good agreement. These cases of close agreement often involved arsenic, molybdenum (both of which occur in solution as anionic complexes), and zinc, which is more soluble than most cationic trace metals in the neutral pH range. In three cases the laboratory concentrations were higher than those in the field (table 20). In the case of mercury release from T6, this was most likely the result of error in analysis of the laboratory drainage. The discrepancy in antimony and arsenic release from T9 is difficult to explain.

In five cases, all involving copper, nickel and zinc, the laboratory concentrations were much lower than the field values. Although the field concentrations were two to three orders of magnitude higher than those in the laboratory, the laboratory data often indicated potential

for metal release. Complexation of these metals, all of which occur in solution as cations, with cyanide probably contributes to the relatively high concentrations in the field.

7. TREATMENT OF ANTIMONY, ARSENIC, AND MOLYBDENUM

Elevated concentrations of antimony (Sb), arsenic (As), and molybdenum (Mo) were observed in laboratory drainages in the initial phase of this project as well as in field drainages (table 19). Investigation of existing methods for treating these parameters was identified as a concern in the initial phase of this project (Lapakko, 1991). Elevated concentrations of copper, lead, nickel, and zinc were also observed in solution in the laboratory or field (table 19). These metals are present as cations in solution and are commonly treated by raising pH, by adding lime for example, and precipitating the metals. This process is not, however, effective for removal of antimony, arsenic, and molybdenum. A bibliography on the release of arsenic, antimony, and molybdenum by mineral dissolution, as well as their aqueous chemistry and treatment is presented in appendix J.

Examination of the literature and communication with mining companies identified treatment with ferric sulfate as the most common method presently used for removal of Sb, As, and Mo from mining waste waters. Variations of this process are used at the Giant and Con Mines near Yellowknife, Northwest Territories (Legge, 1993), and at the David Bell Mine near Marathon, Ontario (Meyer, 1992). The process is referred to as ferric co-precipitation (Legge, 1993, Meyer, 1992), although thermodynamic considerations indicate that arsenic is actually adsorbed to the ferric iron precipitate surface (Twidwell and Huang, 1993, Huang, 1993).

The process consists of a pretreatment step and three additional fundamental steps, although the specific treatment system design may vary among operations. The pretreatment is the addition of hydrogen peroxide for cyanide destruction, and this addition is also reported to oxidize arsenite to arsenate (Legge, 1993). Flow is also pretreated with a carbon column at the David Bell Mine (Meyer, 1992).

The first subsequent step is the addition of ferric sulfate, which depresses the solution pH due to hydrolysis of the ferric iron. The amount of ferric sulfate added is designed to yield a 10:1 ratio of iron to arsenic (Legge, 1993) or antimony (Meyer, 1992) in the solution. No values were found for the ferric sulfate addition required for removal of molybdenum. In the second step lime is added to raise the solution pH and precipitate the iron and facilitate adsorption of the oxyanions. An additional tank may be required to provide adequate time for these reactions. The effluent from this tank, to which a flocculent is added, is pumped to a clarifier to allow settling of the ferric precipitate and the associated Sb, As, and Mo. The underflow from the clarifier is recycled while the treated overflow can be released to the environment (figure 22).

Retention times were reported for the various treatment steps at the Con mine (Legge, 1993). A 20-minute retention time was reported for the hydrogen peroxide oxidation. The same 20 minute value was reported for the ferric sulfate addition, lime addition, and subsequent reaction. A 25 minute retention time was reported for the settling process. These retention times reportedly reduced the arsenic concentration from 27 mg/L in the influent to 0.33 mg/L in the effluent. At the David Bell Mine antimony concentrations were reduced from 3.0 mg/L in the influent to 0.5 mg/L in the effluent (Meyer, 1992).

ACKNOWLEDGEMENTS

Anne Jagunich, with assistance from Kate Willis, Katherine Dahlin, and Cal Jokela conducted dissolution experiments and analyzed drainage samples for pH, specific conductance, alkalinity, and acidity. David Antonson supervised these activities. Albert Klaysmat and Jean Matthew analyzed drainage samples for metals (calcium and magnesium) and sulfate, respectively. Separation of the sulfide mineral fraction of the tailings and analysis of their chemistry and mineralogy were conducted by Louis Mattson of Midland Research, Nashwauk, MN. Specific surface area of the sulfide mineral fraction was analyzed by Eyasu Mekonnen of the Soil Science Department at the University of MN. Jennifer Wessels was responsible for data management and summarized the information presented in section 5.1. J. D. Lehr and Jacqueline Jiran of the MN DNR provided helpful review of section 5.1. Project funding was provided by the Minnesota Minerals Coordinating Committee.

REFERENCES

- American Public Health Association, American Water Works Association, Water Environment Federation. 1992. Standard Methods for the Examination of Water and Wastewater. 18th edition. American Public Health Association, Washington, DC.
- Bradham, W. S., Caruccio, F. T. 1991. A comparative study of tailings analysis using acid/base accounting, cells, columns, and soxhlets. In Proc. of the Second International Conference on the Abatement of Acidic Drainage, V. 1, CANMET, Montreal, Quebec, Canada. p. 157-173.
- Brady, K. B. C., Smith, M. W., Beam, R. L., Cravotta III, C. A. 1990. Effectiveness of the addition of alkaline materials at surface coal mines in preventing or abating acid mine drainage: Part 2. Mine site case studies. In Proc. of the 1990 Mining and Reclamation Conference and Exhibition, Charleston, West Virginia, April 23-26, 1990. p. 227-241.
- Busenberg, E., Clemency, C. 1976. The dissolution kinetics of feldspars at 25°C. *Geochim. Cosmochim. Acta* 40, 41-49.
- Colvine, A. C. 1989. An empirical model to the formation of Archean gold deposits of final cratonization of the Superior Province, Canada: *Econ. Geol. Mon.* 6, p. 37-58.
- Cravotta III, C. A., Brady, K. B. C., Smith, M. W., Beam, R. L. 1990. Effectiveness of the addition of alkaline materials at surface coal mines in preventing or abating acid mine drainage: Part 1. Geochemical considerations. In Proc. of the 1990 Mining and Reclamation Conference and Exhibition, Charleston, West Virginia, April 23-26, 1990. p. 221-225.
- Division of Minerals. 1993a. List of current state metallic mineral leases (Report #4). Minnesota Department of Natural Resources, Division of Minerals, June 2, 1993.
- Division of Minerals. 1993b. Minnesota bedrock geology and state metallic minerals leases: Northern Minnesota, June 1993. Minnesota Department of Natural Resources, Division of Minerals. Geologic map (MGS map S-13) from Morey et al. (1982). Map data were encoded by the Minnesota Land Management Information Center (LMIC). Some modification of the original file was made by the Division of Minerals.
- Eary, E. L., Schramke, J. A. 1990. Rates of inorganic oxidation reactions involving dissolved oxygen. In Chemical Modeling of Aqueous Systems II, Melchior, D. C. and Basset, R. L. eds. ACS Symposium Series 416, American Chemical Society, Washington, D. C. p. 379-396.
- Eckstrand, O. R. (ed.). 1984. Canadian Mineral Deposit Types: A Geologic Synopsis. Economic Geology Report 36. Geological Survey of Canada, 1984, 86 p.

Hem, J. D. 1970. Study and interpretation of the chemical characteristics of natural water. Geological Survey Water-Supply Paper 1473, Washington, D.C. 363 p.

Huang, H. 1993. Introduction to STABCAL program. Montana College of Mineral Science and Technology, Butte, MT, (406) 496-4139. Distributed at Mine Operations and Closure Short Course, April 27-29, 1993, Helena MT. 11 p.

Jiran, J. R. 1990 (unpublished). Archean Lode Gold Deposits in the Superior Province of the Canadian Shield, December 22, 1990. 17 p.

Klein, C., Hurlbut Jr., C. S. 1985. Manual of mineralogy. John Wiley and Sons, New York. 596 p.

Kleinmann, R. L. P., Crerar, D. A., Pacelli, R. R. 1981. Biogeochemistry of acid mine drainage and a method to control acid formation. Mining Eng. March 1981.

Lapakko, K. A. 1991. Non-ferrous mine waste project. Minnesota Department of Natural Resources, Division of Minerals, St. Paul, MN. 68 p. plus appendices.

Lapakko, K.A. 1990. Solid Phase characterization in conjunction with dissolution experiments for prediction of drainage quality. In Proc. Western Regional Symposium on Mining and Mineral Processing Wastes, F. Doyle (ed.), Soc. for Mining, Metallurgy, and Exploration, Inc., Littleton, CO. p. 81-86.

Lapakko, K. A., Antonson, D. A. 1991. The mixing of limestone with acid producing rock. Proc. Second International Conference on the Abatement of Acidic Drainage. Montreal, Canada, September 16-18, 1991.

Legge, M. 1993. Personal communication with Mike Legge, Industrial Coordinator II, Water Resources Division, Yellowknife, Northwest Territories, (403) 920-8243.

Meyer, K. 1992. The David Bell Mine water quality management strategy. CIM Bull. Sept. 1992. p. 27-30.

Nelson, M. 1978. Kinetics and mechanisms of the oxidation of ferrous sulfide. Ph.D. Thesis, Stanford University, Palo Alto, CA.

Nordstrom, D. K. 1982. Aqueous pyrite oxidation and the consequent formation of secondary iron minerals. In Acid Sulfate Weathering. Soil Sci. Am. Madison, WI.

Ojakangas, R. W., Matsch, C. L. 1982. Minnesota's Geology. University of Minnesota Press, Minneapolis, MN, 1982. 255 p.

- Renton, J. J., Rhymer, T. E., Stiller, A.H. 1988. A laboratory procedure to evaluate the acid producing potential of coal associated rocks. *Mining Science and Technology*, 7. p. 227-235.
- Renton, J. J., Stiller, A. H., Rhymer, T. E. 1985. Evaluation of the acid producing potential of toxic rock materials. In *Stopping Acid Mine Drainage: A New Approach*. West Virginia Geological and Economic Survey. p. 7-12.
- Renton, J. J. 1983. Laboratory studies of acid generation from coal associated rocks. In *Proceedings of Surface Mining and Water Quality*, Clarksburg, W.Va. May 26, 1983.
- Singer, P. C., Stumm, W. 1970. Acid mine drainage: The rate determining step. *Science*, 167. p. 1121-1123.
- Stumm, W., Morgan, J. J. 1981. *Aquatic chemistry - an introduction emphasizing chemical equilibria in natural waters*. John Wiley & Sons, Inc. p. 470.
- Sung, W., Morgan, J. J. 1980. Kinetics and product of ferrous iron oxygenation in aqueous systems. *Environ. Sci. Technol.* 14. p. 561-568.
- Twidwell, L. G., Huang, H. H. 1993. Arsenic and heavy metal mobility considerations. Reference notes for Mine Operations Closure Course, April 27-29, 1993, Helena, MT. 40 p.
- Windley, B. F. 1977. *The Evolving Continents*. John Wiley and Sons, New York, NY, 1977. 385 p.

Table 1. Particle size distribution of tailings (wet screening by Hanna Research Center).

Particle Size Distribution, Weight Percent				
Sample	+100M	+270M	+500M	-500M
T1	14.37	35.01	16.66	33.96
T2	0.27	2.48	6.24	91.01
T3	4.04	22.77	19.06	54.13
T4	1.83	18.25	18.60	61.32
T5	8.97	26.82	19.45	44.76
T6	12.88	40.32	20.54	26.26
T7	13.72	27.77	15.87	42.64
T8	7.99	24.49	17.19	50.33
T9	1.42	28.90	28.05	41.63
T10	0.58	16.63	18.16	64.63
T11	83.75	14.28	1.22	0.75
T12	56.04	15.04	12.84	16.08

Table 2. Chemical analysis for regulatory parameters in nonferrous tailing samples.

	Concentrations in PCT				Concentrations in PPM														
	S _{TOT}	SO ₄	S ²⁻	CO ₂	Ag	As	Ba	Be	Cd	Cr	Cu	Hg	Mo	Ni	Pb	Sb	Se	Tl	Zn
T1	0.51	0.06	0.49	9.86	<.5	38	67	<.5	1	146	26	.23	<1	32	15	<5	<1	<1	339
T2	7.63	1.00	7.3	8.91	<.5	429	36	<.5	3	165	155	1.80	<1	125	122	<5	2	<1	931
T3	1.03	0.05	1.01	7.50	<.5	151	22	<.5	<1	209	117	.05	<1	118	22	<5	7	3	114
T4	1.15	0.14	1.10	6.84	<.5	115	25	<.5	<1	212	149	.03	<1	110	19	<5	<1	1	110
T5	0.67	0.04	0.66	2.94	<.5	47	38	<.5	1	64	39	.02	2	27	55	<5	1	2	84
T6	2.12	0.16	2.07	7.54	<.5	1240	42	<.5	<1	104	67	.03	<1	18	21	<5	3	4	66
T7	0.10	0.05	0.08	10.23	<.5	1346	53	<.5	<1	281	33	.05	<1	126	14	18	2	1	60
T8	1.73	0.07	1.70	4.88	<.5	>2000	102	<.5	<1	213	124	1.38	<1	140	106	41	1	<1	85
T9	5.58	5.83	3.64	0.61	1.0	234	402	<.5	1	78	32	21.6	1130	19	26	288	<1	33	152
T10	4.08	0.57	3.89	21.85	<.5	281	90	<.5	2	52	23	.06	<1	26	28	<5	2	4	61
T11	<0.02	0.02	<0.01	0.17	<.5	72	72	<.5	5	2368	1098	.04	<1	463	40	<5	<1	<1	97
T12	<0.02	0.03	<0.01	0.16	<.5	17	42	<.5	<1	156	1615	.03	<1	620	19	<5	<1	1	103

Table 3. Mineralogical composition of non-ferrous tailings (analysis by Hanna Research Center).

		Weight Percent Minerals											
		T1	T2	T3	T4	T5	T6	T7	T8	T9	T10	T11 ¹	T12 ¹
<u>Carbonates</u>													
Calcite		0.2	1.5	0.5	0.6	6.0	1.3	0.2	- ³	1.4	2.1	0.4	0.4
Dolomite		18.9	16.1	14.5	13.0	-	-	20.9	10.1	-	-	-	-
Ankerite		-	-	-	-	0.5	3.6	-	-	-	19.7	-	-
Siderite		1.9	1.3	0.9	1.1	0.2	14.0	0.2	0.1	-	31.4	-	-
CaCO ₃ +MgCO ₃ ²		18.9	18.9	16.3	14.7	6.5	4.5	22.9	11.0	1.4	20.0	0.4	0.4
<u>Regulatory Element-Bearing Minerals</u>													
Pyrite	S	0.86	13.58	1.82	1.99	1.09	1.29	0.04	2.43	6.57	7.32	-	-
Pyrrhotite	S	0.04	0.02	0.10	0.05	0.22	3.50	0.54	1.04	0.13	-	tr ⁵	tr ⁵
Barite	Ba,SO ₄	-	-	-	-	-	-	-	-	14.22	-	-	-
Arsenopyrite	As	0.01	0.09	0.03	0.03	0.01	0.27	0.29	0.40	0.05	0.06	-	-
Chalcopyrite	Cu	0.01	0.04	0.03	0.04	0.01	0.02	0.01	0.04	0.01	0.01	tr ⁵	tr ⁵
Molybdenite	Mo	-	-	-	-	-	-	-	-	0.19	<0.01	-	-
Galena	Pb	<0.01	0.01	<0.01	<0.01	<0.01	<0.01	<0.01	0.01	<0.01	-	-	-
Stibnite	Sb	-	-	-	-	-	-	<0.01	0.01	0.04	0.01	-	-
Sphalerite	Zn	0.05	0.14	0.02	0.02	0.01	0.01	0.01	0.01	0.02	-	-	-

43

- 1 The trace amounts of the sulfides observed in this sample were partially oxidized and generally poorly liberated. Most of the nickel in T11 and T12 occurred in olivine and serpentine rather than in sulfide minerals.
- 2 Total calcium carbonate and magnesium carbonate expressed as percent calcium carbonate, i.e. CaCO₃ + 1.19*(MgCO₃).
- 3 - = not present
- 4 Barite was the only sulfate mineral detected. Sulfate in other samples is probably due to pyrite and/or pyrrhotite oxidation which often forms melanterite, FeSO₄·7H₂O.
- 5 tr = trace

Table 4. Mineralogic Acid Production Potential and Neutralization Potential for tailings.

Solid	% S ²⁻ ¹	APP ²	NP ³
T1	0.50	15.6	189
T2	7.9	247	189
T3	1.08	33.8	163
T4	1.18	36.9	147
T5	0.59	9.06	65
T6	2.10	65.6	45
T7	0.30	9.38	229
T8	1.79	55.9	110
T9	5.03	157	14
T10	6.30	197	200
T11	0.01	0.31	4
T12	0	0	4

¹ Sulfur analysis by Lerch.

² APP = Acid Production Potential, calculated as $31.25 \times \%S^{2-}$.

³ NP = Neutralization Potential, calculated as $10(CaCO_3) + 11.9(MgCO_3)$.

Table 5. Variable Rinse Interval Experiment temperature and relative humidity summary statistics.

	One Week Interval		Three Week Interval	Five Week Interval	Seven Week Interval	Ten Week Interval
	weeks 30-57 ¹	weeks 58-151 ²				
Temperature (°C)						
min	21.7	22.2	24.4	24.3	22.2	22.2
ave	26.0	25.2	25.7	25.5	25.0	25.0
max	27.5	28.3	27.6	27.6	28.3	28.3
sd	1.13	1.24	1.01	0.963	1.32	1.25
n	28	91	20	32	56	68
Relative Humidity (%)						
min	46.2	43.0	46.0	43.0	45.0	43.0
ave	54.2	52.6	56.7	53.4	52.0	51.3
max	64.7	66.0	66.0	66.0	63.3	63.3
sd	6.14	4.90	6.54	6.87	3.44	3.63
n	28	91	20	32	56	68

¹ Solids T1, T3, T4, T5, T7, T8, T11, and T12

² Solids T2, T6, T9, and T10

Table 6. Percent depletion of APP and NP from Long Term Dissolution Experiment for weeks 0-151.

Solid	Reactor	Initial Total Sulfur	APP	APP Released	Percent Released
		%	mg CaCO ₃ /g	mg CaCO ₃	
T2	3	7.63	238	3.18	106
T6	11	2.12	66.2	0.88	8.03
T9	17	5.58	174	2.33	13.7
T10	19	4.08	128	1.70	8.95

Solid	Reactor	Initial NP	Calcium Released	Magnesium Released	NP Released	Percent Released
		mg CaCO ₃ /g	mg CaCO ₃ /g	mg CaCO ₃	mg CaCO ₃ /g	
T2	3	189	33.4	24.1	57.5	30.4
T6	11	45	13.5	9.92	23.4	52.0
T9	17	14	15.6	1.65	17.2	123
T10	19	200	34.8	28.8	63.6	31.8

Table 7. Rates of release for the Long Term Dissolution Experiment for weeks 0-151.

Solid	Reactor	Period (weeks)	No. of Measured Values	Sulfate		Ca + Mg		Calcium		Magnesium	
				rate	r ²	rate	r ²	rate	r ²	rate	r ²
T2	3	19-66	48	0.096	0.986	0.202	0.994	0.102	0.996	0.101	0.990
		67-151	85	0.065	0.995	0.182	1.000	0.103	0.999	0.079	0.997
		19-151	133	0.079	0.986	0.195	0.998	0.103	1.000	0.092	0.992
T6	11	20-51	32	0.033	0.995	0.099	0.999	0.058	1.000	0.041	0.998
		52-69	18	0.048	0.993	0.102	1.000	0.052	1.000	0.050	0.999
		70-151	82	0.034	0.999	0.106	1.000	0.060	1.000	0.046	0.999
		20-151	132	0.035	0.998	0.105	1.000	0.057	0.999	0.048	0.999
T9	17	13-56	44	0.017	0.987	0.060	0.996	0.058	0.996	0.000	1.000
		57-66	10	0.076	0.999	0.115	0.999	0.110	0.999	0.000	1.000
		68-100	33	0.023	0.988	0.050	0.995	0.045	0.995	0.004	0.975
		101-130	30	0.058	0.994	0.082	0.987	0.053	0.986	0.029	0.988
		131-142	12	0.088	1.000	0.016	0.994	0.011	0.997	0.005	0.983
		143-151	9	0.143	0.999	0.016	0.999	0.012	0.999	0.004	1.000
		13-151	139	0.043	0.948	0.067	0.991	0.057	0.978	0.010	0.838
T10	19	11-52	42	0.094	0.993	0.265	0.997	0.132	1.000	0.134	0.991
		53-68	16	0.203	0.999	0.332	1.000	0.143	1.000	0.188	1.000
		69-151	83	0.134	0.989	0.277	0.999	0.151	0.992	0.126	0.998
		11-151	141	0.127	0.995	0.283	0.999	0.141	0.997	0.142	0.995

Table 8. Total years of dissolution for depletion of neutralization potential and acid production potential.

SAMPLE	COMPOSITION				RATE OF DEPLETION		TOTAL YEARS TO DEPLETION ¹	
	mg CaCO ₃ /g		mmole CaCO ₃ /g		mmole/g-wk		NP	APP
	NP _o	APP _o	NP _o	APP _o	NP	APP		
T2	189	246	1.89	2.46	0.0026	0.0011	14.0	45.1
T6	45	66	0.45	0.66	0.0014	0.00047	6.2	27.2
T10	200	197	2.0	1.97	0.0038	0.0017	10.2	22.4

¹ $\text{Years}_{\text{NP}} = (\text{NP}_o / \text{RATE OF NP DEPLETION}) / 52$ and $\text{Years}_{\text{APP}} = (\text{APP}_o / \text{RATE OF APP depletion}) / 52$. This assumes that the average rates observed during the experiment will remain constant over time.

Table 9. Rates of release from weeks 20-57 from the Long Term Dissolution Experiment.

Solid	Reactor	% S	NP ¹	No. of Meas. Values	Sulfate		Ca + Mg		Calcium		Magnesium	
					rate ²	r ²	rate	r ²	rate	r ²	rate	r ²
T1	1	0.51	189	38	0.003	0.942	0.080	1.000	0.050	1.000	0.030	0.997
	2	0.51	189	36	0.004	0.990	0.072	1.000	0.047	0.999	0.026	0.999
T2	3	7.63	189	38	0.086	0.995	0.191	0.993	0.098	0.995	0.094	0.991
	4	7.63	189	36	0.083	0.993	0.213	0.999	0.108	1.000	0.105	0.998
T3	5	1.03	163	38	0.010	0.987	0.102	0.999	0.057	0.999	0.046	0.998
	6	1.03	163	36	0.010	0.991	0.102	0.999	0.058	1.000	0.044	0.997
T4	7	1.15	147	38	0.013	0.970	0.106	0.999	0.061	1.000	0.044	0.996
	8	1.15	147	36	0.014	0.988	0.097	1.000	0.057	1.000	0.040	0.998
T5	9	0.67	65	38	0.001	0.567	0.055	0.998	0.050	1.000	0.005	0.849
	10	0.67	65	36	0.001	0.608	0.054	1.000	0.050	1.000	0.003	0.992
T6	11	2.12	45	38	0.035	0.991	0.100	0.999	0.058	1.000	0.042	0.997
	12	2.12	45	36	0.037	0.994	0.096	1.000	0.057	0.999	0.040	0.997
T7	13	0.10	229	38	0.004	0.972	0.077	0.999	0.052	1.000	0.025	0.991
	14	0.10	229	36	0.004	0.987	0.077	1.000	0.051	1.000	0.026	0.999
T8	15	1.73	110	38	0.005	0.991	0.072	1.000	0.054	1.000	0.018	0.992
	16	1.73	110	36	0.005	0.992	0.073	1.000	0.054	1.000	0.019	0.999
T9	17	5.58	14	38	0.016	0.982	0.060	0.993	0.059	0.993	0.002	0.974
	18	5.58	14	35	0.016	0.975	0.057	0.998	0.056	0.998	0.002	0.988
T10	19	4.08	200	38	0.098	0.981	0.284	0.997	0.134	0.999	0.150	0.993
	20	4.08	200	36	0.097	0.984	0.273	0.999	0.133	1.000	0.139	0.994
T11	21	<0.02	4	38	0.002	0.929	0.004	0.975	0.002	0.964	0.002	0.981
	22	<0.02	4	36	0.002	0.983	0.004	0.993	0.002	0.994	0.002	0.984
T12	23	<0.02	4	38	0.002	0.955	0.022	0.998	0.005	0.956	0.017	0.999
	24	<0.02	4	36	0.003	0.975	0.023	0.998	0.006	0.991	0.017	0.998

¹ kg CaCO₃/t rock. Based on CaCO₃ and MgCO₃ content.

² Rate expressed as mmole/week.

Table 10. Specific surface area analysis (m²/g) and percent recovery.

Sample	Superpanner Separation ¹			Heavy Liquid Separation ²		
	Untreated	6N HCl Rinse ³	Recovery (%)	Untreated	6N HCl Rinse ³	Recovery (%)
T1	1.18 ⁴	NA	59	NA	NA	NA
T2	0.323 ⁴	NA	23	NA	NA	NA
T4	0.450 ⁴	NA	48	NA	NA	NA
T9	0.174 ⁴	0.122 ⁴	41	0.304 ⁴	0.256 ⁵	71.1
T10	0.511 ⁴	NA	19	1.398 ⁵	0.342 ⁵	71.0

NA: not analyzed

- 1 Sulfide mineral separation using superpanner followed by heavy liquid (3.75 specific gravity) separation.
- 2 Sulfide mineral separation using two heavy liquid separations (2.95/3.30 and 3.75 specific gravity).
- 3 1 g sulfide concentrate was leached with 50 mL 6N HCl. Sulfide minerals leached with 6N HCl for 60 minutes to remove surface coatings.
- 4 3-point and 1-point BET measurements averaged as [2(3-point) + 1-point]/3. The 3-point and 1-point measurements were within four percent of their mean.
- 5 1-point BET only

Table 11. Oxidation rates expressed in terms of pyrite mass and surface area.

Solid	FeS Content	A_s : Specific Surface Area ¹	Rate of Sulfate Release ²	Rate of Sulfate Release ³	Rate of Sulfate Release ⁴
	g/75 g tailings	m ² /g	mmole/week	mol/g (FeS)•s	mol/m ² (FeS)•s
				x 10 ⁻¹¹	x 10 ⁻¹¹
T1	0.68	1.18	0.004	0.97	0.82
T2	10.2	0.323	0.084	1.4	4.2
T4	1.53	0.450	0.014	1.5	3.4
T9	5.03	0.174	0.016	0.52	3.0
T10	5.49	0.511	0.098	3.0	5.8
T3	1.44	NA ⁵	0.010	1.2	NA
T5	0.98	NA	0.001	0.17	NA
T6 ⁶	3.59	NA	0.036	1.7	NA
T7	0.44	NA	0.004	1.5	NA
T8	2.6	NA	0.005	0.32	NA

¹ Superpanner separation, untreated; sulfide mineral separation using superpanner followed by heavy liquid (3.75 specific gravity) separation. 3-point and 1-point BET measurements averaged as [2(3-point) + 1-point]/3. The 3-point and 1-point measurements were within four percent of their mean.

² For weeks 20-57, average of the two reactors.

³ Calculated as Rate (mmol/wk)/(86,400)(7)(g FeS)(1000).

⁴ Calculated as Rate (mmol/wk)/(86,400)(7)(grams FeS)(A_s)(1000).

⁵ NA = Not Analyzed

⁶ Pyrrhotite comprises 3.50%, 0.54%, and 1.04% of the iron sulfide in samples T6, T7, and T8, respectively.

Table 12A. Variable Mass Experiment: Acid neutralization by carbonate minerals based on regression data for $([Ca] + [Mg])$ vs. $[SO_4]$, all data¹.

Solid	Neutralization ²	Slope	Y-Intercept ⁴	r ²	n ⁵
T2	2.03	0.985	0.798	0.971	102
T2 ³	2.02	0.990	0.660	0.981	101
T4	2.26	0.886	0.790	0.864	100
T10	1.98	1.009	0.680	0.981	108
ALL	2.01	0.997	0.717	0.982	310
ALL ³	2.01	0.997	0.687	0.986	309

Table 12B. Variable Mass Experiment: Acid neutralization by carbonate minerals based on regression data for $([Ca] + [Mg])$ vs. $[SO_4]$, for sulfate values less than 1.0 mmole/L¹.

Solid	Neutralization ²	Slope	Y-Intercept ⁴	r ²	n ⁵
T2	1.63	1.230	0.515	0.190	6
T4	1.55	1.292	0.577	0.832	72
T10	1.57	1.272	0.641	0.428	15
ALL	1.56	1.285	0.581	0.824	93

¹ Weeks 0-37 of the Long Term Dissolution Experiment for the 75 gram sample and weeks 1-37 of the Variable Mass Experiment.

² Moles of acid neutralized per mole of calcium carbonate and magnesium carbonate dissolved. Calculated as $2/\text{slope}$.

³ One outlier removed.

⁴ Represents the sum of calcium and magnesium concentrations when the sulfate concentration is zero. That is, the y-intercept represents the calcium and magnesium carbonate mineral dissolution which does not neutralize acid (reaction 17).

⁵ n = number of data points for regression.

Table 12C. Variable Mass Experiment: Acid neutralization by carbonate minerals based on regression data for $([Ca] + [Mg])$ vs. $[SO_4]$, for sulfate values less than 0.5 mmole/L¹.

Solid	Neutralization ²	Slope	Y-Intercept ³	r ²	n ⁴
T4	1.25	1.606	0.508	0.588	43

Table 12D. Variable Mass Experiment: Acid neutralization by carbonate minerals based on regression data for $([Ca] + [Mg])$ vs. $[SO_4]$, for sulfate values less than 0.25 mmole/L¹.

Solid	Neutralization ²	Slope	Y-Intercept ³	r ²	n ⁴
T4	1.05	0.903	0.469	0.334	24

¹ Weeks 0-37 of the Long Term Dissolution Experiment for the 75 gram sample and weeks 1-37 of the Variable Mass Experiment.

² Moles of acid neutralized per mole of calcium carbonate and magnesium carbonate dissolved. Calculated as $2/\text{slope}$.

³ Represents the sum of calcium and magnesium concentrations when the sulfate concentration is zero. That is, the y-intercept represents the calcium and magnesium carbonate mineral dissolution which does not neutralize acid (reaction 17).

⁴ n = number of points for regression.

Table 13. Trends in pH, sulfate, calcium, magnesium, calcium plus magnesium, and alkalinity vs. oxidation interval¹.

Solid	pH	Sulfate	Calcium	Magnesium	Ca + Mg	Alkalinity
T1	no variation	increase to 3 week, then plateau	increase	increase to 3 week, then plateau	increase	increase
T2 ²	no variation	increase to 5 week, then plateau	increase	increase to 5 week, then slight decrease	increase	increase to 5 week, then plateau
T3	no variation	slight increase	increase	increase to 3 week, then plateau	increase	increase
T4	no variation	slight increase to 3 week, then plateau	increase	increase to 5 week, then plateau	increase	increase to 5 week, then plateau
T5	no variation	variable	increase	no variation	increase	increase
T6 ²	decrease	increase	slight increase	slight increase	increase	plateau to 5 week, then slight decrease
T7	slight decrease (?)	slight increase (?)	increase	increase	increase	increase to 3 week, then plateau
T8	slight decrease (?)	increase to 3 week, then slight decrease	increase	increase	increase	increase to 5 week, then plateau
T9 ²	no variation	decrease after 5 week	no variation	no variation	no variation	slight increase to 5 week then plateau
T10 ²	slight decrease (?)	increase	increase	increase	increase	no variation
T11	increase to 3 week, then slight decrease	no variation	slight increase	increase	increase	plateau to 5 week, then increase
T12	increase to week 7, then decrease	slight decrease	increase	increase	increase	increase

¹ Based on visual examination.

² Solids have only 1 week, 5 week, and 7 week oxidation intervals

Table 14. Percent APP released during the Elevated Temperature Experiment, weeks 0-48.

Solid	Reactor	Initial Total Sulfur	APP	APP Released	Percent Released
		%	mg CaCO ₃ /g	mg CaCO ₃ /g	
T1	3	0.51	15.9	15.6 ¹	98.1 ¹
	4	0.51	15.9	8.43	52.8
T2	14	7.63	238	171	71.5
	15	7.63	238	163	68.5
	16 ¹	7.63	238	165	69.4
T4	5	1.15	35.9	20.5	57.3
	6	1.15	35.9	19.9	55.2
T8	7	1.73	54.1	11.6	21.6
	8	1.73	54.1	11.3	20.2
T9	9	5.58	174	43.9	25.2
	10	5.58	174	42.0	24.1
T10	11	4.08	128	128	101
	12	4.08	128	135	106
	13 ¹	4.08	128	130	102
T12	1	0.02	0.63	1.03	166
	2	0.02	0.63	0.894	143

¹ The total APP release was skewed by a single anomalously high sulfate analysis. The values from reactor 4 are assumed to be more realistic.

² Reactors were rinsed with room temperature water.

Table 15. Percent NP released during the Elevated Temperature Experiment, weeks 0-48.

Solid	Reactor	Initial NP	Calcium Released	Magnesium Released	NP Released	Percent Released
		mg CaCO ₃ /g				
T1	3	189	12.0	5.09	17.1	9.04
	4	189	11.5	4.84	16.3	8.62
T2	14	189	94.7	54.2	149	78.8
	15	189	94.5	57.8	152	80.6
	16 ¹	189	87.6	56.4	144	76.2
T4	5	147	19.8	8.36	28.2	19.2
	6	147	20.0	8.62	28.6	19.5
T8	7	110	13.8	4.57	18.4	16.7
	8	110	13.0	4.37	17.4	15.8
T9	9	14	12.4	1.87	14.3	102
	10	14	12.9	1.91	14.8	106
T10	11	200	80.7	33.5	114	57.1
	12	200	90.6	31.3	122	61.0
	13 ¹	200	82.4	28.1	110	55.3
T12	1	4	1.52	4.61	6.14	153
	2	4	1.09	3.64	4.73	118

¹ Reactors were rinsed with room temperature water.

Table 16. Comparison of percent APP and NP released in Elevated Temperature and Long Term Dissolution Experiments.

Solid	Elevated Temperature			Long Term Dissolution		
	Number of Weeks	APP Released (%)	NP Released (%)	Number of Weeks	APP Released (%)	NP Released (%)
T1	48	98	9.0	57	8.3	3.4
	48	53	8.6	55	8.2	3.0
T2	48	71	79	57	11	18
	48	68	81	55	11	18
T4	48	57	19	57	6.1	5.6
	48	55	19	55	6.5	5.3
T8	48	22	17	57	2.9	5.6
	48	20	16	55	2.8	5.4
T9	48	25	100	57	3.5	69
	48	24	100	54	3.8	65
T10	48	100	57	57	13	14
	48	100	61	55	12	13
T12	48	160	150	57	88	36
	48	143	120	55	98	34

Table 17. Comparison of sulfate release rates between Elevated Temperature Experiment and overall rates in the Long Term Dissolution Experiment.

Solid	Reactor	% S	Period (weeks) ¹	Sulfate ²	
				rate	rate ³
T1	odd	0.51	6-18	0.157	0.003
			22-48	0.101	
	even	0.51	2-32	0.149	0.004
			36-48	0.066	
T2	odd	7.63	2-22	4.318	0.086
			24-48	1.096	
	even	7.63	2-32	3.504	0.083
			40-48	0.289	
T4	odd	1.15	2-28	0.475	0.013
			32-48	0.120	
	even	1.15	2-28	0.435	0.014
			34-48	0.152	
T8	odd	1.73	2-8	0.061	0.005
			8-18	0.431	
			18-48	0.143	
	even	1.73	12-22	0.319	0.005
24-48			0.127		
T9	odd	5.58	8-12	2.846	0.016
			20-48	0.210	
	even	5.58	6-12	2.079	0.016
			14-20	0.129	
			22-30	0.977	
			36-48	0.084	
T10	odd	4.08	2-8	5.087	0.098
			10-20	2.076	
			22-38	1.624	
			40-48	0.398	
	even	4.08	2-18	3.102	0.097
			20-30	2.867	
			32-48	0.741	
T12	odd	<0.02	12-22	0.008	0.002
			24-34	0.009	
			40-48	0.006	
	even	<0.02	10-20	0.008	0.003
			22-48	0.004	

¹ For Elevated Temperature Experiment only.

² Release rate in mmole/week.

³ From Long Term Dissolution Experiment, weeks 20-57.

Table 18. Comparison of neutralization from the Elevated Temperature Experiment and the Long Term Dissolution Experiment¹.

Solid	Reactor	Elevated Temperature			Long Term Dissolution		
		APP Released	NP Released	H^+ prod. ² carb. diss.	APP Released	NP Released	H^+ prod. ² carb. diss.
		mg CaCO ₃ /g	mg CaCO ₃ /g		mg CaCO ₃ /g	mg CaCO ₃ /g	
T1	odd	15.6	17.1	1.83	1.32	6.46	0.409
	even	8.42	16.3	1.03	1.31	5.70	0.460
T2	odd	170	149	2.29	25.8	34.2	1.51
	even	163	152	2.14	25.6	33.8	1.52
T4	odd	20.6	28.1	1.46	2.20	8.26	0.533
	even	19.8	28.6	1.39	2.34	7.75	0.604
T8	odd	11.7	18.4	1.27	1.57	6.22	0.505
	even	10.9	17.4	1.26	1.49	5.95	0.501
T9	odd	43.9	14.3	6.13	6.14	9.60	1.28
	even	42.0	14.8	5.68	6.64	9.15	1.45
T10	odd	128	114	2.25	17.0	27.8	1.22
	even	135	122	2.22	15.8	26.6	1.19
T12	odd	1.04	6.14	0.337	0.550	1.46	0.753
	even	0.894	4.73	0.378	0.610	1.38	0.884

¹ Elevated Temperature Experiment data based on 48 weeks of release and Long Term Dissolution Experiment based on 57 weeks of release.

² H^+ produced per mole of calcium and magnesium carbonate mineral dissolved. Calculated as $(2 * \text{APP Released}) / \text{NP Released}$.

Table 19. Summary of field vs. laboratory drainage quality data.

Sample	Parameter	Field (mg/L)	Laboratory (mg/L)	Comments
T3/T4 ¹	Arsenic	0.02 - 0.17	<0.030 ² - 0.055	Field = Lab x 3
	Copper	1.0 - 14.2	0.002 - 0.015	Field = Lab x 1000
	Nickel	1.9 - 6.6	<0.010 - 0.012	Field = Lab x 500
	Lead	0.3 - 0.14	<0.020 - 0.023	Field = Lab x 30
	Zinc	0.01 - 0.14	<0.005 - 0.030	Field = Lab x 5
T5	Barium	NA ³	<0.05 - 0.111	
	Zinc	0.02	<0.01 - 0.021	Field = Lab
T6	Arsenic	0 - 0.370	<0.05	NC ⁴
	Cadmium	0.002 - 0.015	<0.01	Field =? Lab ⁵
	Chromium	0.003 - 0.019	<0.01	Field =? Lab
	Copper	0.004 - 0.027	<0.01	Field =? Lab x 3
	Lead	0.012 - 0.090	<0.02	NC
	Mercury	0.0001 - 0.0003	0 - 0.001 ⁶	Field = Lab x 0.3
	Silver	0.002 - 0.011	<0.005 - 0.007 ⁷	Field = Lab
	Zinc	0.021 - 0.533	<0.010 - 0.028	Field = Lab x 20
T7	Antimony	NA	<0.05 - 0.257	
	Arsenic	1.77 - 11.60	0.181 - 4.871	Field = Lab
	Copper	0.34 - 20.00	<0.01 - 0.025	Field = Lab x 1000 ⁸
	Nickel	1.22 - 27.20	<0.01 - 0.014	Field = Lab x 2000
	Zinc	0.10 - 24.8	<0.01 - 0.059	Field = Lab x 500
T9	Antimony	<0.002 - 0.024	0.233 - 2.833	Field = Lab x 0.01
	Arsenic	<0.002 - 0.004	<0.05 - 0.142	Field = Lab x 0.03
	Barium	NA	<0.05 - 0.247	
	Molybdenum	0.13 - 0.62	<0.01 - 0.746	Field = Lab
	Zinc	<0.01 - 0.07	<0.01 - 0.030	Field = Lab
T10	Copper	<0.01 - 0.01	<0.01	Field = Lab
	Nickel	<0.01 - 0.18	<0.01 - 0.037	Field = Lab x 5
	Zinc	<0.01 - 0.15	<0.01 - 0.142	Field = Lab

- 1 Solids were from the same site. The ranges of data were below or slightly above the detection limit for both samples.
- 2 < = below detection limit
- 3 NA = Not Analyzed
- 4 NC = Not Calculated since laboratory concentrations were below detection limit.
- 5 =? means field concentrations were low and laboratory concentrations were undetectable, assumed to be approximately equal.
- 6 Mercury analyses of laboratory samples were questionable.
- 7 Only two samples had concentrations above the detection limit of 0.005 mg/L.
- 8 Although copper concentrations in the field were considerably higher than those observed in the laboratory, the laboratory data suggested elevated copper release.

Table 20. Ratio of trace metal concentrations in the field to those in the laboratory. The upper ends of the observed ranges were used for calculation.

Parameter	T3/T4	T5	T6	T7	T9	T10
Antimony	NA ¹	NA	NA	NA	0.01	NA
Arsenic	3	NA	NC ²	2	0.03	NA
Cadmium	NA	NA	1	NA	NA	NA
Chromium	NA	NA	1	NA	NA	NA
Copper	1000	NA	3	1000 ³	NA	1
Lead	30	NA	5	NA	NA	NA
Mercury	NA	NA	NC	NA	NA	NA
Molybdenum	NA	NA	NA	NA	1	NA
Nickel	500	NA	NA	2000	NA	5
Silver	NA	NA	1	NA	NA	NA
Zinc	5	1	20	500	2	1

¹ NA: not analyzed in the field.

² NC = Not Calculated.

³ Although copper concentrations in the field were considerably higher than those observed in the laboratory, the laboratory data suggested elevated copper release.

Figure 1. Long Term Dissolution Experiment reactor.

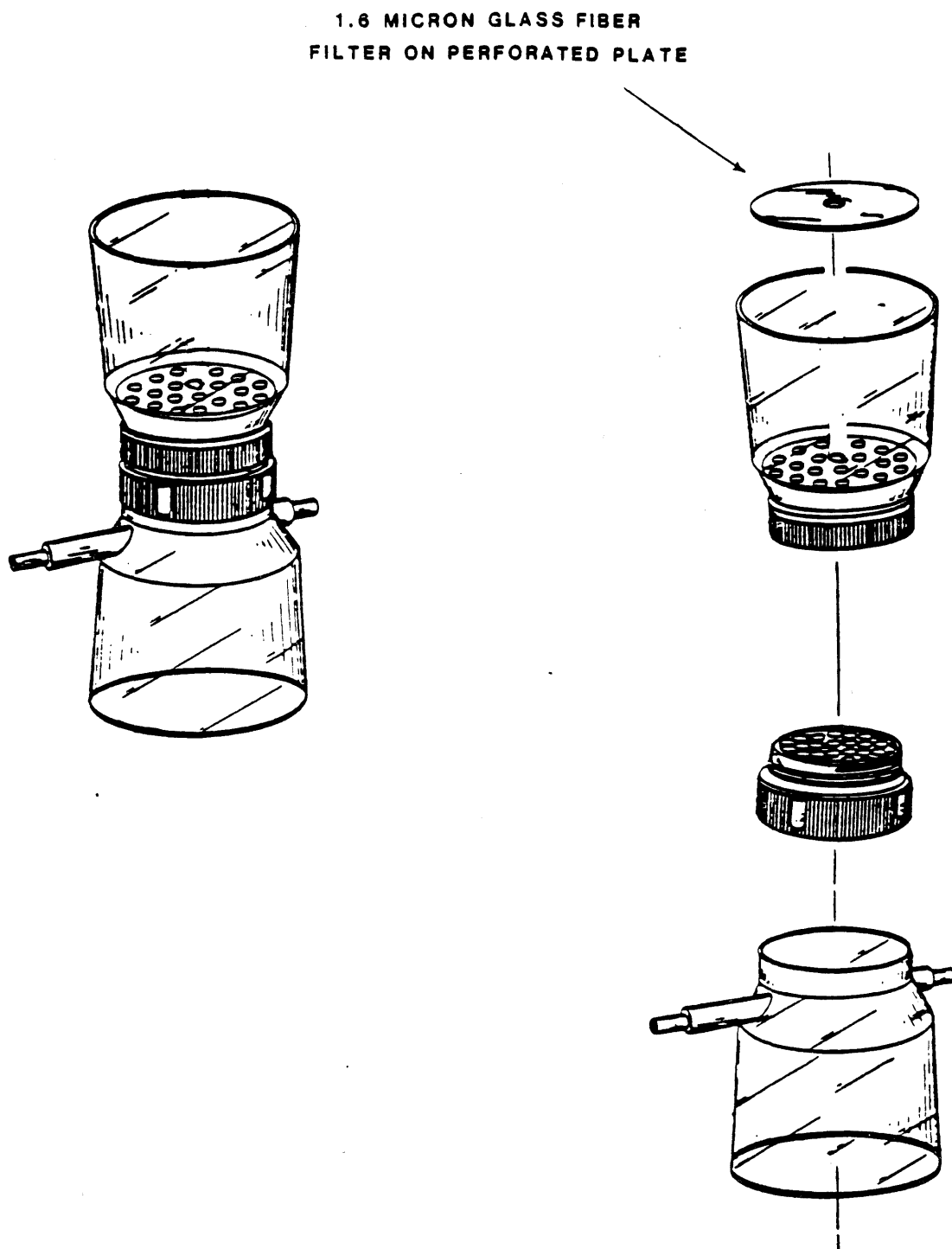


Figure 2. Temperature and relative humidity for the Long Term Dissolution Experiment, weeks 0-151.

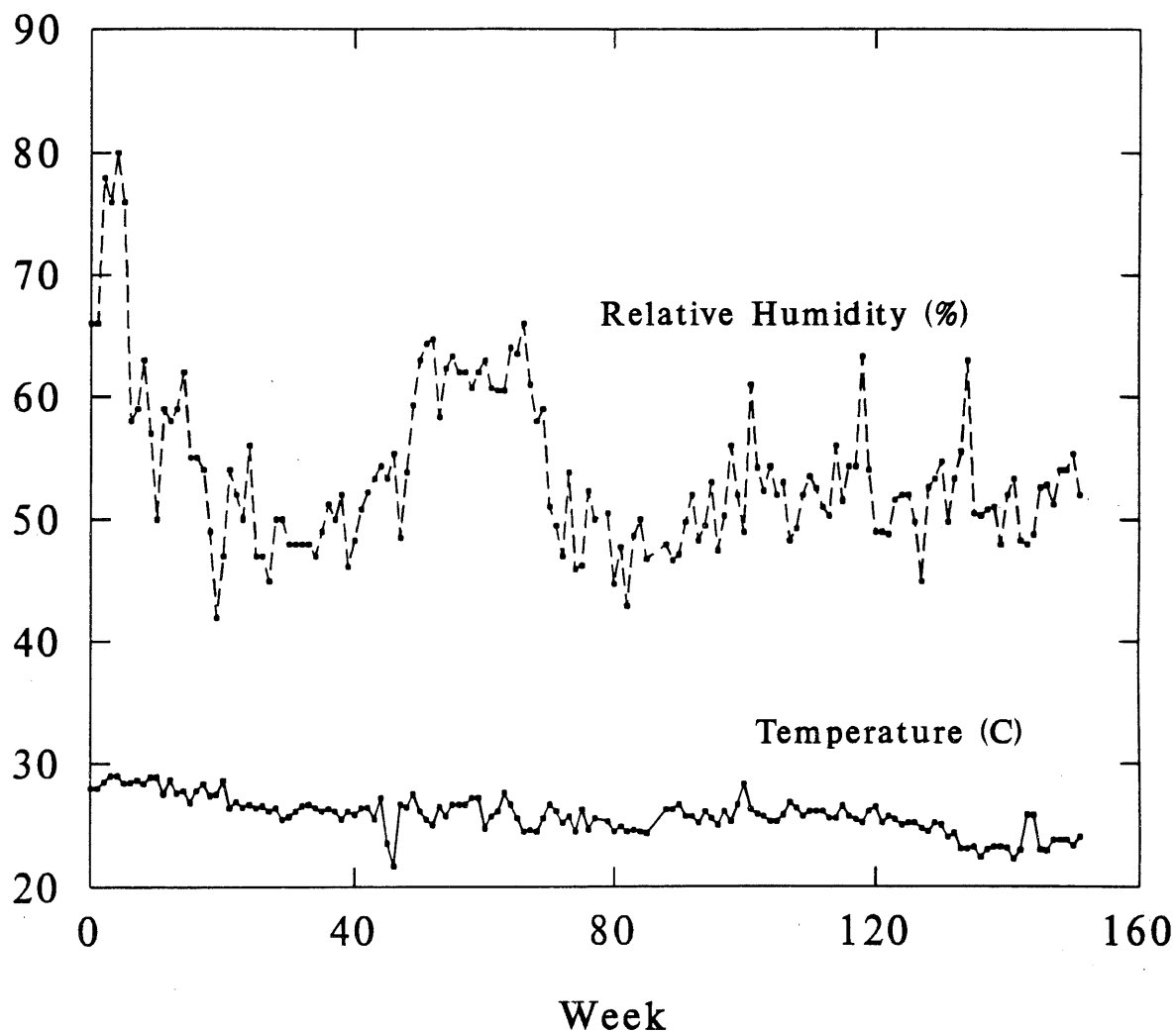
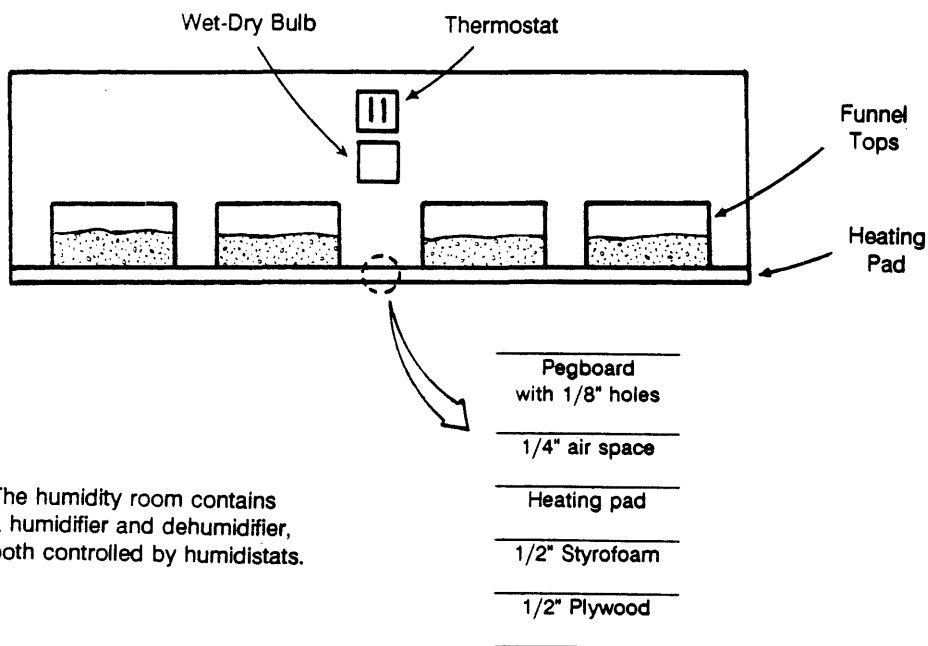
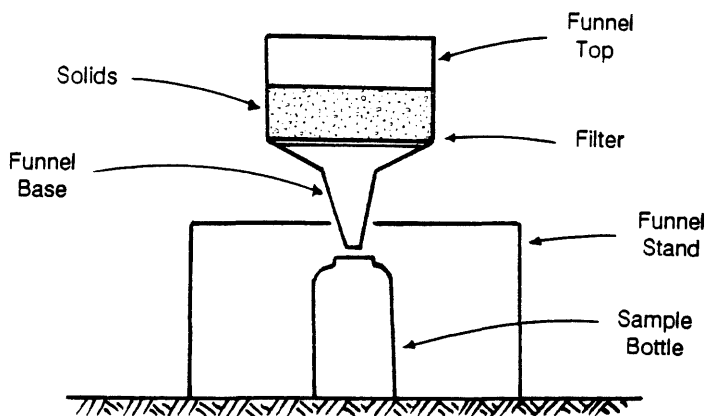


Figure 3. Variable Mass Experiment reactor (top) and experimental apparatus (bottom).



Note: The humidity room contains a humidifier and dehumidifier, both controlled by humidistats.

Figure 4. pH, sulfate, calcium, and magnesium concentrations vs. time for T9, reactor 17 from the Long Term Dissolution Experiment.

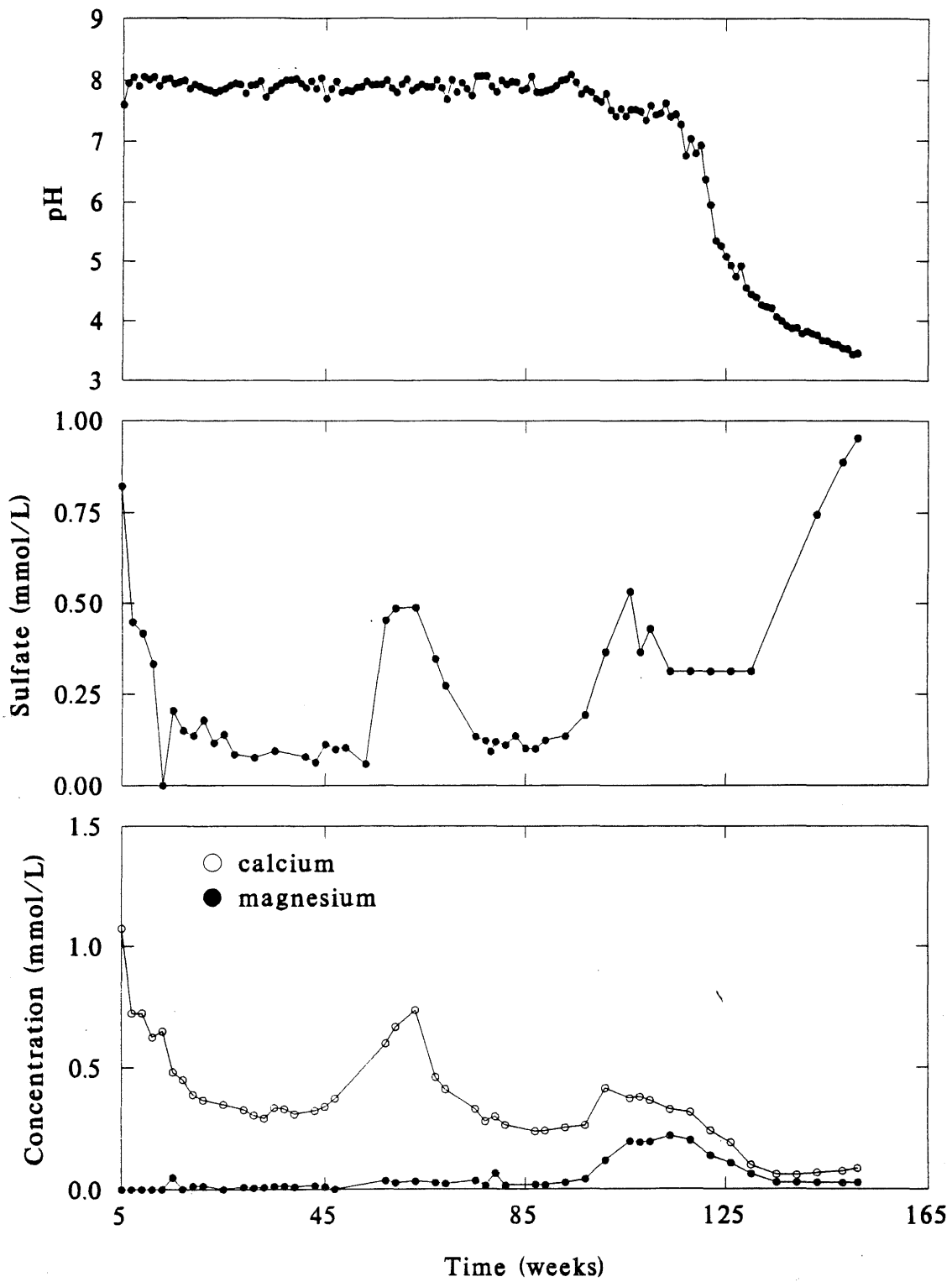


Figure 5. Sulfate, calcium plus magnesium, calcium, and magnesium cumulative mass release vs. time for T9, reactor 17 from the Long Term Dissolution Experiment.

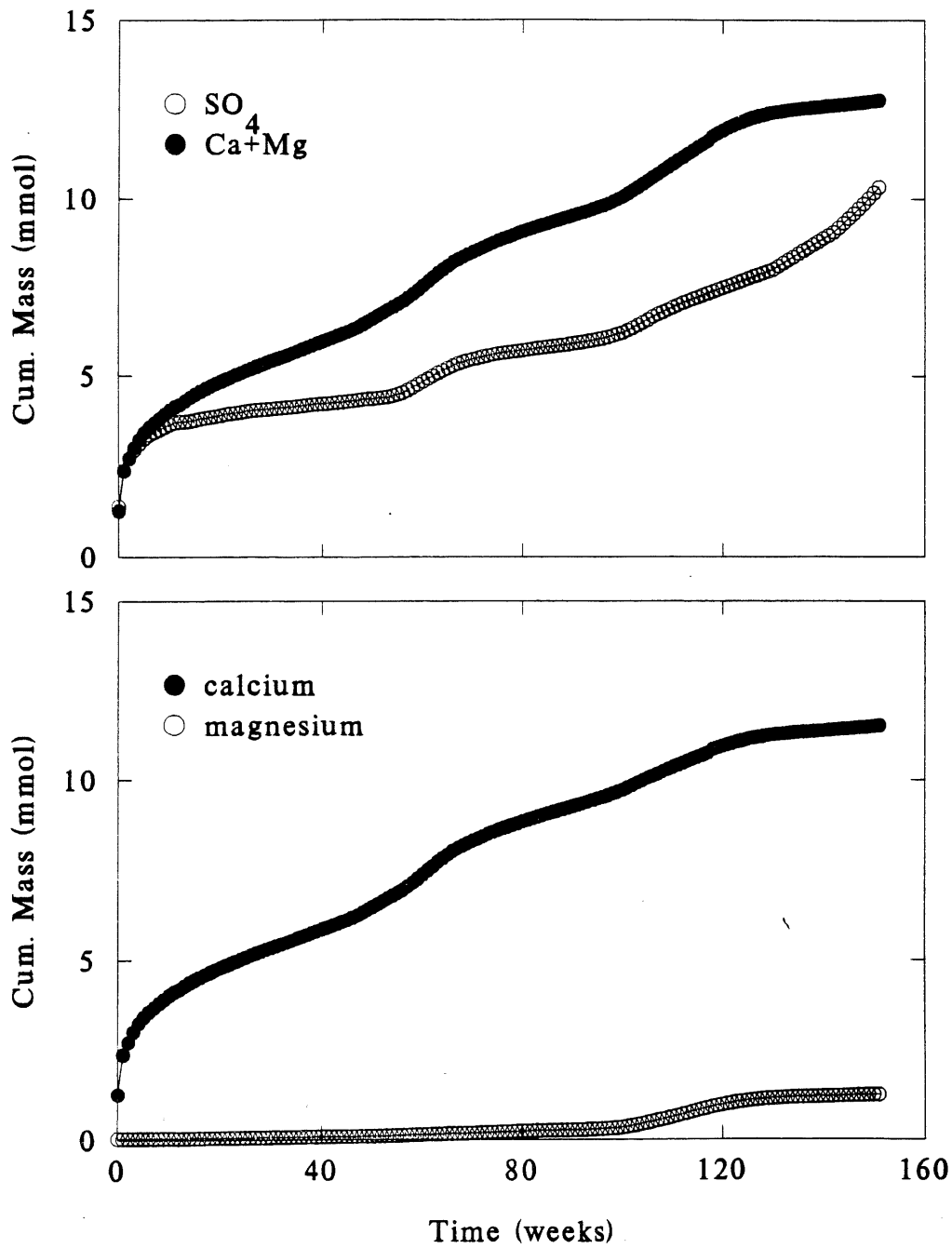


Figure 6. Sulfate concentration vs. time for T2, T6, and T10 from the Long Term Dissolution Experiment.

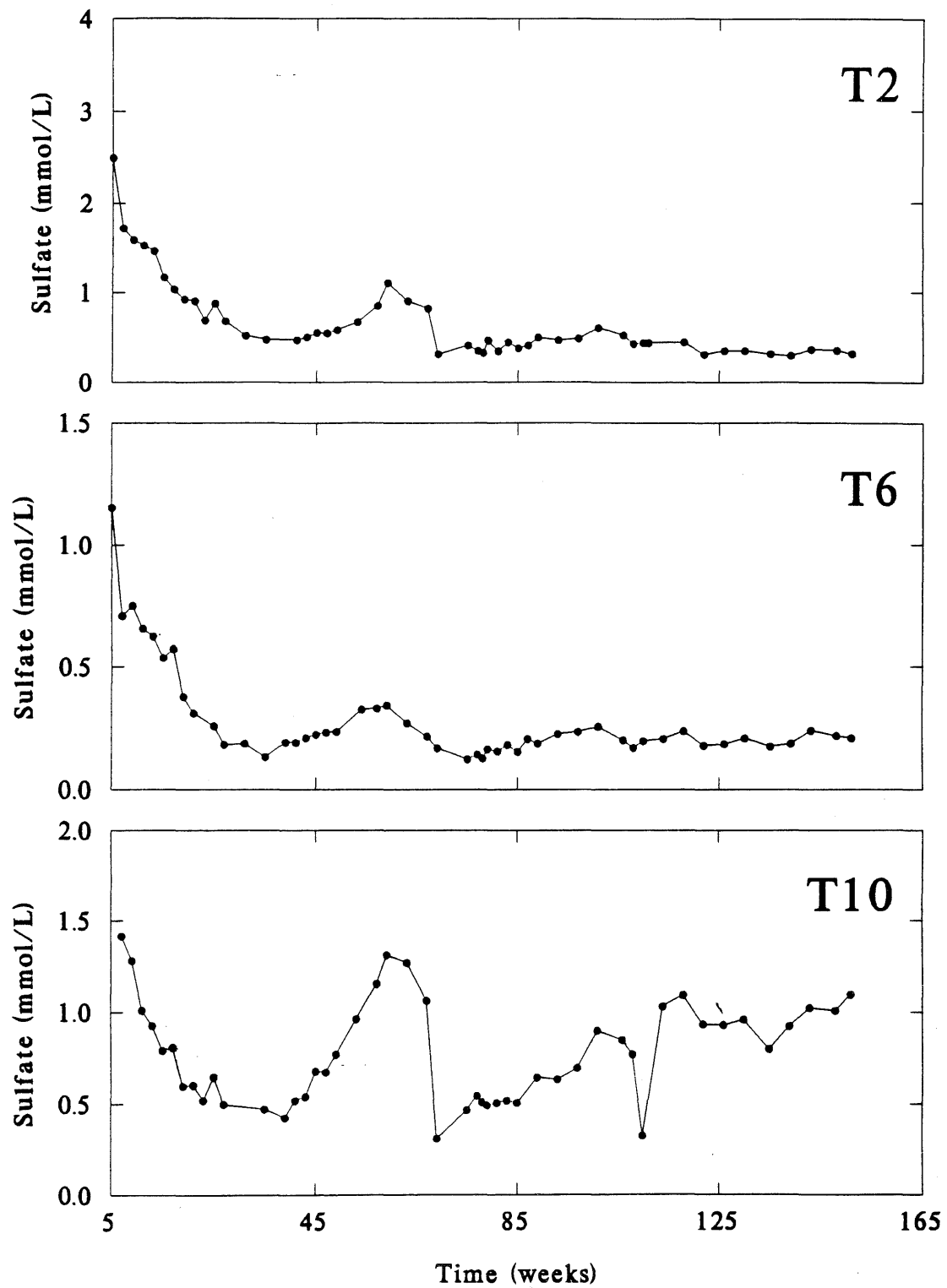


Figure 7. Calcium and magnesium concentrations vs. time for T2, T6, and T10 from the Long Term Dissolution Experiment.

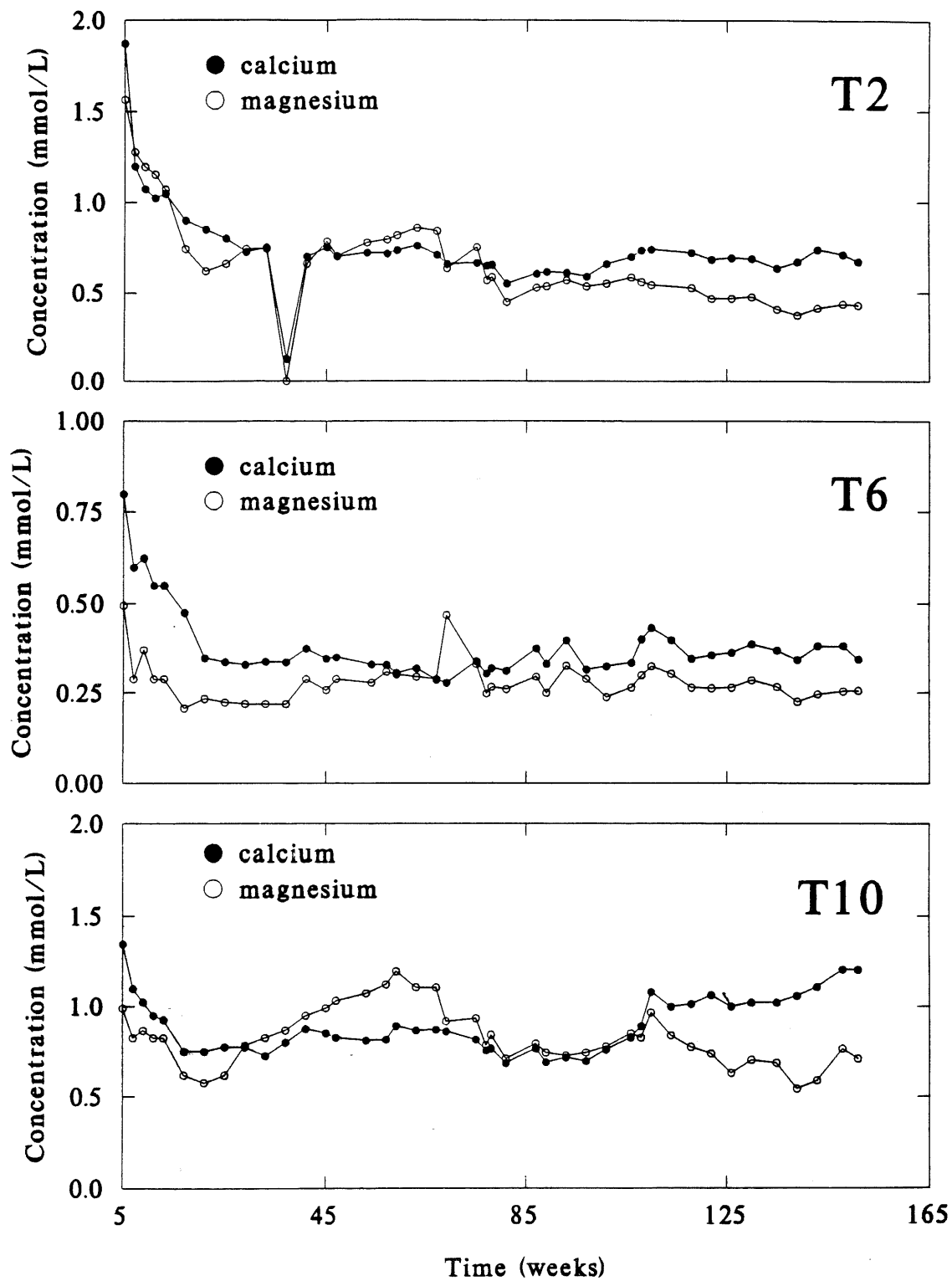


Figure 8. Long Term Dissolution Experiment depletion of APP and NP in 151 weeks.

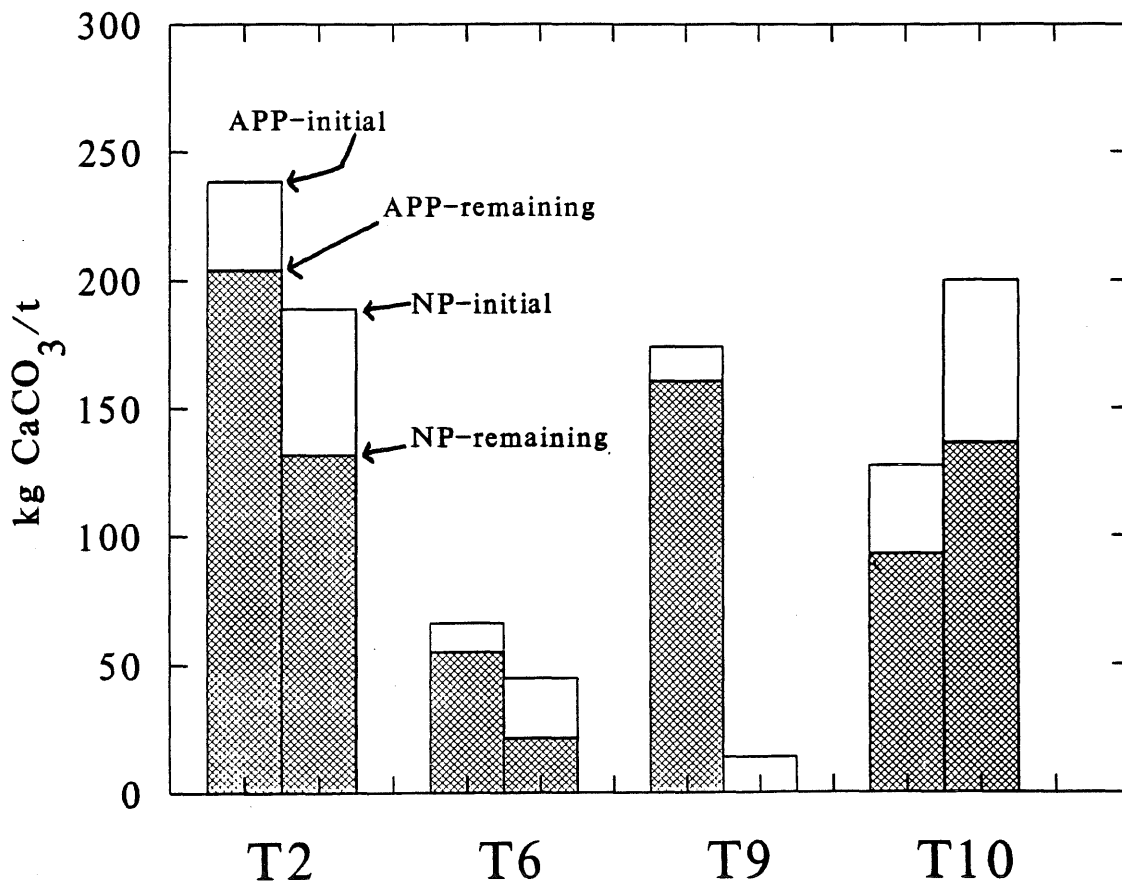


Figure 9. Rate of sulfate release vs. percent sulfide for the Long Term Dissolution Experiment (Solids T2, T6, T9, and T10), weeks 0-151. Regression statistics given on plot are exclusive of sample T10, considered to be an outlier (with T10: $y = 0.007x + 0.042$; $n = 4$; $r^2 = 0.130$).

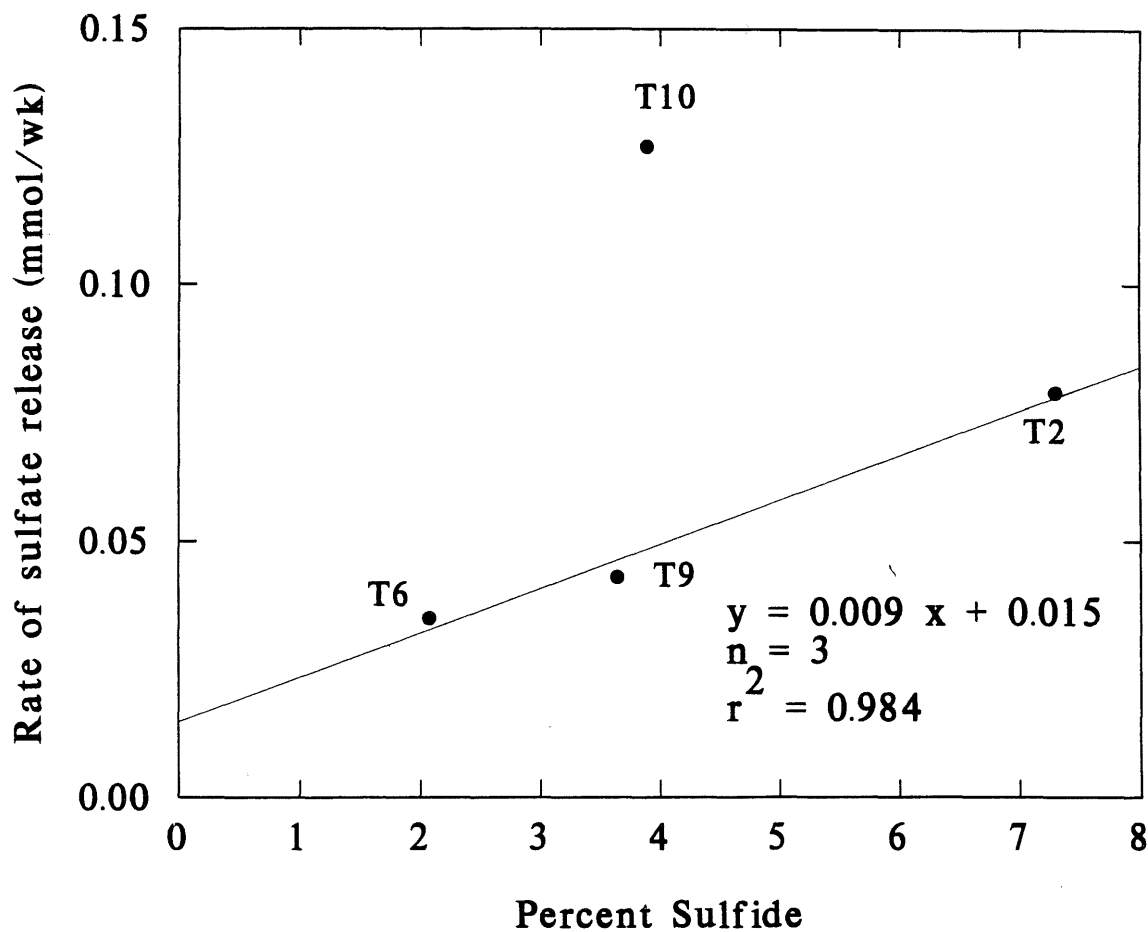


Figure 10. Rate of sulfate release vs. percent sulfide for all twelve solids, weeks 20-57. Regression statistics given on the plot include all solids. If solid T10 were considered an outlier then $y = 0.011x - 0.001$; $n = 22$; $r^2 = 0.841$.

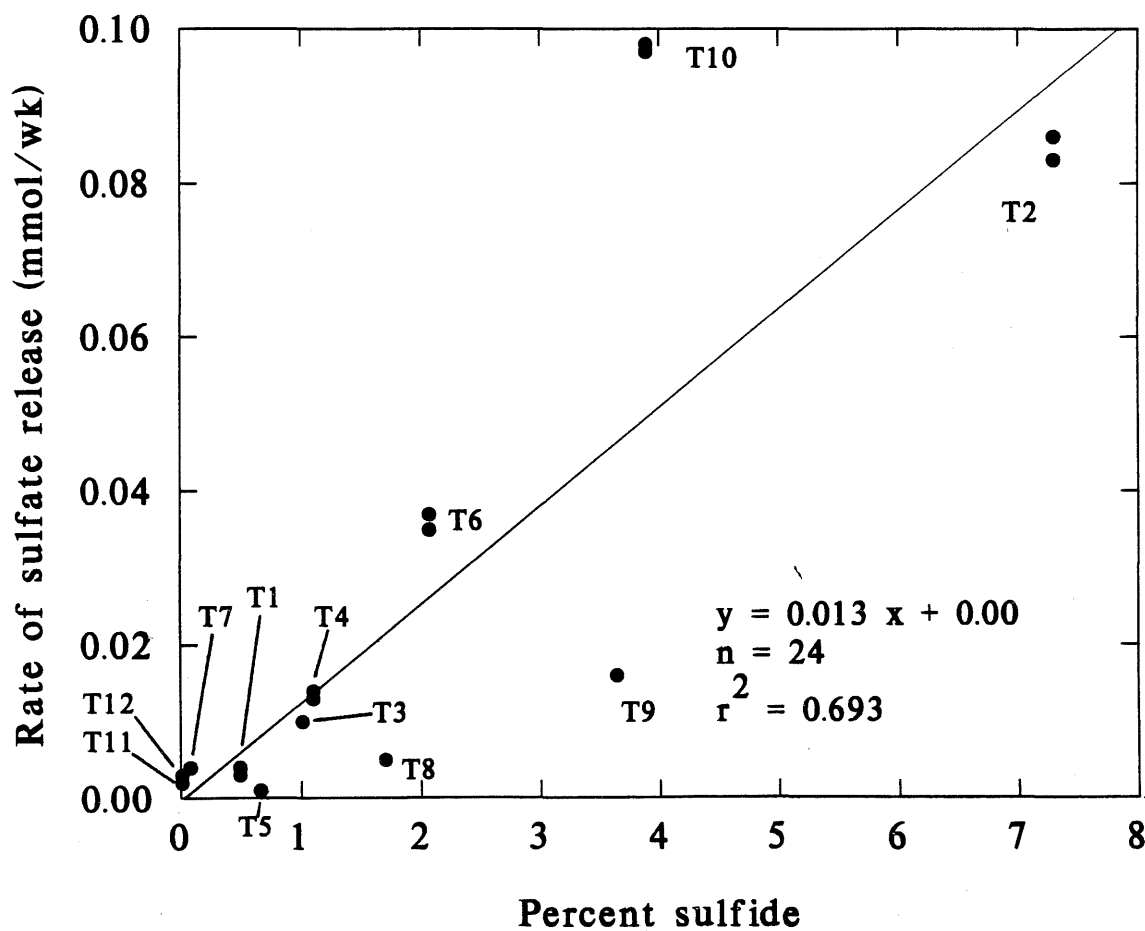
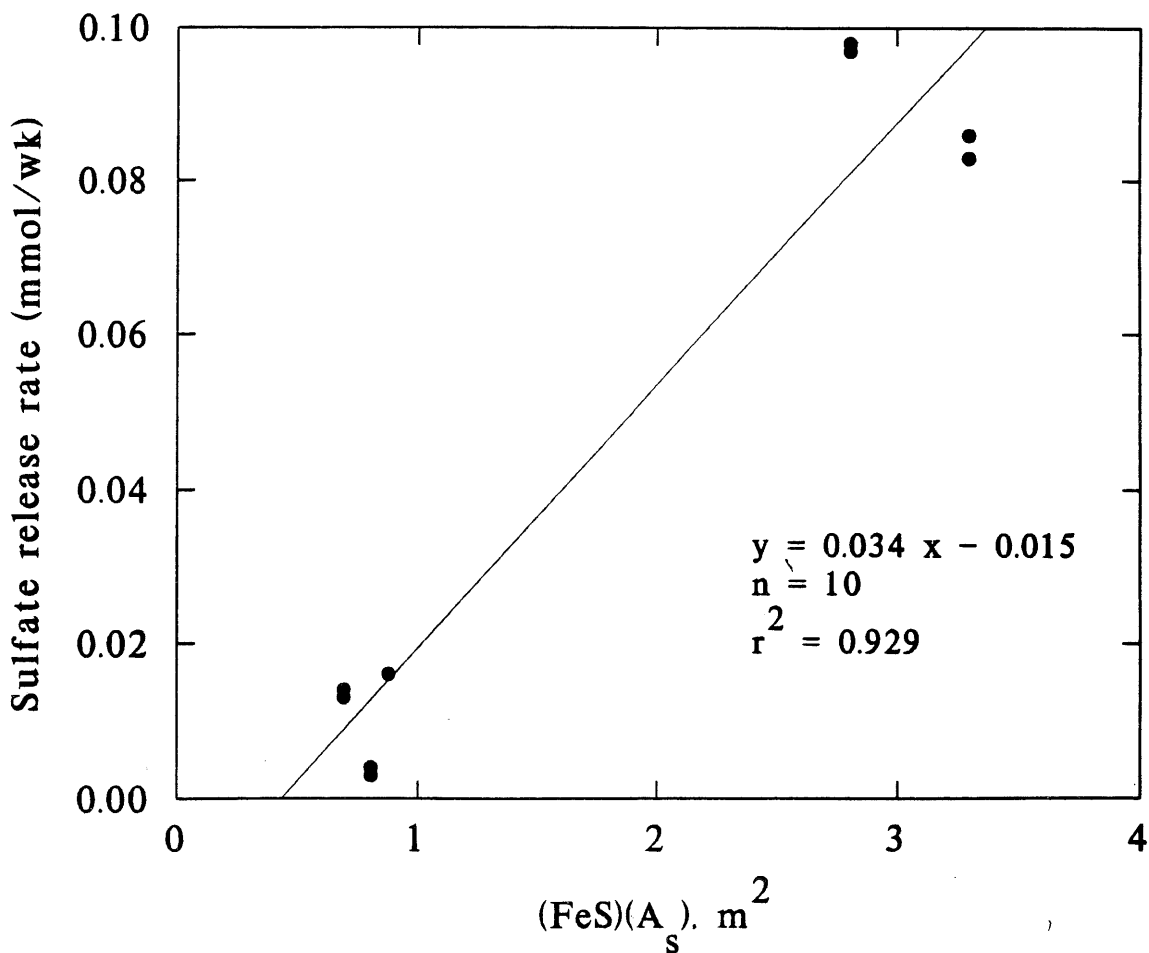


Figure 11. Rate of sulfate release vs. iron sulfide surface area for solids T1, T2, T4, T9, and T10. The iron sulfide specific area determinations are qualitative.



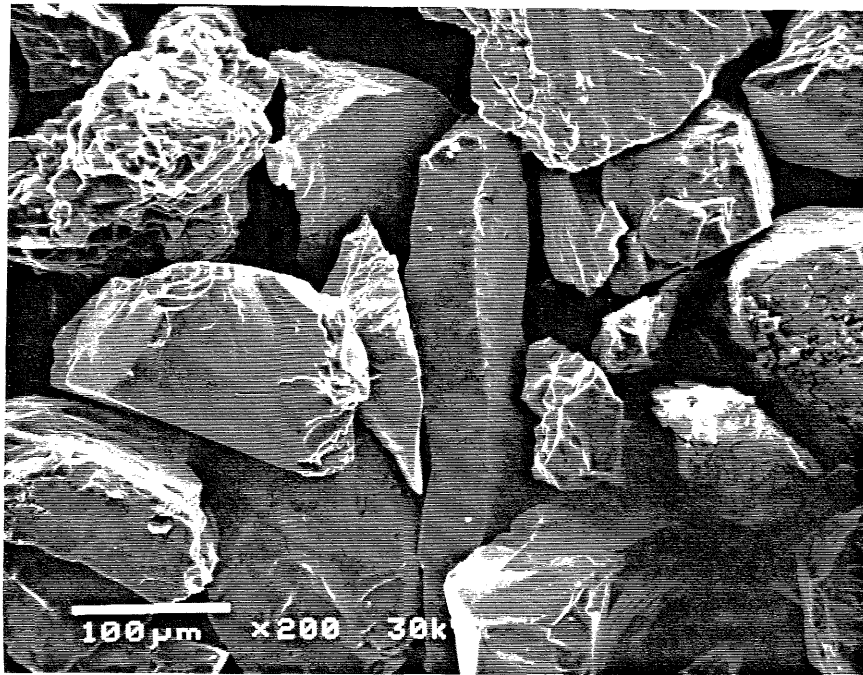


Figure 11A. T1 (flowsheet A sulfide concentrate).

Typical coarse grained pyrite recovered from this sample. Approximately 15-20% of the pyrite is rough textured and/or porous as illustrated by upper left and center right grains. Note magnification of this photo is 200X (scale bar = 100 microns) compared to all other photos at 500X (figures 11A - 11F captions by Lou Mattson, Midland Research Center).

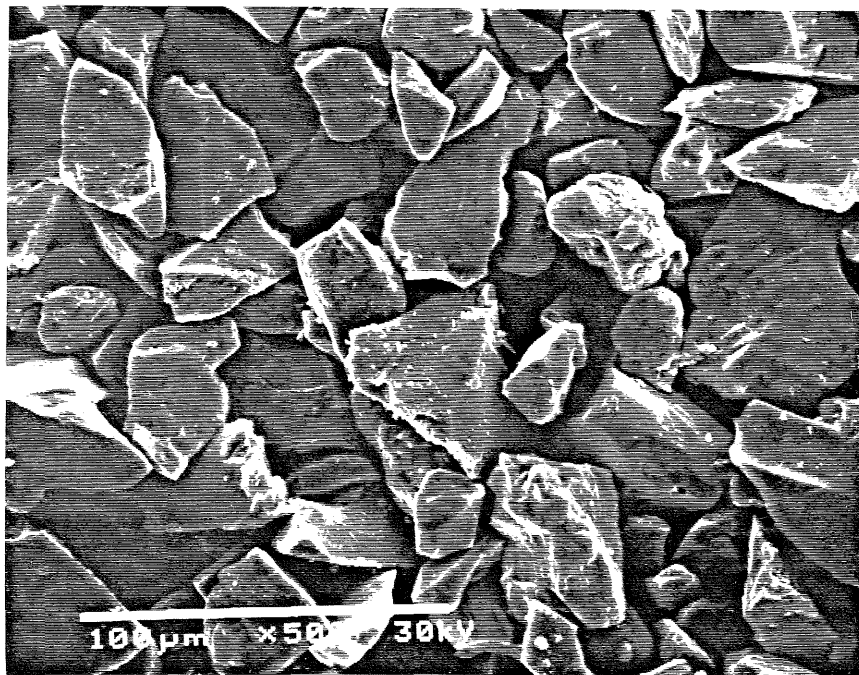


Figure 11B. T2 (flowsheet A sulfide concentrate)

Typical mostly smooth textured pyrite grains recovered. Note scattered rough textured surfaces. Magnification 500X, scale bar = 100 microns.

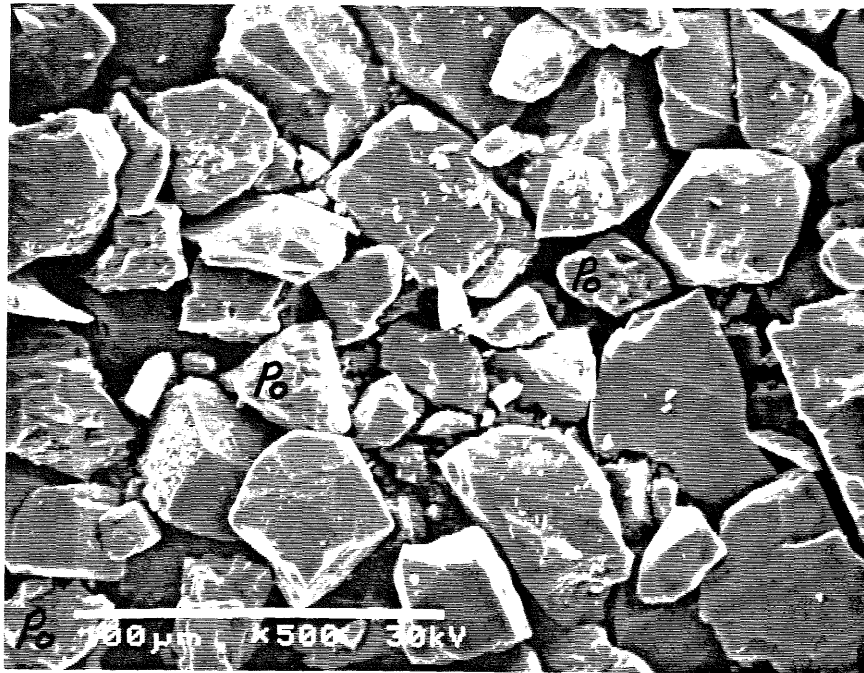


Figure 11C. T4 (flowsheet A sulfide concentrate)

Concentrate is dominantly smooth textured pyrite with some (10%) generally rough textured pyrrhotite (po). The grain mount indicates more fines in this concentrate than were observed in other concentrates. Note the apparent iron sulfate on the surface of the lower pyrite "cube." Magnification 500X, scale bar = 100 microns.

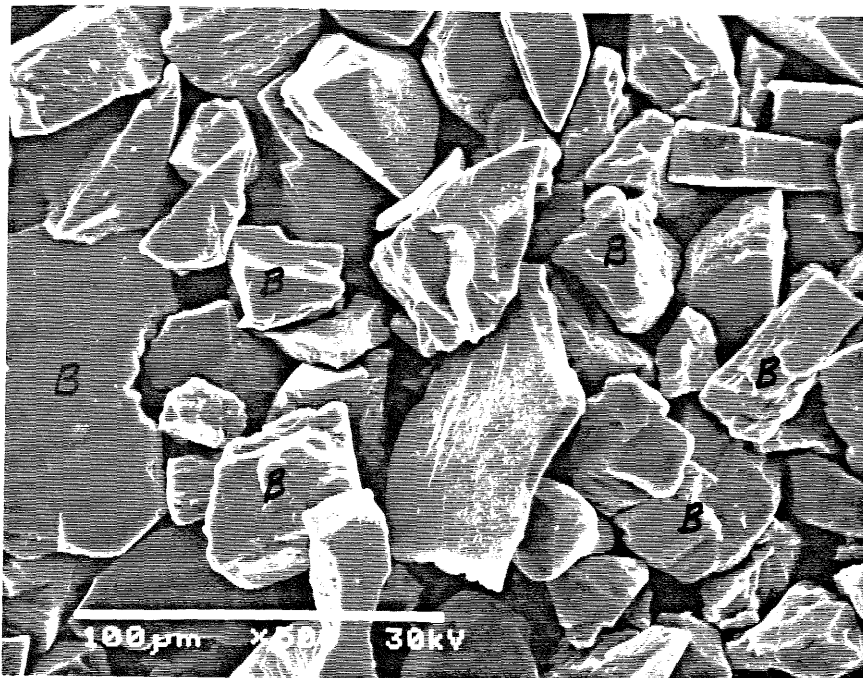


Figure 11D. T9 (flowsheet A sulfide concentrate)

The concentrate is mixed smooth textured pyrite and barite (B). Magnification 500X, scale bar = 100 microns.

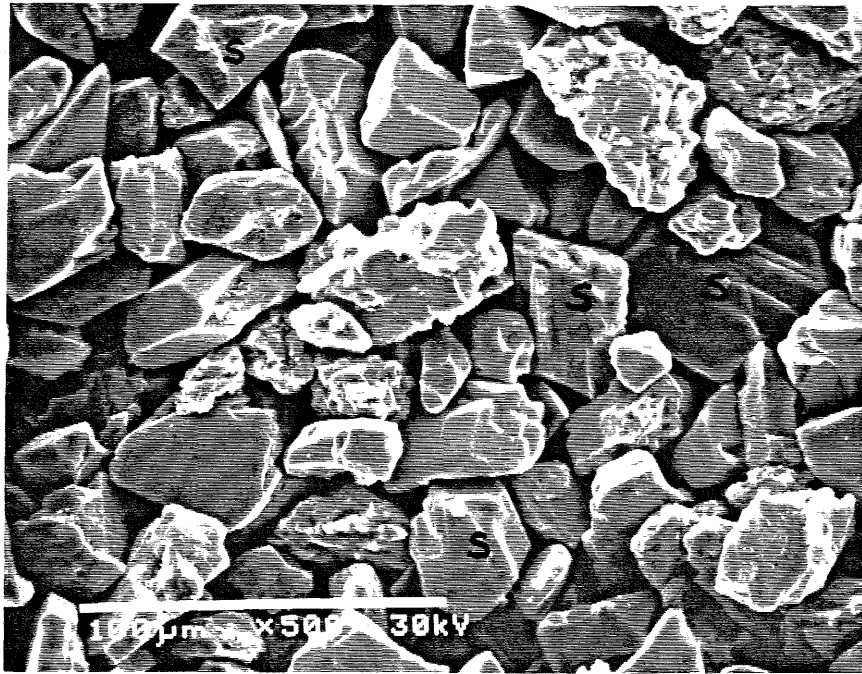


Figure 11E. T10 (flowsheet A sulfide concentrate)

This concentrate is mixed smooth and rough textured pyrite mixed with siderite (s). The pyrite is approximately 1/3 rough textured. Magnification 500X, scale bar = 100 microns.

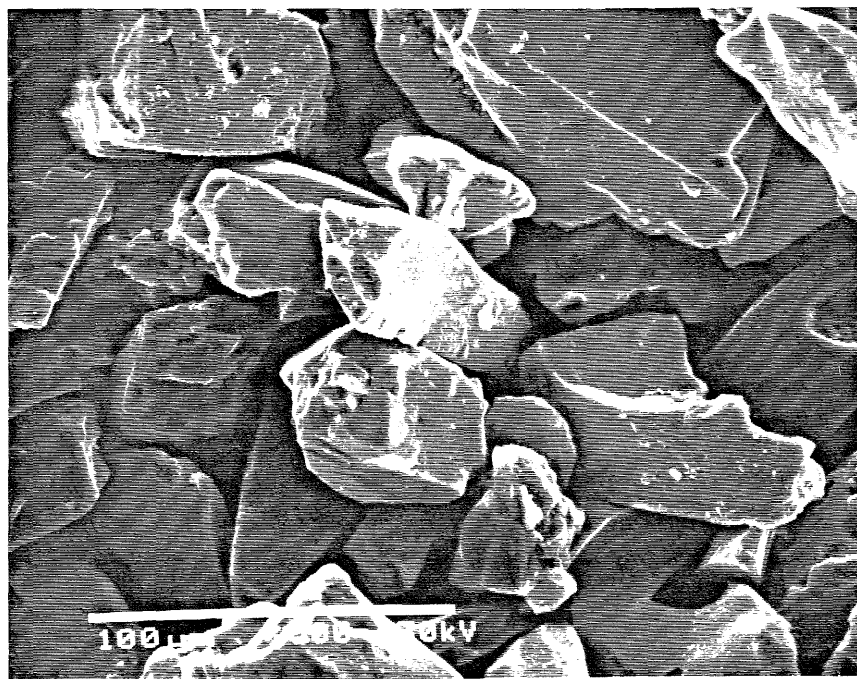


Figure 11F. T5 (flowsheet B (superpanner only) sulfide concentrate)

Typical smooth textured pyrite grains recovered. Some of the grains, while dominantly smooth, exhibit one or more rough textured surfaces. Magnification 500X, scale bar = 100 microns.

Figure 12. Extent of acid neutralization as a function of iron sulfide mass (neutralization calculated as $2(\text{SO}_4)/(\text{Ca} + \text{Mg})$).

For $0 \text{ g} \geq \text{Mass Iron sulfide (g)} \leq 50 \text{ g}$:

$$y = 0.043 x + 0.401$$

$$n = 11$$

$$r^2 = 0.894$$

For Neutralization ≥ 1.8 :

$$y = 0.001 x + 1.753$$

$$n = 8$$

$$r^2 = 0.664$$

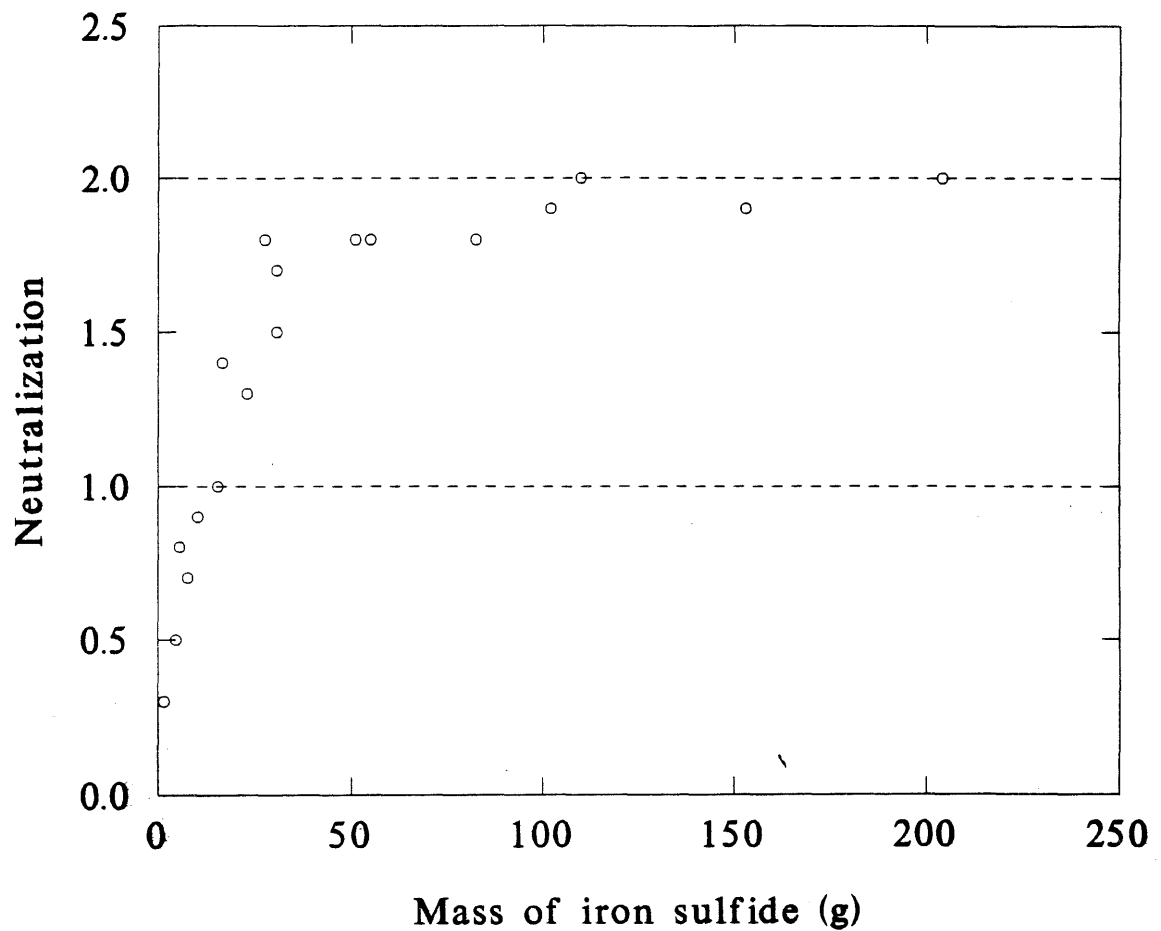


Figure 13. Rate of sulfate release vs. mass of iron sulfide in sample for the Variable Mass Experiment. Regression analysis included on plot. Regressions for T2 and T10 excluded the 1500 gram sample as an outlier (with 1500 gram sample T2: $y = 0.021 x - 0.517$, $n = 6$, $r^2 = 0.926$; T10: $y = 0.030 x - 0.379$, $n = 6$, $r^2 = 0.839$).

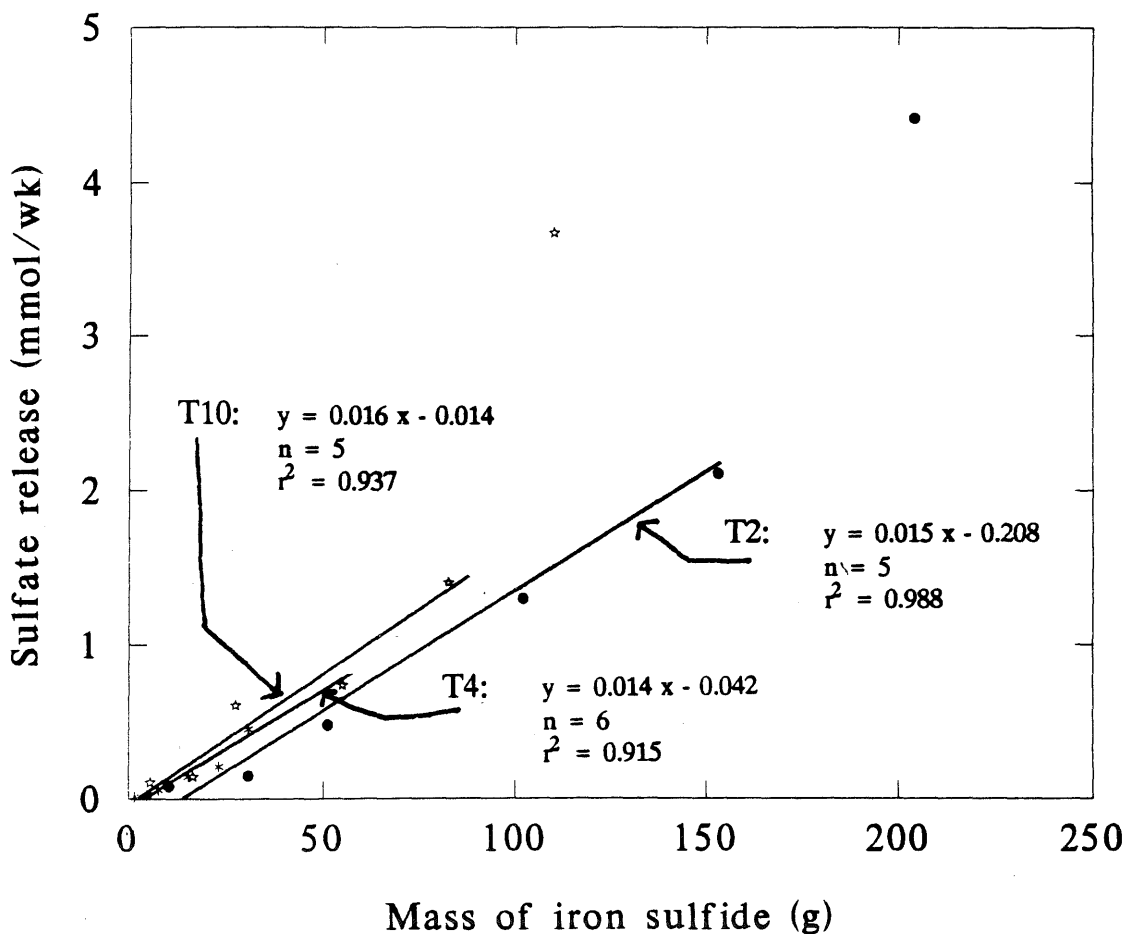


Figure 14. pH vs. oxidation interval box plots for the Variable Rinse Interval Experiment: T1, T2, and T3.

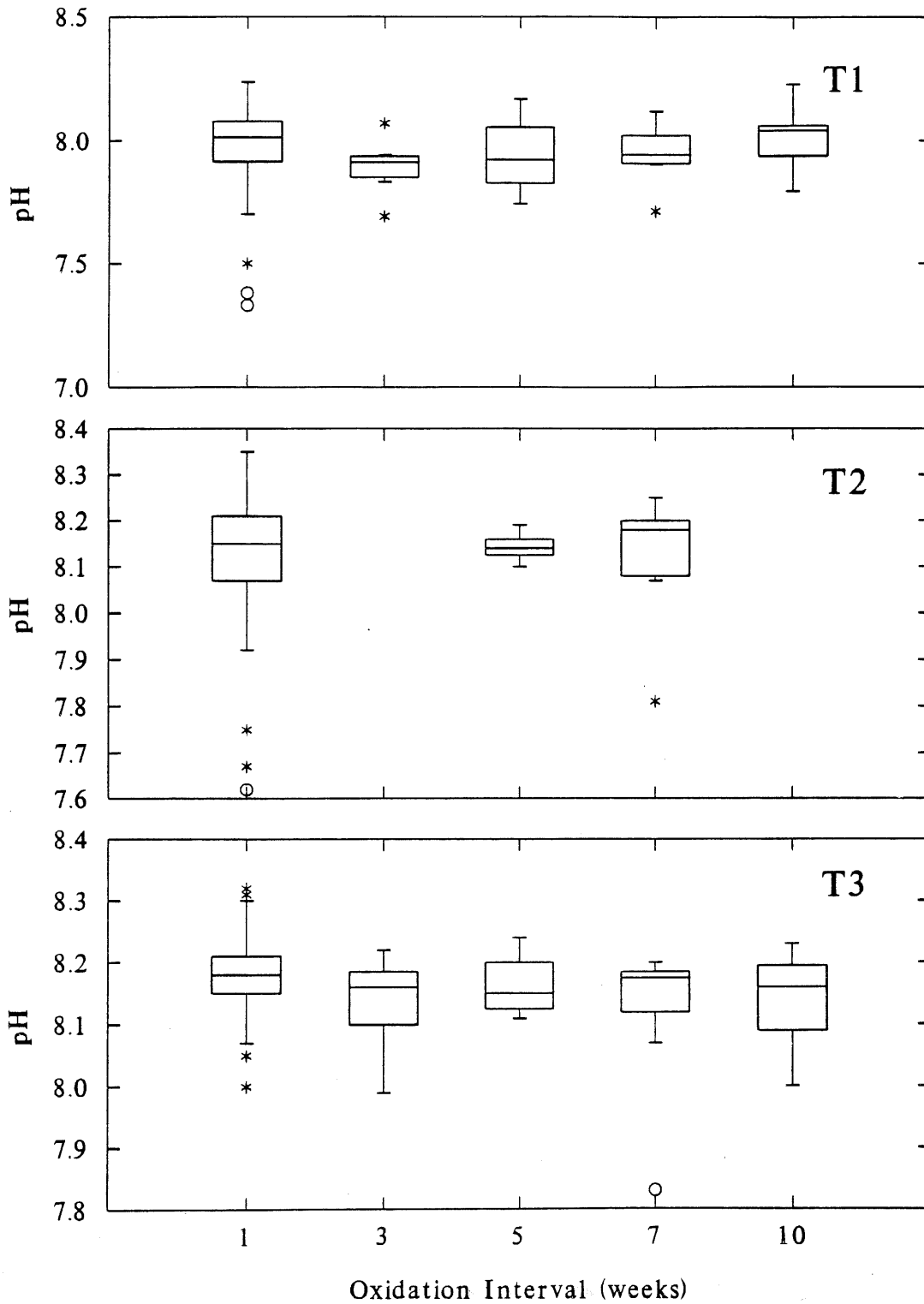


Figure 14 (cont.). pH vs. oxidation interval box plots for the Variable Rinse Interval Experiment: T4, T5, and T6.

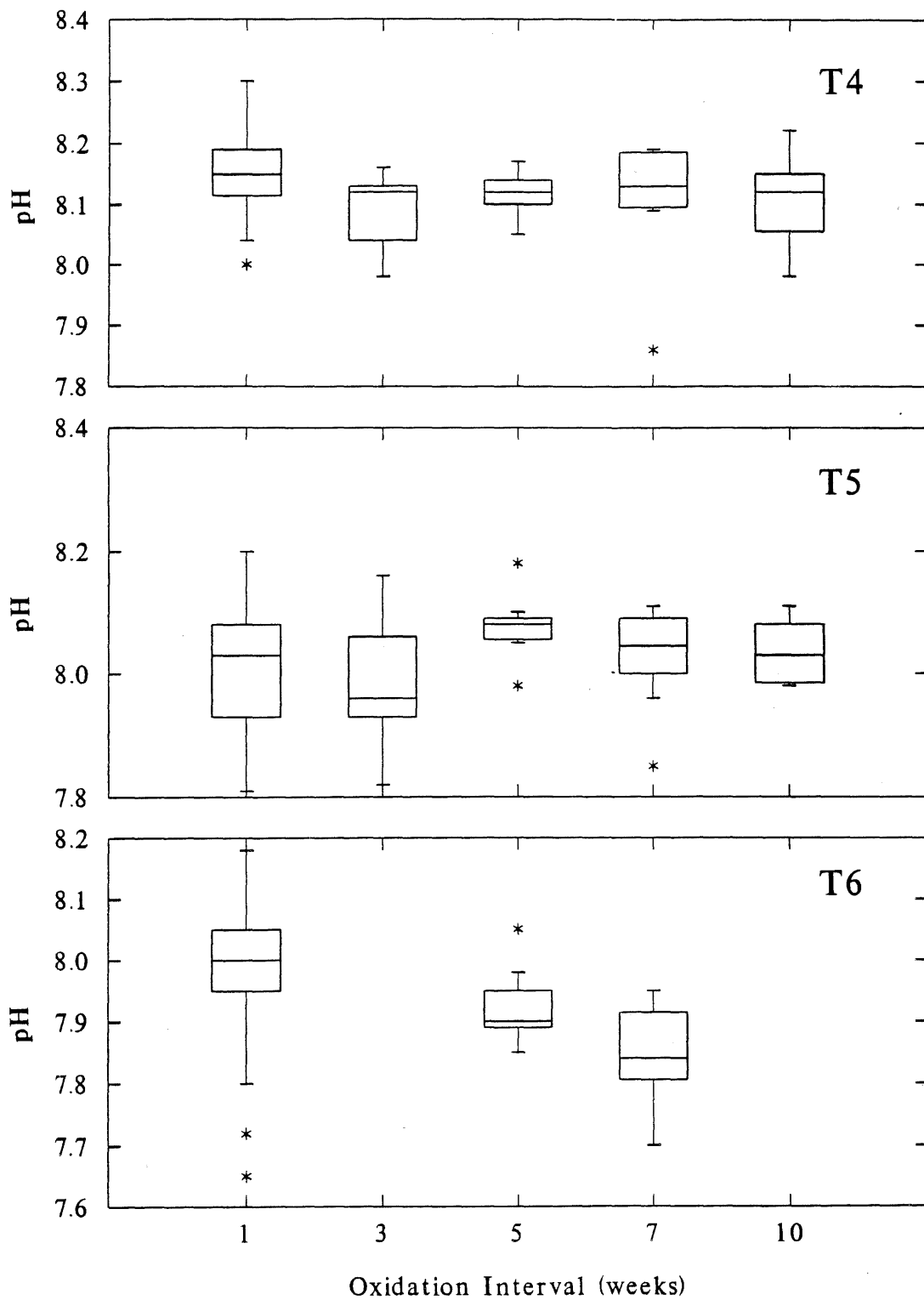


Figure 14 (cont.). pH vs. oxidation interval box plots for the Variable Rinse Interval Experiment: T7, T8, and T9.

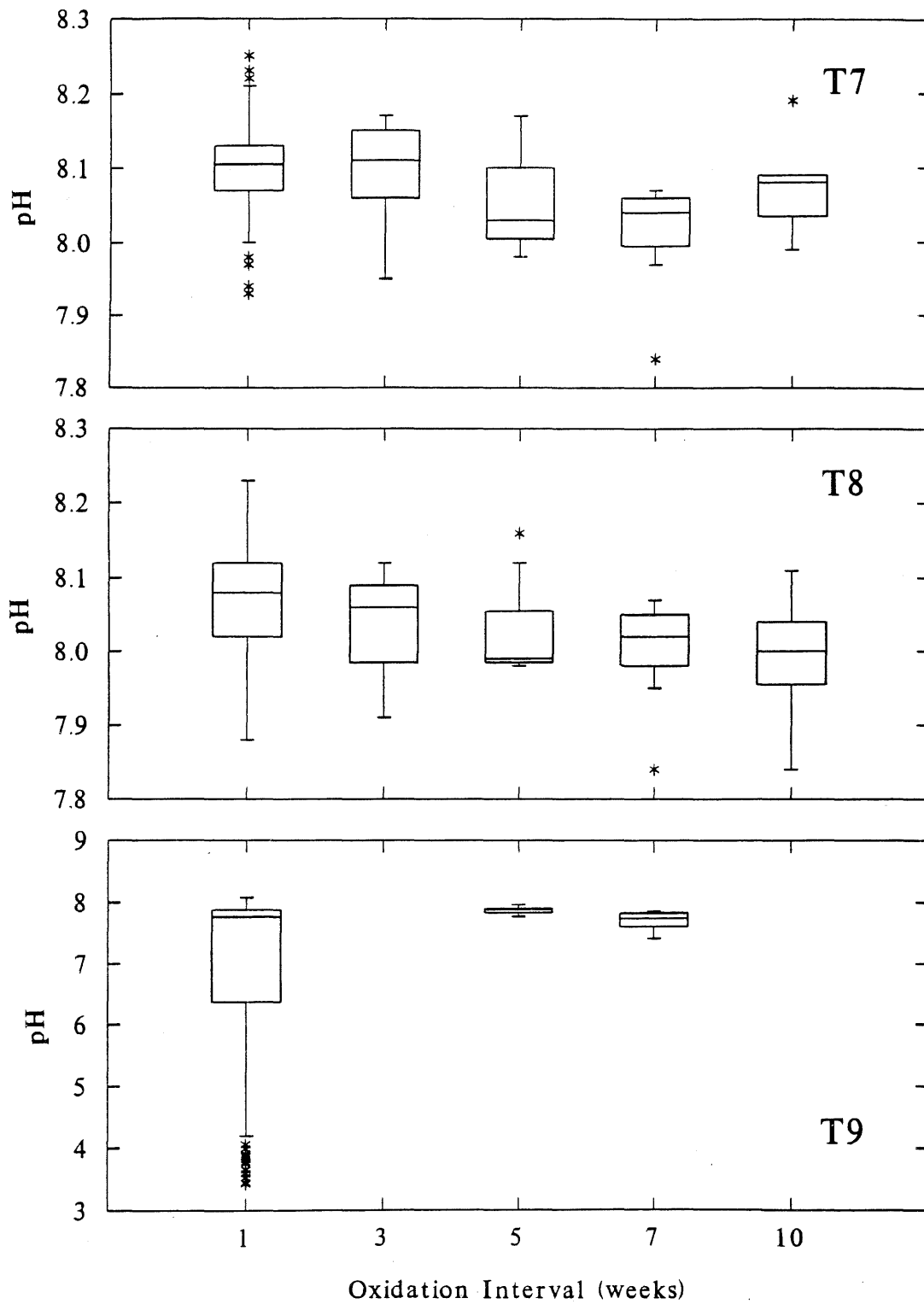


Figure 14 (cont.). pH vs. oxidation interval box plots for the Variable Rinse Interval Experiment: T10, T11, and T12.

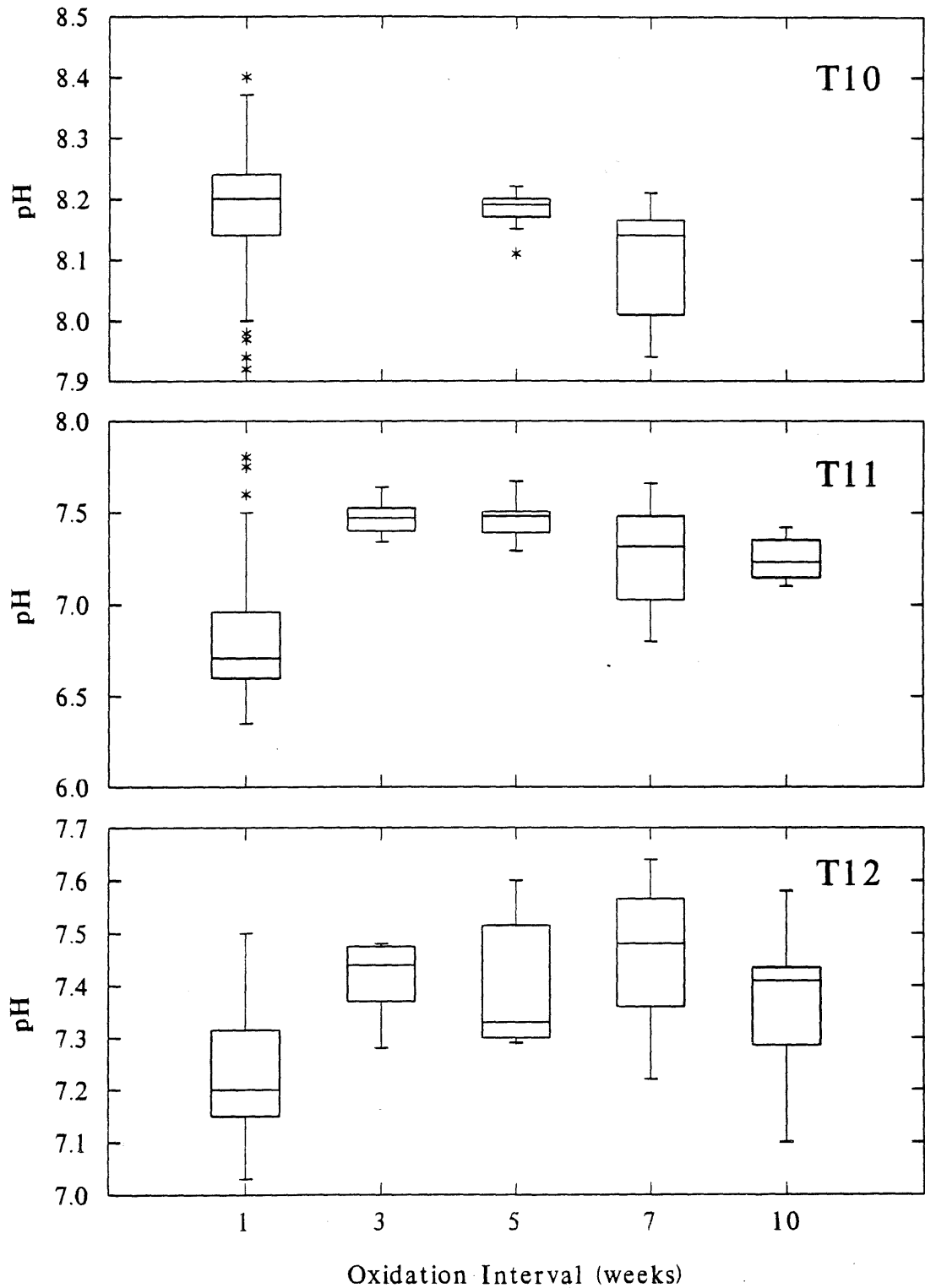


Figure 15. Sulfate concentration vs. oxidation interval box plots for the Variable Rinse Interval Experiment: T1, T2, and T3.

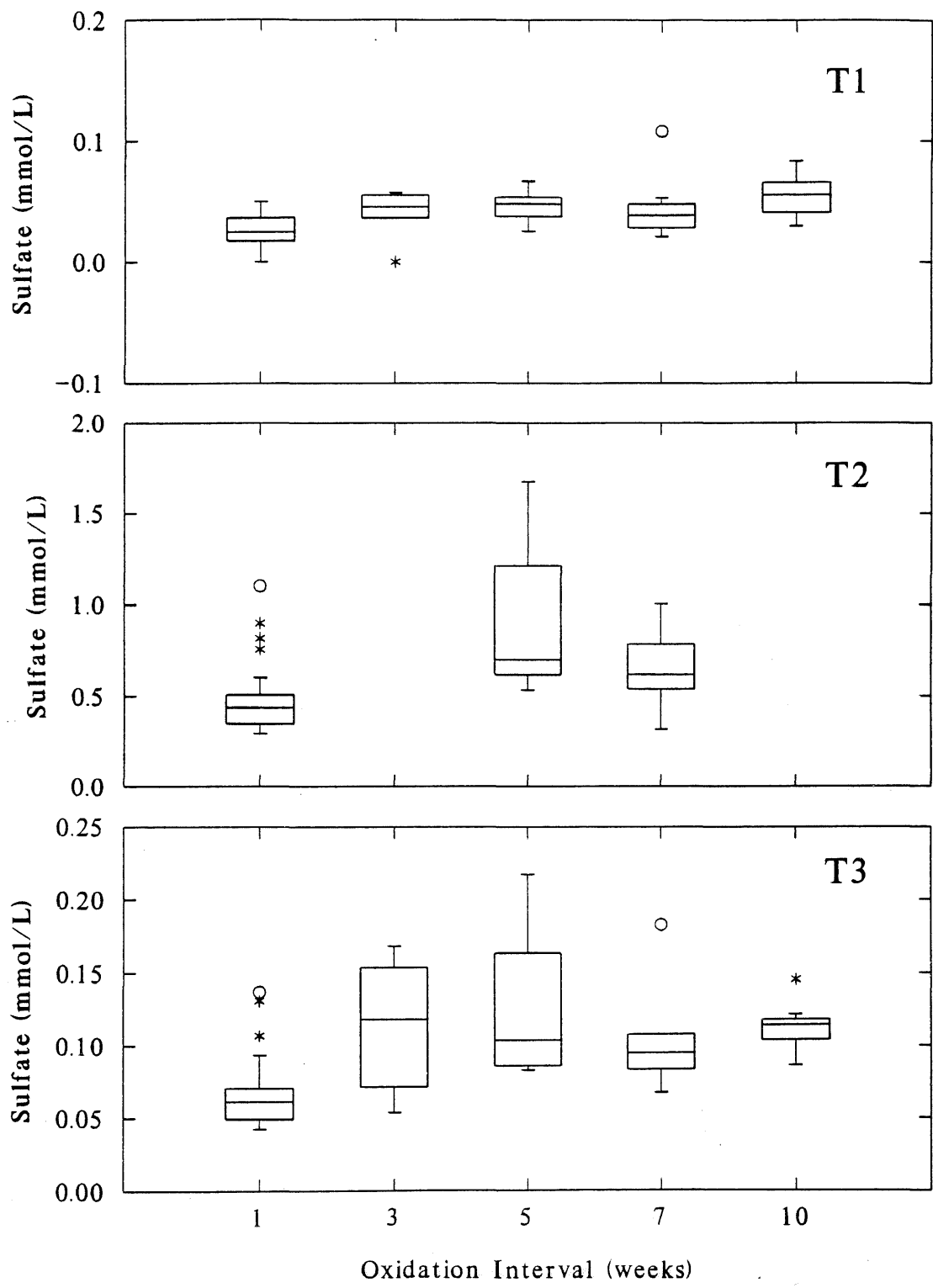


Figure 15 (cont.). Sulfate concentration vs. oxidation interval box plots for the Variable Rinse Interval Experiment: T4, T5, and T6.

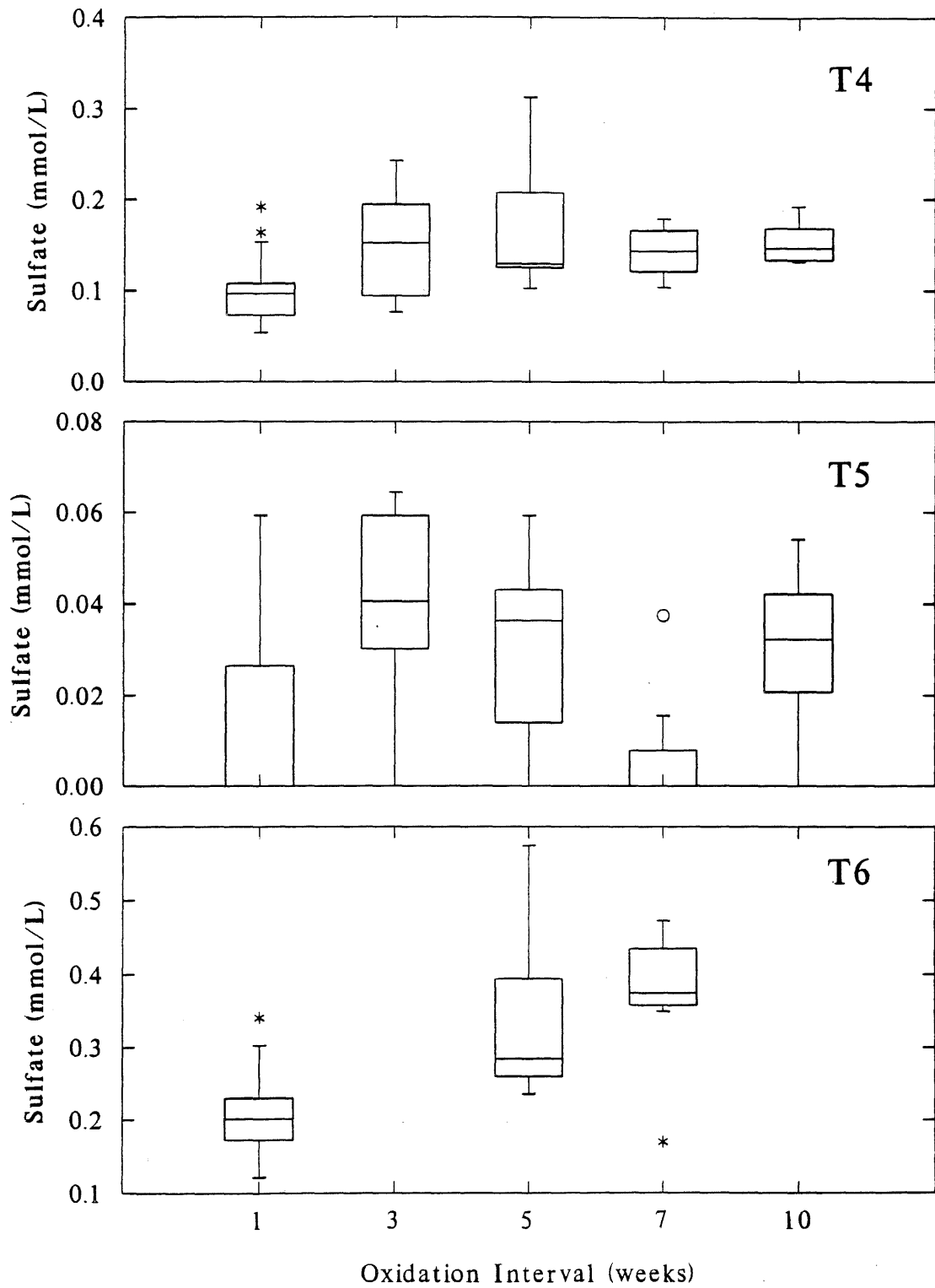


Figure 15 (cont.). Sulfate concentration vs. oxidation interval box plots for the Variable Rinse Interval Experiment: T7, T8, and T9.

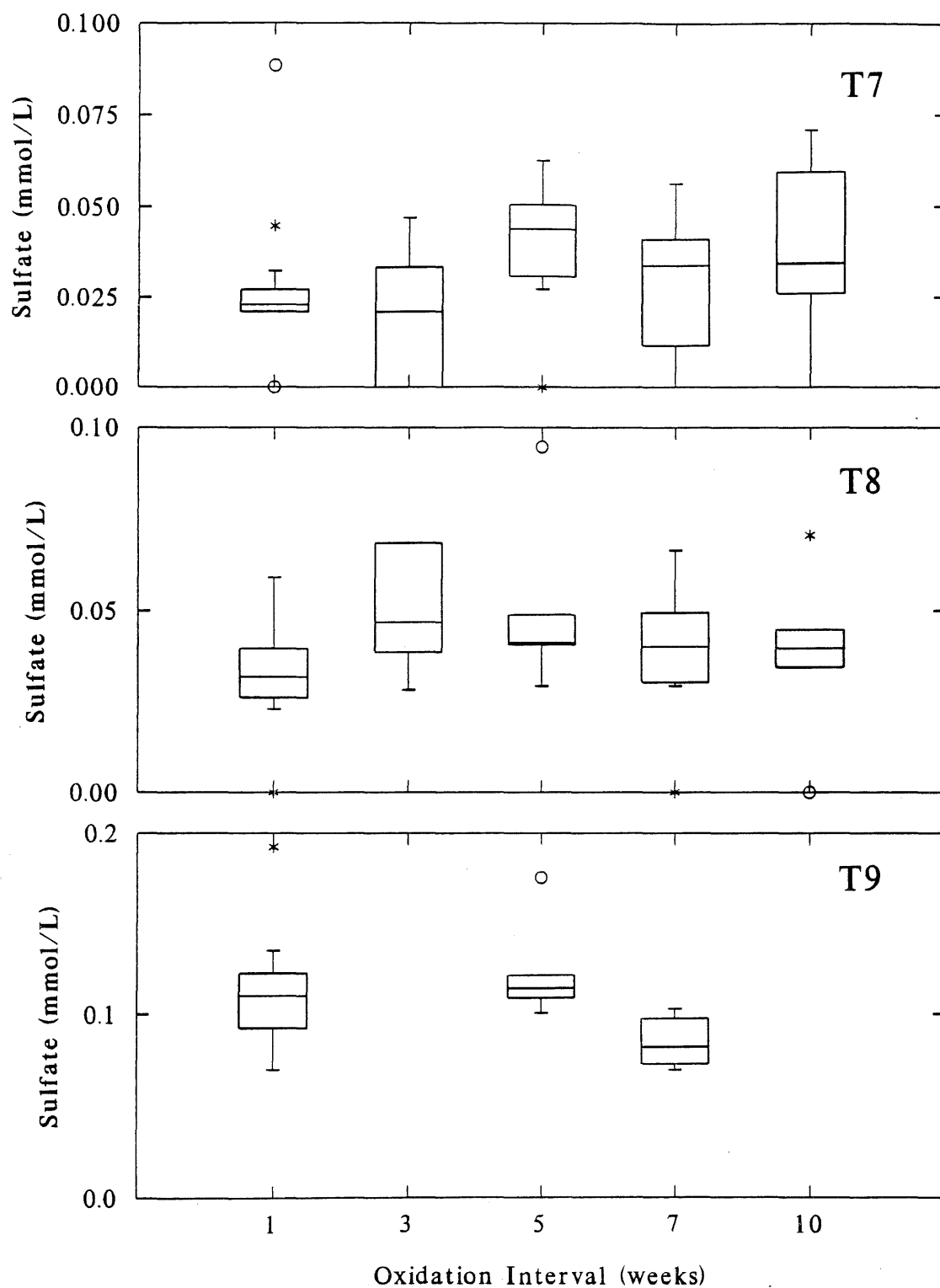


Figure 15 (cont.). Sulfate concentration vs. oxidation interval box plots for the Variable Rinse Interval Experiment: T10, T11, and T12.

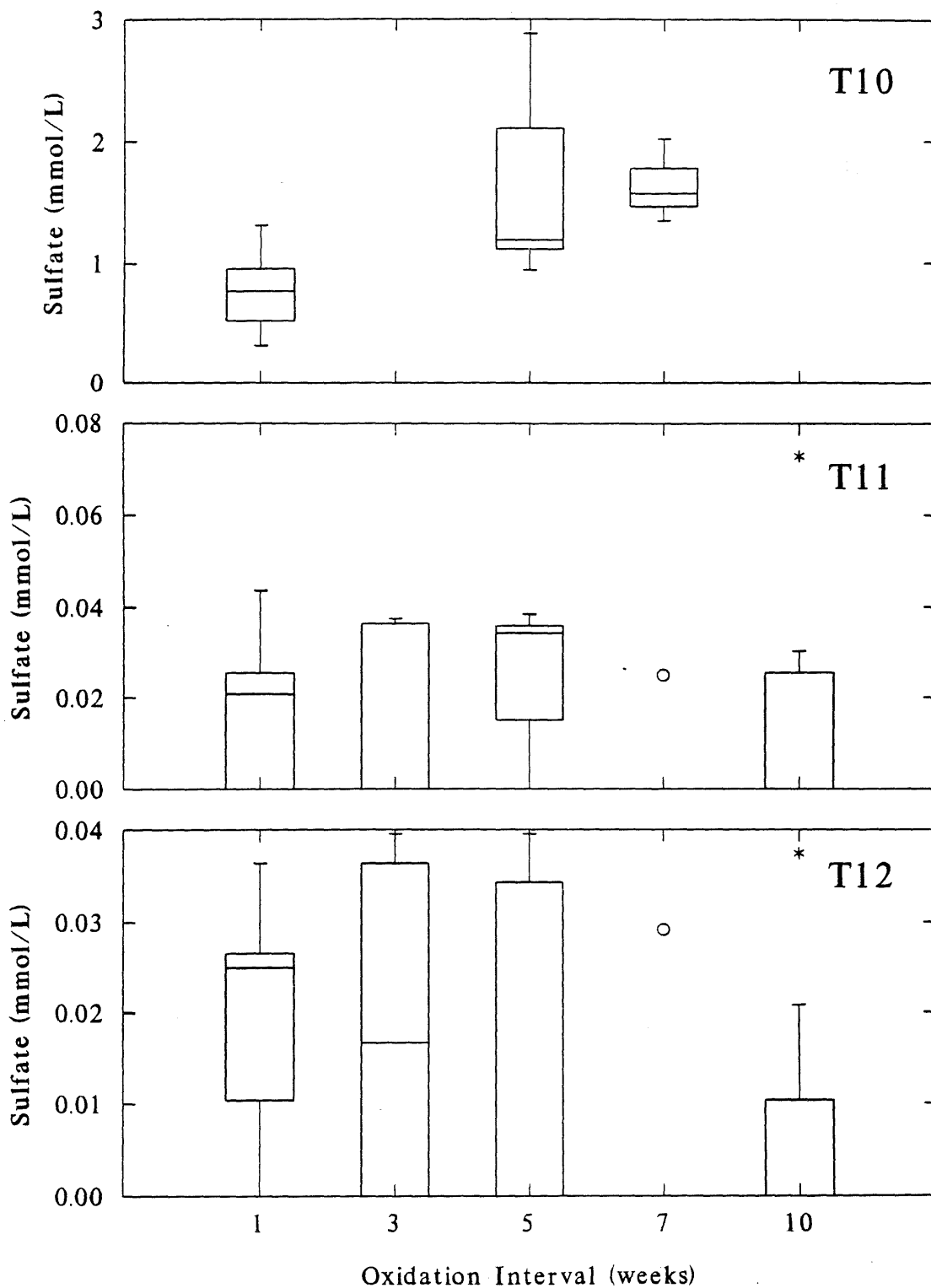


Figure 16. Calcium and magnesium concentrations vs. oxidation interval box plots for the Variable Rinse Interval Experiment: T1, T2, and T3.

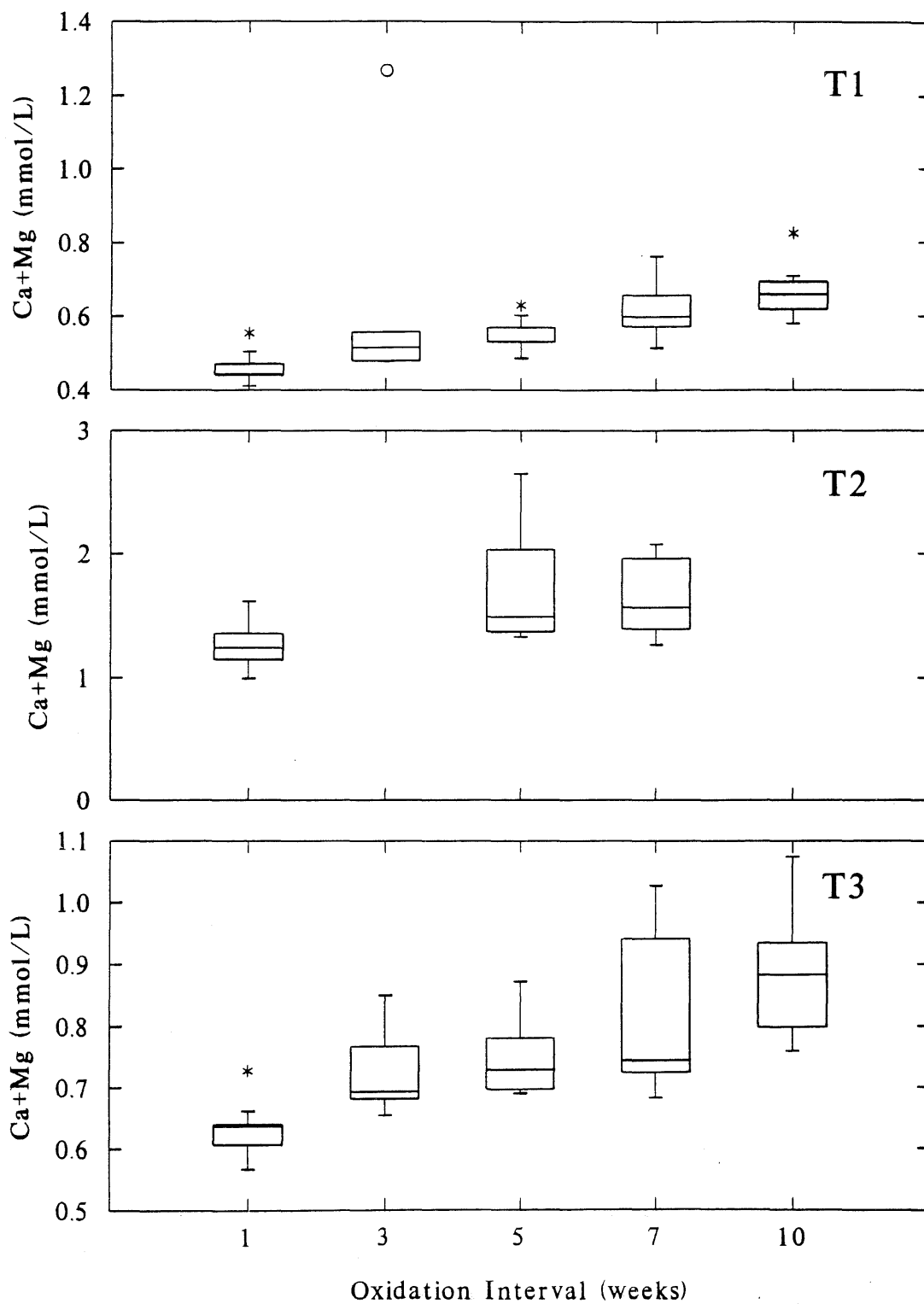


Figure 16 (cont.). Calcium and magnesium concentrations vs. oxidation interval box plots for the Variable Rinse Interval Experiment: T4, T5, and T6.

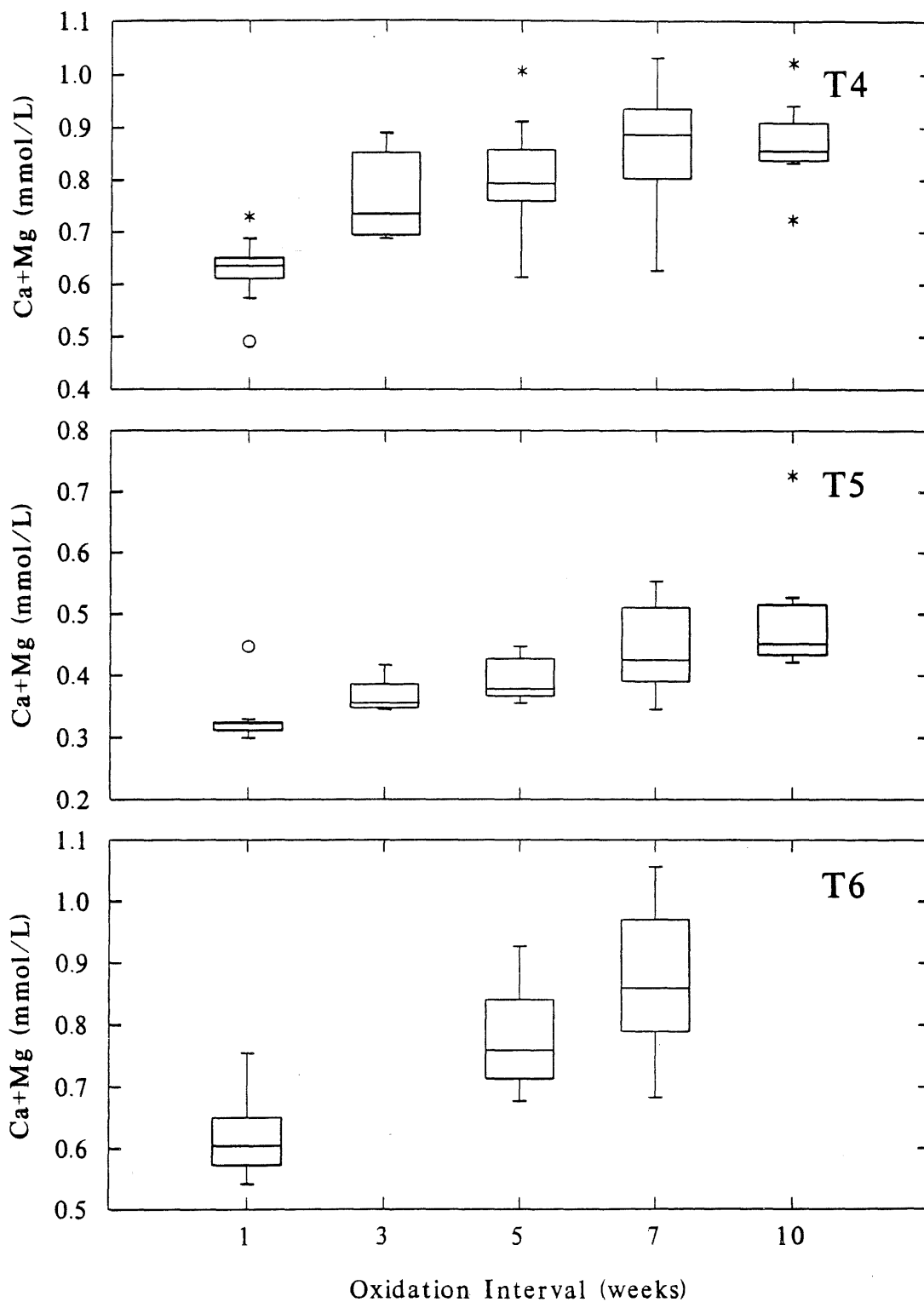


Figure 16 (cont.). Calcium and magnesium concentrations vs. oxidation interval box plots for the Variable Rinse Interval Experiment: T7, T8, and T9.

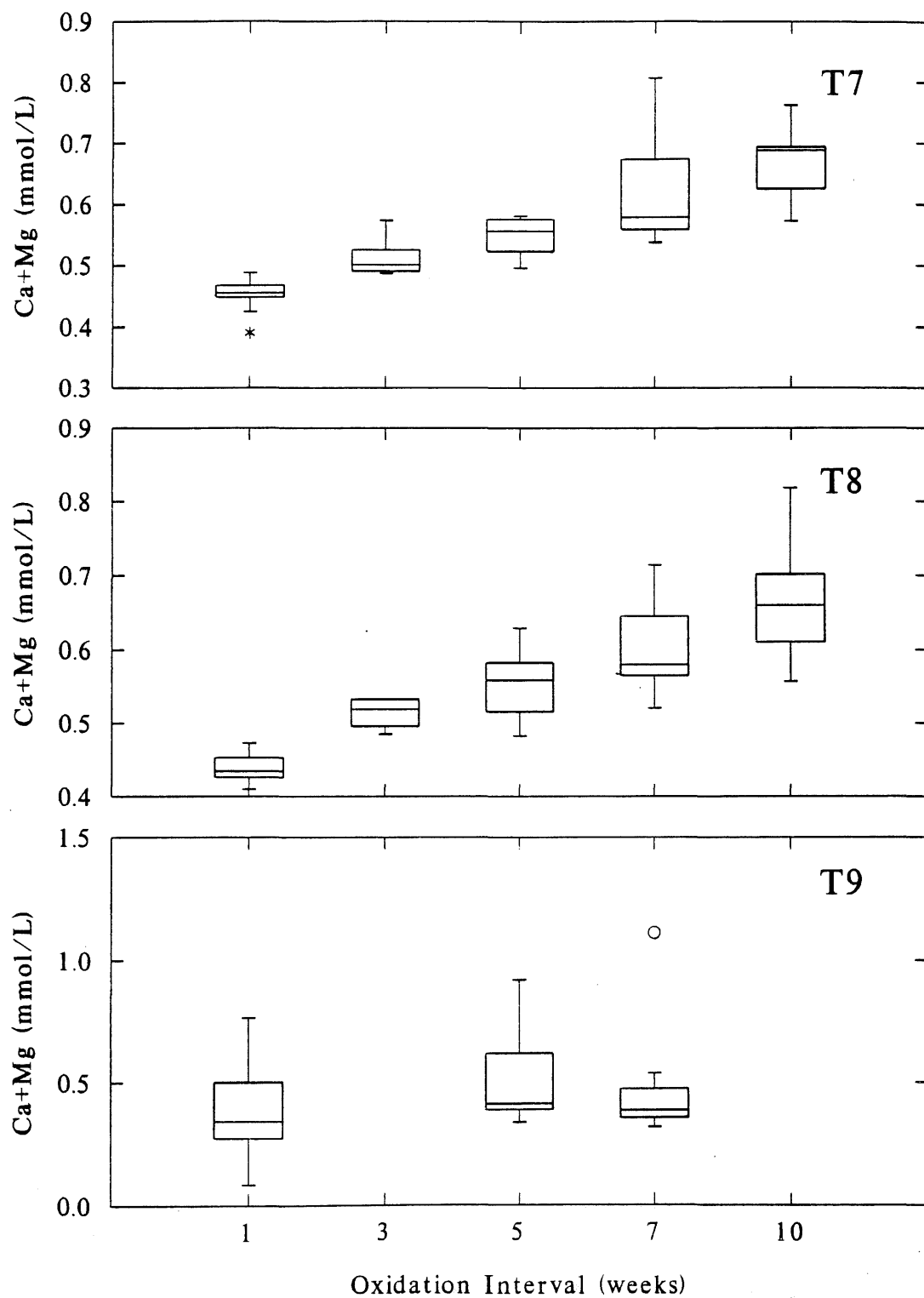


Figure 16 (cont.). Calcium and magnesium concentrations vs. oxidation interval box plots for the Variable Rinse Interval Experiment: T10, T11, and T12.

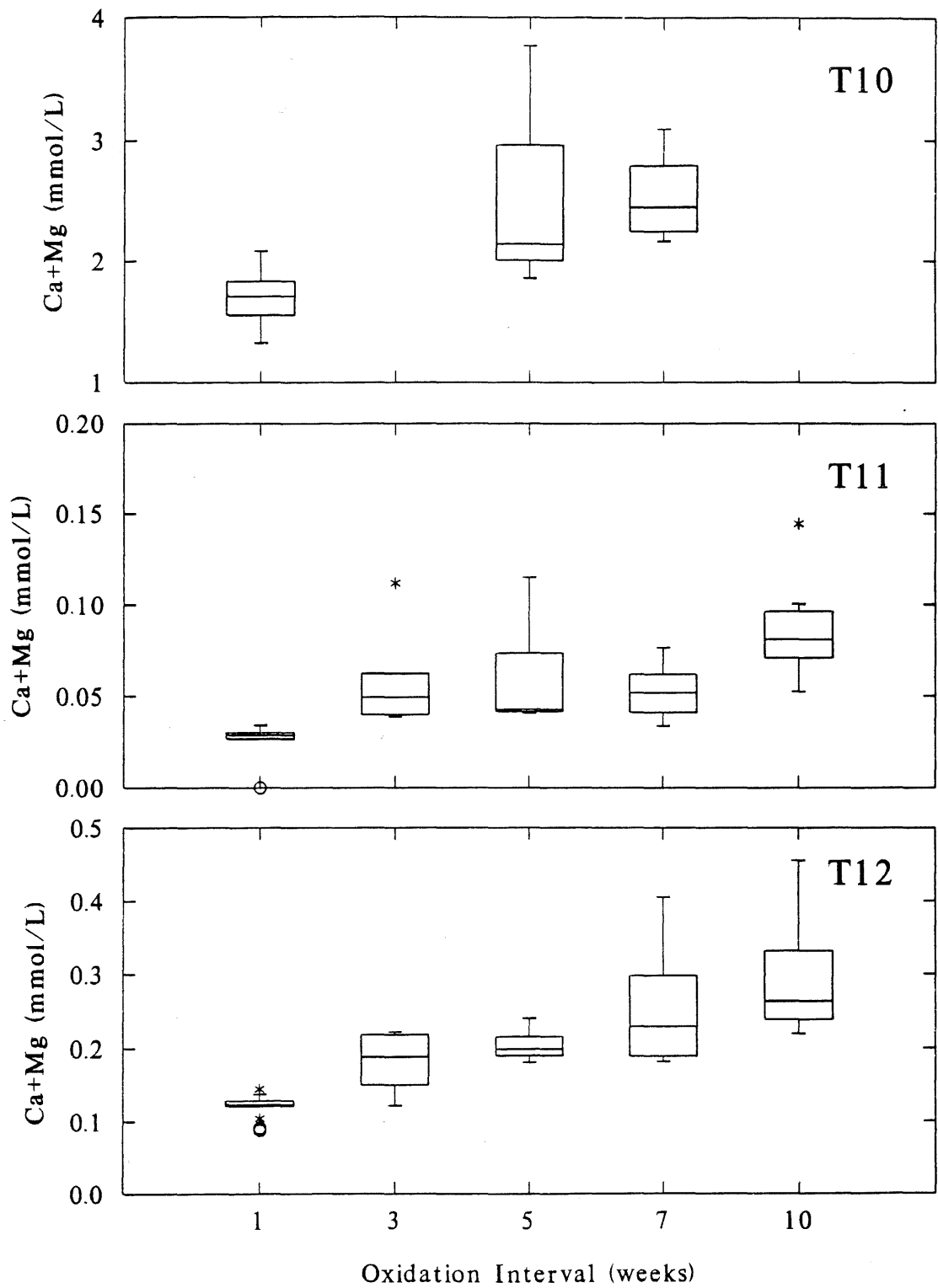


Figure 17. Alkalinity vs. oxidation interval box plots for the Variable Rinse Interval Experiment: T1, T2, and T3.

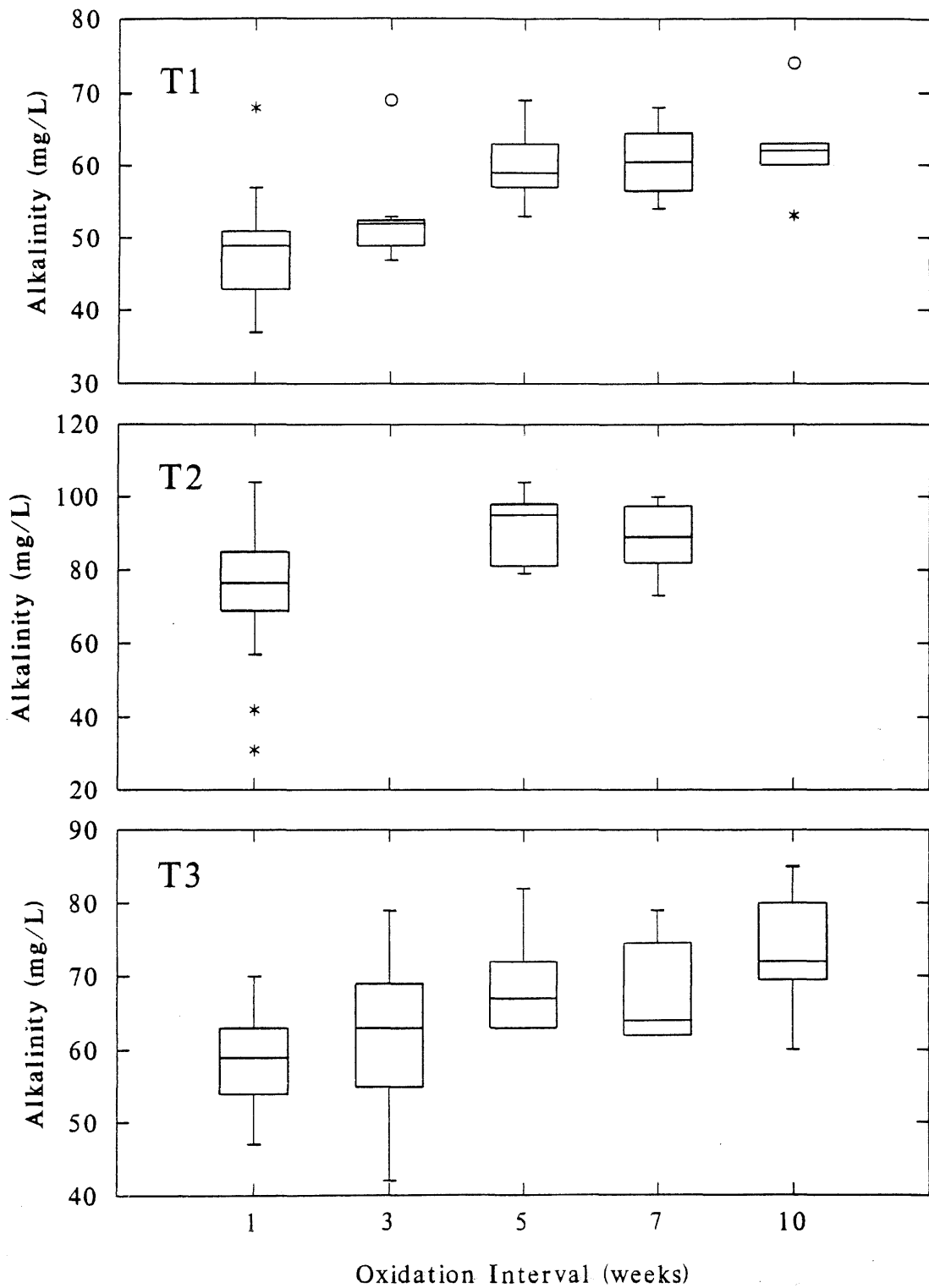


Figure 17 (cont.). Alkalinity vs. oxidation interval box plots for the Variable Rinse Interval Experiment: T4, T5, and T6.

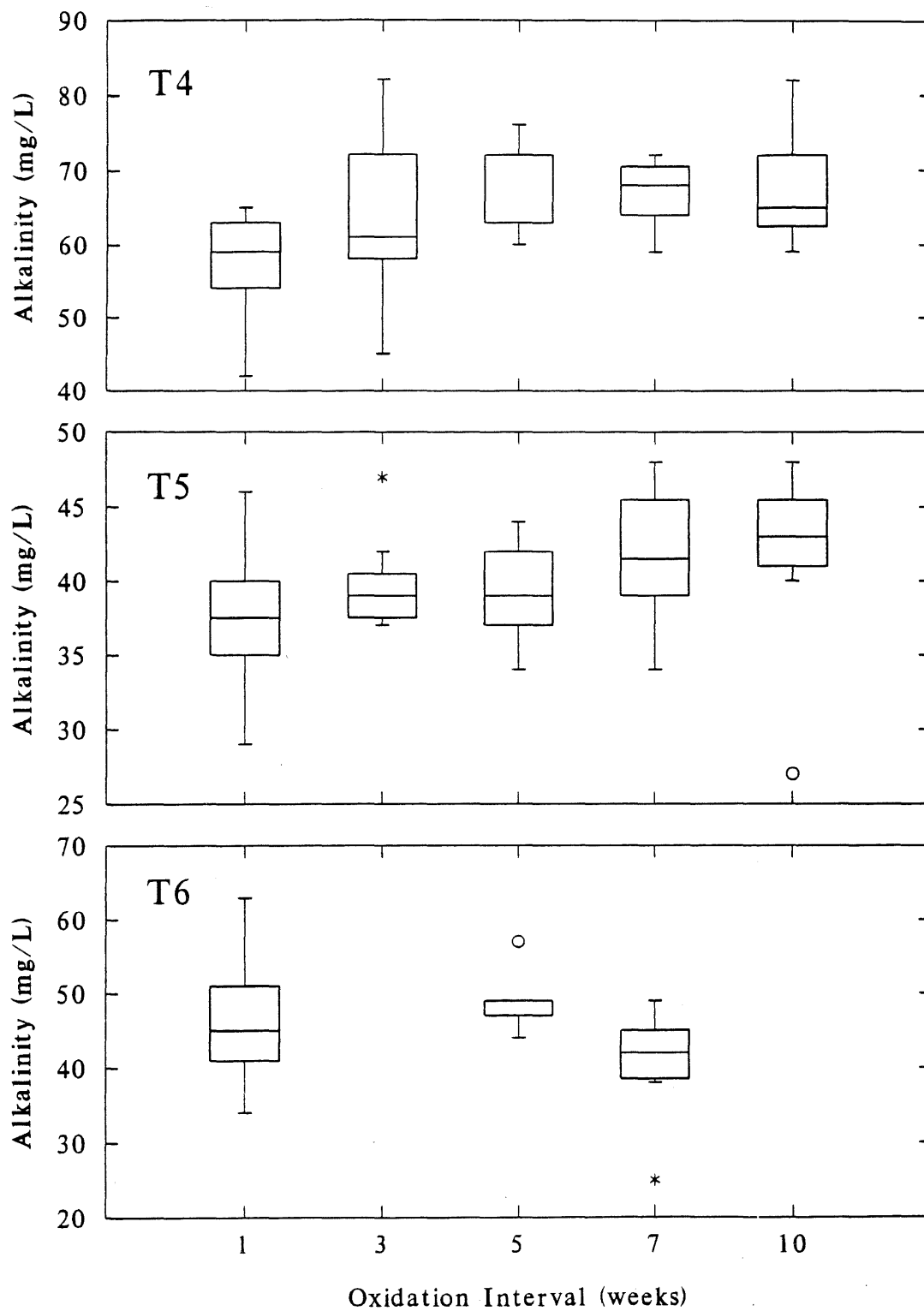


Figure 17 (cont.). Alkalinity vs. oxidation interval box plots for the Variable Rinse Interval Experiment: T7, T8, and T9.

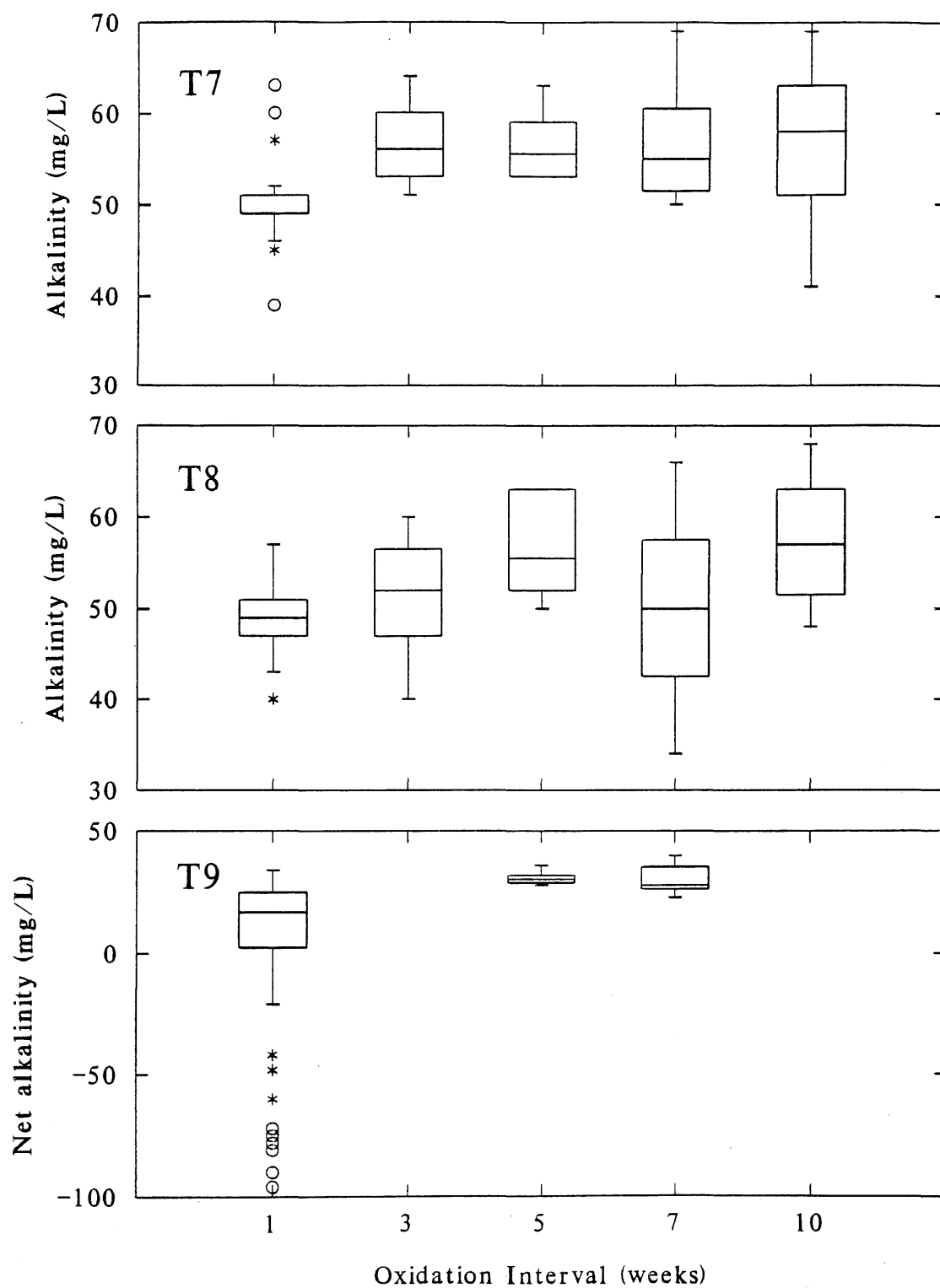


Figure 17 (cont.). Alkalinity vs. oxidation interval box plots for the Variable Rinse Interval Experiment: T10, T11, and T12.

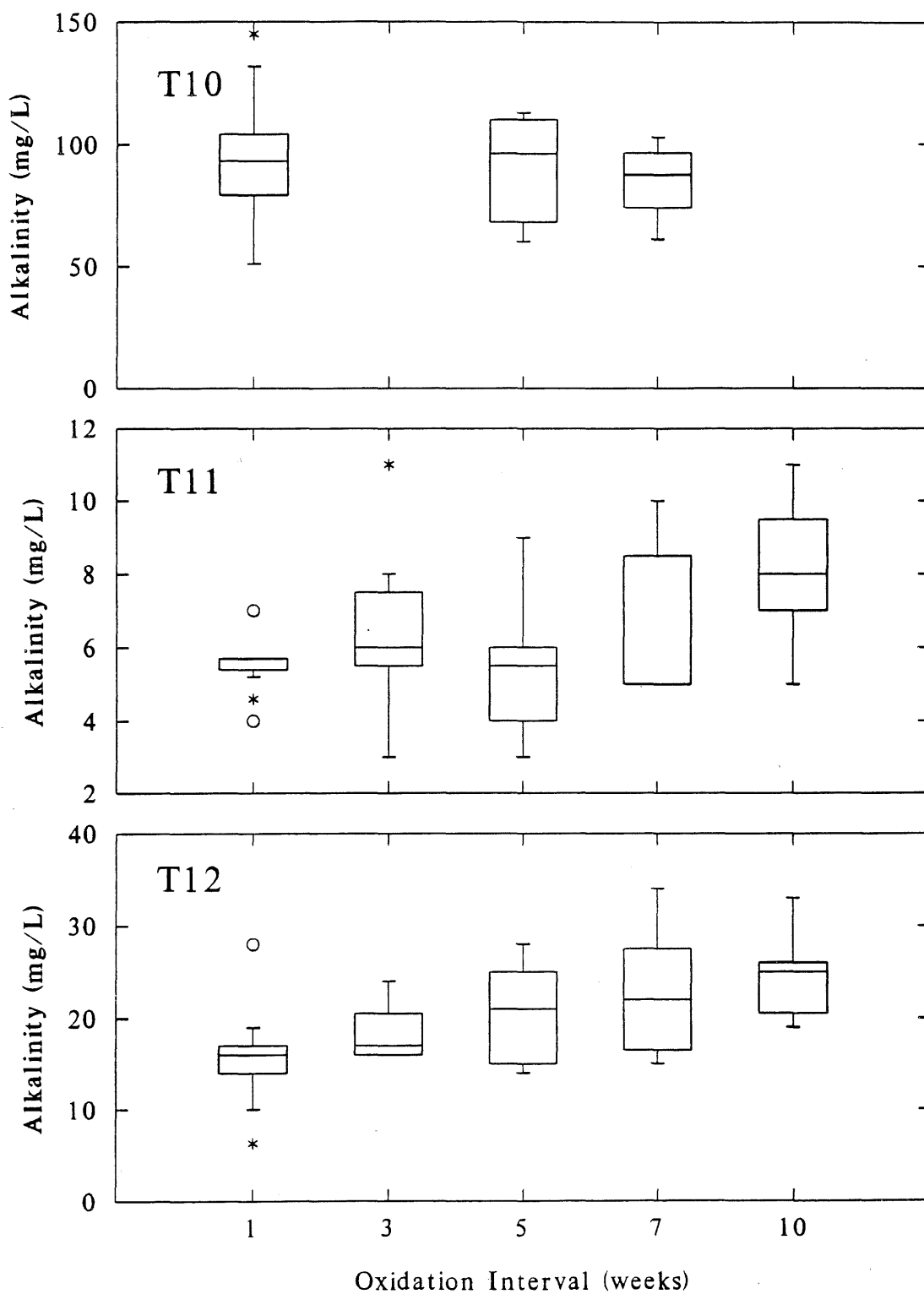


Figure 18. pH, sulfate, calcium, and magnesium concentrations vs. time for T1 (reactors 3: open symbols; and 4: closed symbols) from the Elevated Temperature Experiment.

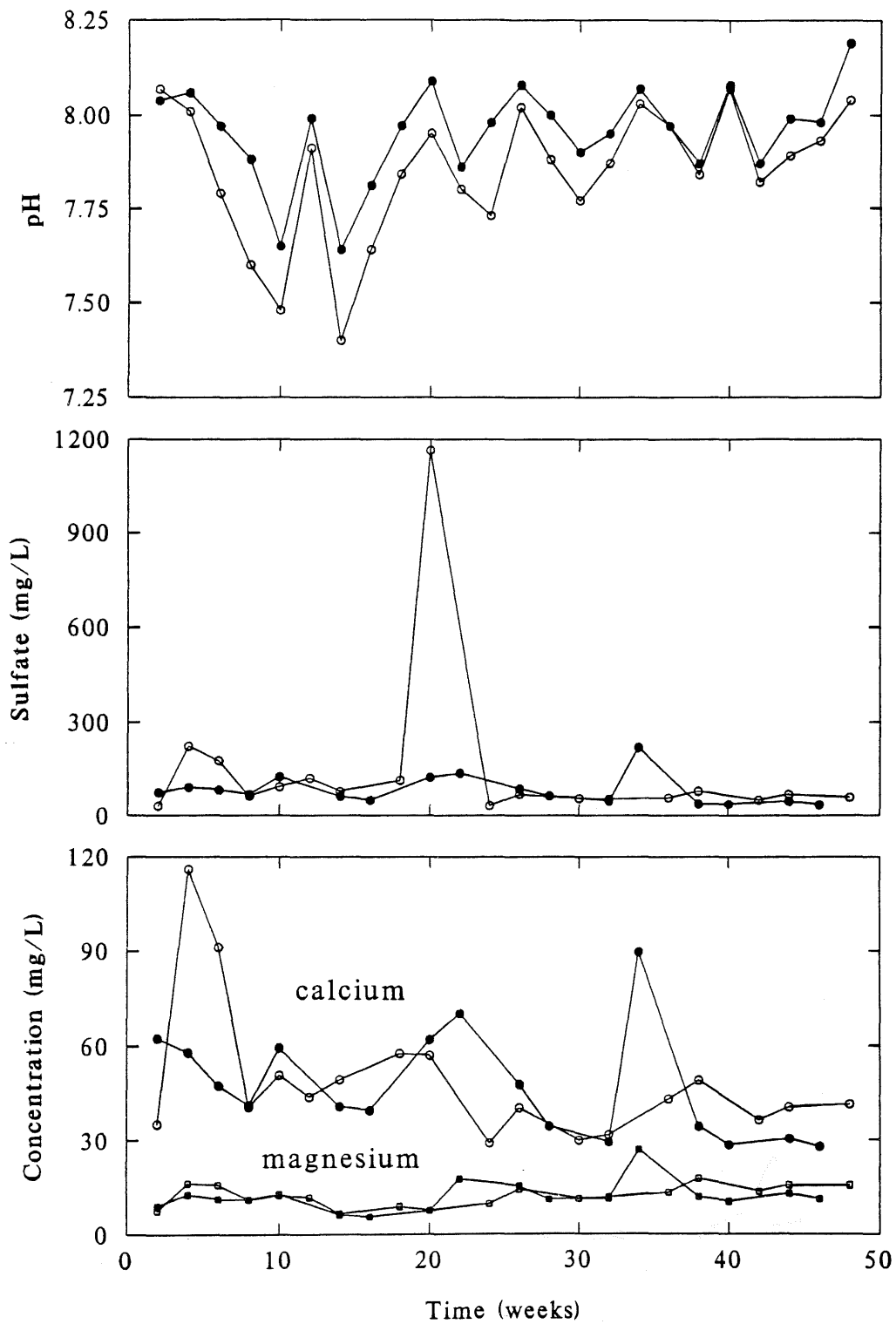


Figure 19. pH, sulfate, calcium, and magnesium concentrations vs. time for T9 (reactors 9: open symbols; and 10: closed symbols) from the Elevated Temperature Experiment.

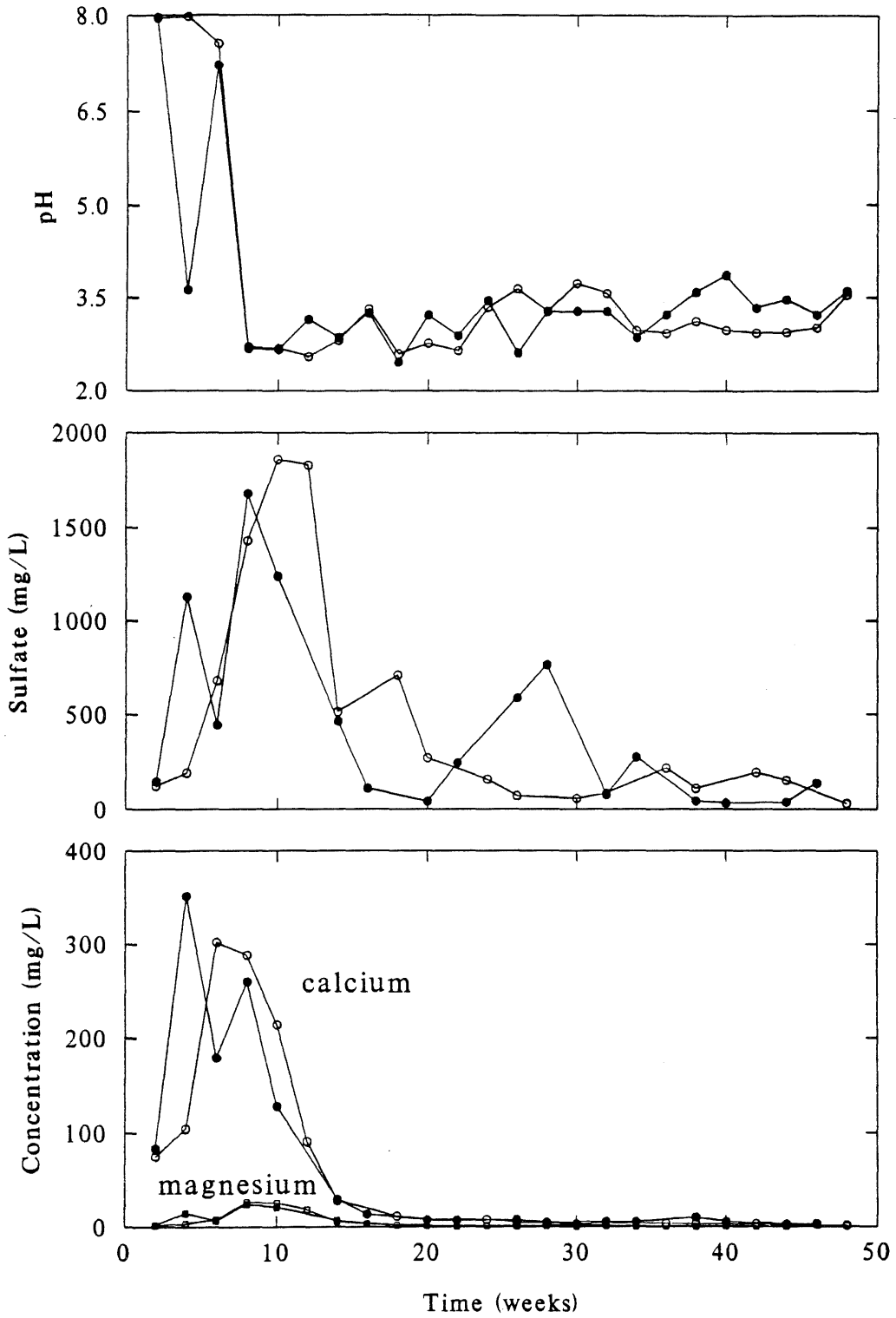


Figure 20. Cumulative mass release vs. time for the Elevated Temperature Experiment, weeks 2-48: Solid T9, reactor 10.

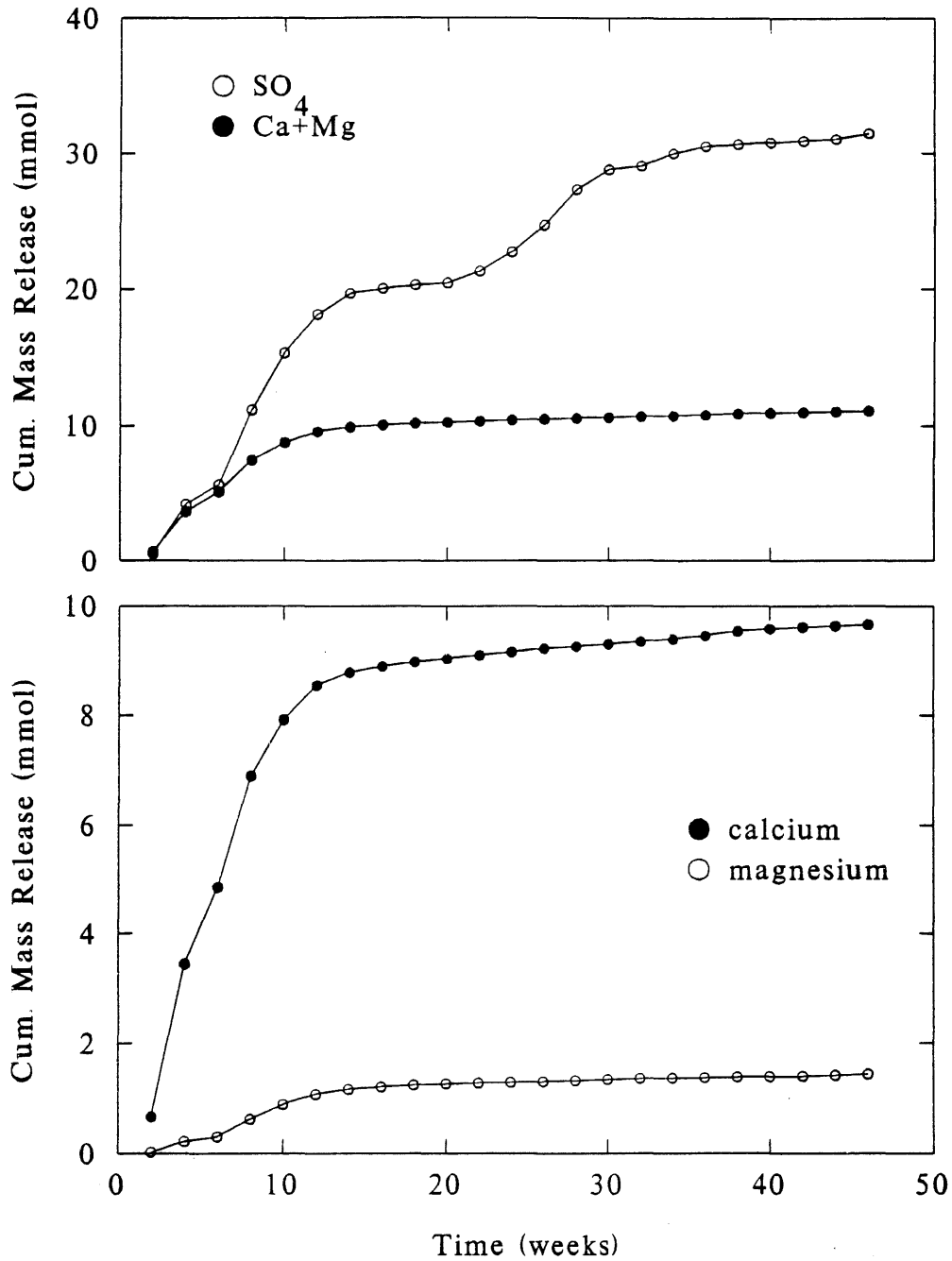


Figure 21. pH, sulfate, calcium, and magnesium concentrations vs. time for the Elevated Temperature Experiment: Solid T2, reactors 14 (open symbols) and 15 (closed symbols).

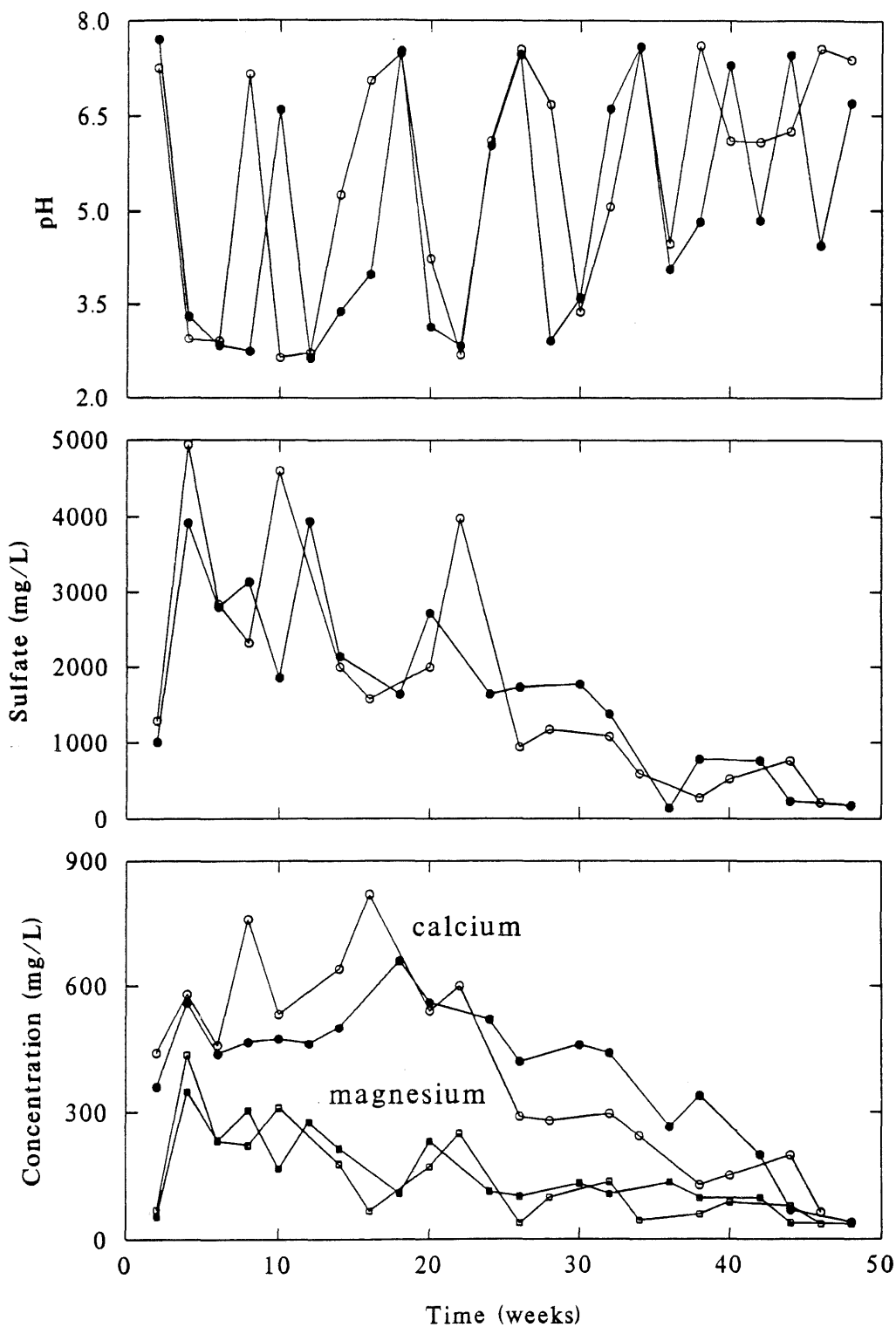


Figure 22. Treatment system designs for arsenic removal from tailings water at the Giant and Con mines.

